Slope Stability Verification Manual

SEEQUENT

GeoStudio

Email: sales@geoslope.com
www.geoslope.com

Table of Contents

1 Introduction

The word "Verification", when used in connection with computer software, can be defined as the ability of the computer code to provide a solution consistent with the physics of the problem. There are also other factors such as initial conditions, boundary conditions, and control variables that may affect the accuracy of the code to perform as stated.

Verification is generally achieved by solving a series of so-called benchmark problems. Benchmark problems are those for which a closed-form solution exists, or for which the solution has become "reasonably certain" because of longhand calculations that have been performed. Publication of the "benchmark" solutions in research journals or textbooks also lends credibility to the solution.

There are also example problems that have been solved and published in documentation associated with other comparable software packages. While these are valuable comparisons, the possibility exists for the published analysis definition and solution to comprise errors; consequently, care must be taken when verifying by means of comparison with other software. Furthermore, it is not possible to verify numerical software for all possible scenarios. Rather, it is an ongoing process that establishes credibility with time.

2 Verifications

The following examples compare the results of stability analyses against published solutions presented in textbooks or journal papers. There is a group of models that was distributed to geomechanics professional as part of a survey sponsored by the Association for Computer Aided Design (ACADS). The problems were designed to test the numerical procedures for handling various aspects of slope stability analysis. Several participants submitted solutions generated by a wide array of slope stability programs. The results were reviewed by an expert panel to establish the most likely correct solution. Giam and Donald (1989) authored the complete report of the study. These verifications contain ACADS in the title.

2.1 ACADS Simple Slope

Project File: ACADS Simple Slope.gsz

This model contains a simple case of a total stress analysis without considering pore-water pressures. It is a simple analysis that represents a homogenous slope with given soil properties. The entry-exit search technique was used to locate the critical slip surface. This model is originally published by the ACADS study (Giam and Donald, 1989).

2.1.1 Geometry and Material Properties
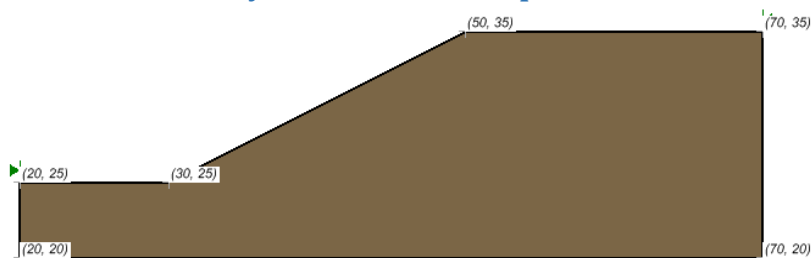
Figure 1 Simple Slope: Geometry

Table 1 Simple Slope: Material Properties

c (kN/m^2)	ϕ (degrees)	γ (kN/m^3)
3.0	19.6	20.0

2.1.2   Results and Discussions

The results of the factor of safety calculations are shown in the following table and figures. The Factor of Safety published by the ACADS study was 1.00

Table 2 Simple Slope: Results

Method	Factor of Safety	
	Moment	Force
Bishop	0.963	
Janbu		0.992
Morgenstern-Price	0.991	0.991
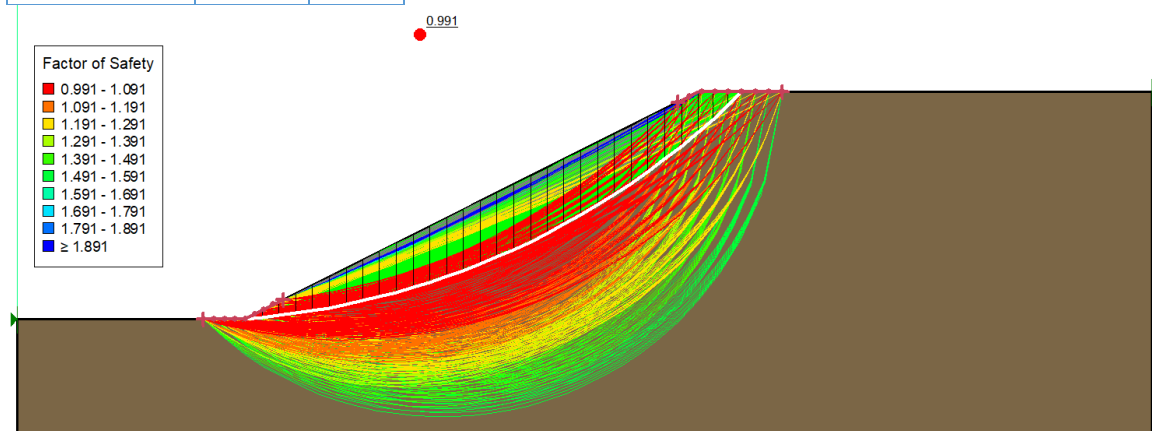
Figure 2 Simple Slope: Critical Slip Surface
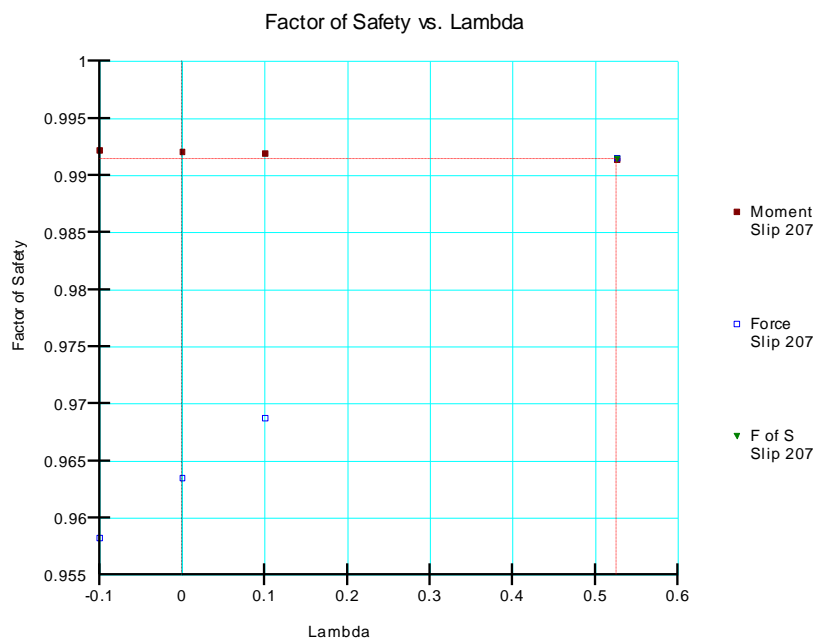
Figure 3 Simple Slope: Factor of Safety vs Lambda.

2.2   ACADS Tension Crack

Project File: ACADS Simple Slope.gsz

This model has the same slope geometry as verification problem #1, with the exception that a tension crack zone has been added as shown in Figure 4.

For this problem, a suitable tension crack depth is required. Water is assumed to fill the tension crack. The formula used to calculate the tension crack depth is given by (Craig, 1997):

$$Depth = \frac{2c}{\gamma\sqrt{k_a}}, k_a = \frac{1 - sin\,\varphi}{1 + sin\,\varphi}$$

which results in a tension crack depth of about 3.6 m. The entry-exit search technique was used to locate the critical slip surface.

2.2.1   Geometry and Material Properties

Figure 4 Tension Crack: Geometry

Table 3 Tension Crack: Material Properties

c (kN/m²)	φ (degrees)	γ (kN/m3)
32.0	10.0	20.0

2.2.2   Results and Discussions

The results of the factor of safety calculations are shown in the following table and figures. The Factor of Safety published by the ACADS study is 1.65 to 1.70.

Table 4 Tension Crack: Results

Method	Factor of Safety	
	Moment	Force
Bishop	1.664	
Janbu		1.471
Morgenstern-Price	1.660	1.660
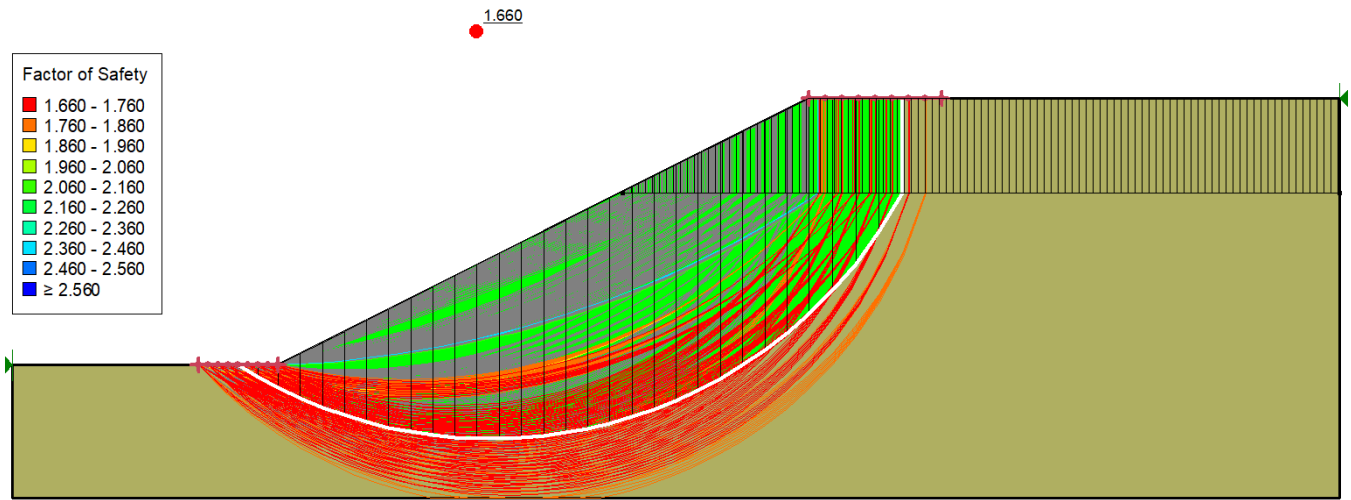
Figure 5 Tension Crack: Critical Slip Surface
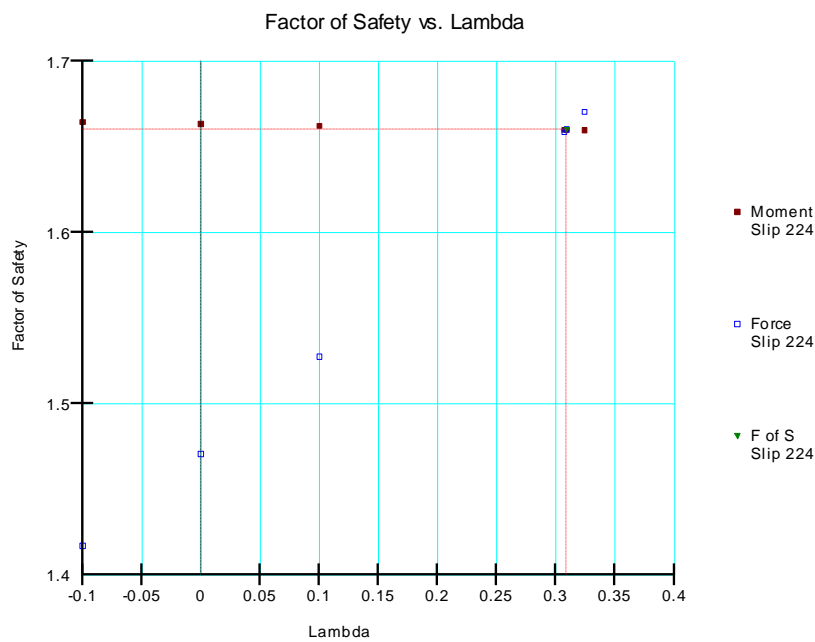
Figure 6 Tension Crack: Factor of Safety vs Lambda.

2.3   ACADS Non-Homogeneous

Project File: ACADS Non-Homogeneous Slope.gsz

This model is a non-homogeneous three-layer slope with geometry shown in Figure 7 and material properties shown in Table 5. The entry-exit search technique was used to locate the critical slip surface.

2.3.1 Geometry and Material Properties
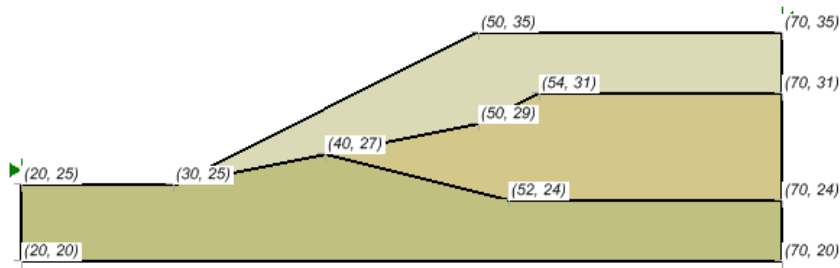
Figure 7 Non-Homogeneous Slope: Geometry

Table 5 Non-Homogeneous Slope: Material Properties

	c (kN/m²)	φ (degrees)	γ (kN/m³)
Soil #1	0.0	38.0	19.5
Soil #2	5.3	23.0	19.5
Soil #3	7.2	20.0	19.5

2.3.2 Results and Discussions

The results of the factor of safety calculations are shown in the following table and figures. The Factor of Safety published by the ACADS study was 1.39.

Table 6 Non-homogeneous Slope: Results

Method	Factor of Safety	
	Moment	Force
Bishop	1.414	
Janbu		1.319
Morgenstern-Price	1.382	1.382
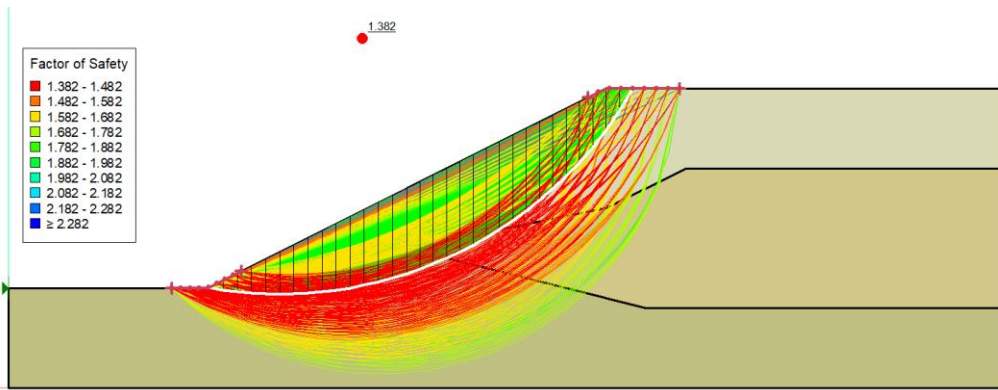
Figure 8 Non-homogeneous Slope: Critical Slip Surface
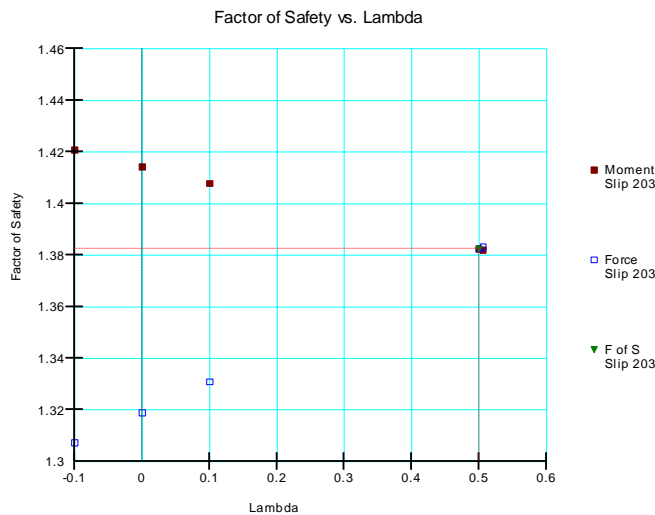
Figure 9 Non-homogeneous Slope: Factor of Safety vs Lambda.

2.4 ACADS Non-Homogenous with Seismic Load

Project File: ACADS Non-Homogeneous Slope.gsz

This model is identical to the previous model with the exception that a horizontal seismically induced acceleration of 0.15g was included in the analysis. The entry-exit search technique was used to locate the critical slip surface. No pore-water pressures are designated and therefore a total stress analysis is performed.

2.4.1 Geometry and Material Properties
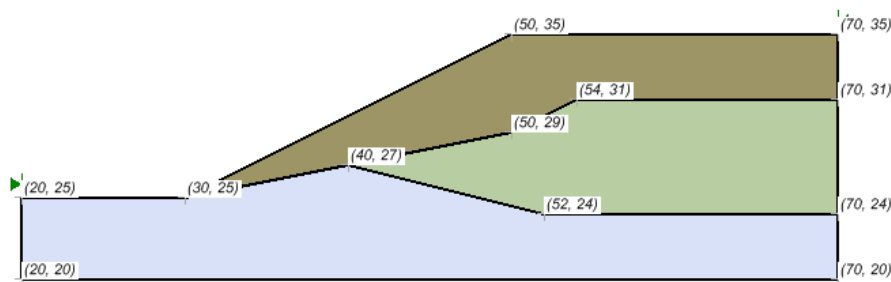
Figure 10 Non-Homogeneous Slope with Seismic Load: Geometry

Table 7 Non-Homogenous Slope with Seismic Load: Material Properties

	c kN/m²)	ϕ (degrees)	γ (kN/m³)
Soil #1	0.0	38.0	19.5
Soil #2	5.3	23.0	19.5
Soil #3	7.2	20.00	19.5

2.4.2 Results and Discussions

The results of the factor of safety calculations are shown in the following table and figures. The Factor of Safety published by the ACADS study was 1.00.

Table 8 Non-Homogenous Slope with Seismic Load: Results

Method	Factor of Safety	
	Moment	Force
Bishop	1.02	
Janbu		0.903
Morgenstern-Price	0.989	0.989
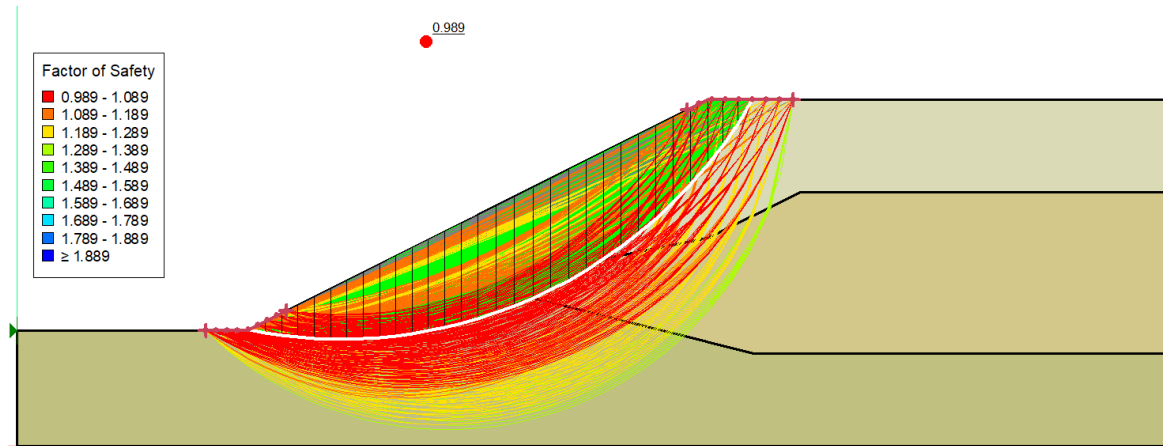
Figure 11 Non-Homogenous Slope with Seismic Load: Critical Slip Surface
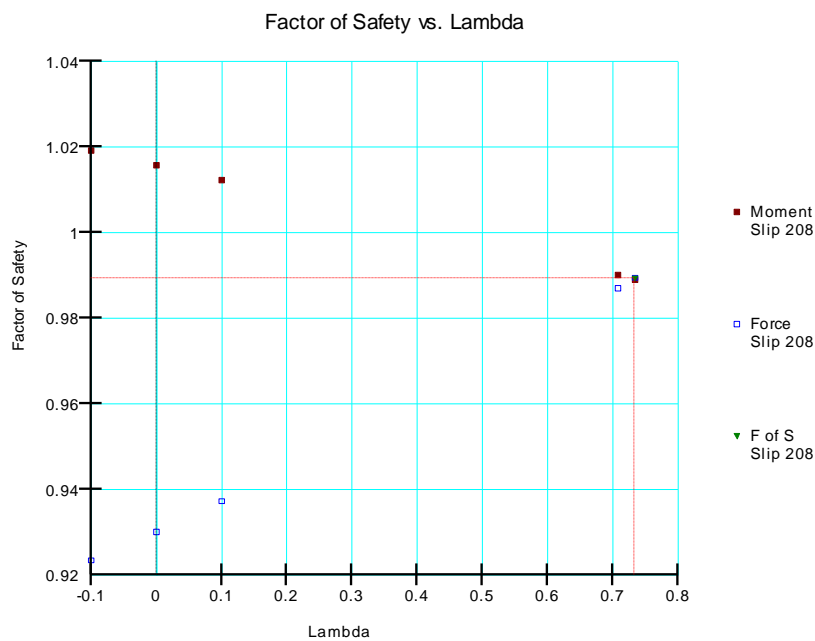
Figure 12 Non-homogenous Slope with Seismic Load: Factor of Safety vs Lambda.

2.5   ACADS Talbingo Dam – Dry

Project File: ACADS Talbingo Dam.gsz

This model is the Talbingo Dam (Giam and Donald, 1989) for the end-of-construction stage. The entry-exit search technique was used to locate the critical slip surface.

2.5.1 Geometry and Material Properties
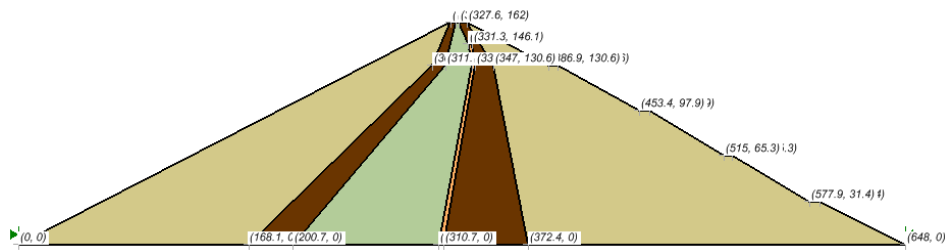
Figure 13 Talbingo Dam: Geometry

Table 9 Talbingo Dam: Material Properties

	c (kN/m²)	φ (degrees)	γ (kN/m³)
Rock fill	0	45	20.4
Transitions	0	45	20.4
Filter	0	45	20.4
Core	85	23	18.1

Table 10 Talbingo Dam: Geometry Data

Pt. #	Xc (m)	Yc (m)	Pt. #	Xc (m)	Yc (m)	Pt. #	Xc (m)	Yc (m)
1	0	0	10	515	65.3	19	307.1	0
2	315.5	162	11	521.1	65.3	20	331.3	130.6
3	319.5	162	12	577.9	31.4	21	328.8	146.1
4	321.6	162	13	585.1	31.4	22	310.7	0
5	327.6	162	14	648	0	23	333.7	130.6
6	386.9	130.6	15	168.1	0	24	331.3	146.1
7	394.1	130.6	16	302.2	130.6	25	372.4	0
8	453.4	97.9	17	200.7	0	26	347	130.6
9	460.6	97.9	18	311.9	130.6	-	-	-

2.5.2 Results and Discussions

The results of the factor of safety calculations are shown in the following table and figures. The Factor of Safety published by the ACADS study is (1.95)/1.90. The critical slip surface corresponds to the infinite slope case in which the slip surface is very shallow.

Table 11 Talbingo Dam: Results

Method	Factor of Safety	
	Moment	Force
Bishop	1.951	
Janbu		1.949
Morgenstern-Price	1.951	1.951

Color	Name	Slope Stability Material Model	Unit Weight (kN/m³)	Effective Cohesion (kPa)	Effective Friction Angle (°)	Phi-B (°)
	core	Mohr-Coulomb	18.1	85	23	0
	filter	Mohr-Coulomb	20.4	0	45	0
	rock fill	Mohr-Coulomb	20.4	0	45	0
	transition	Mohr-Coulomb	20.4	0	45	0
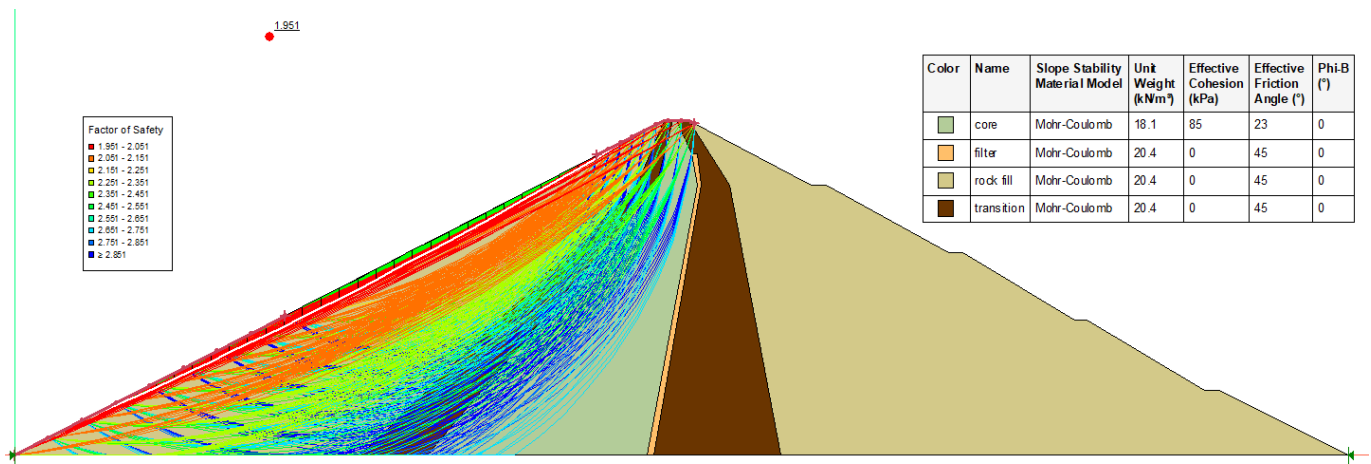
Figure 14 Talbingo Dam: Critical Slip Surface
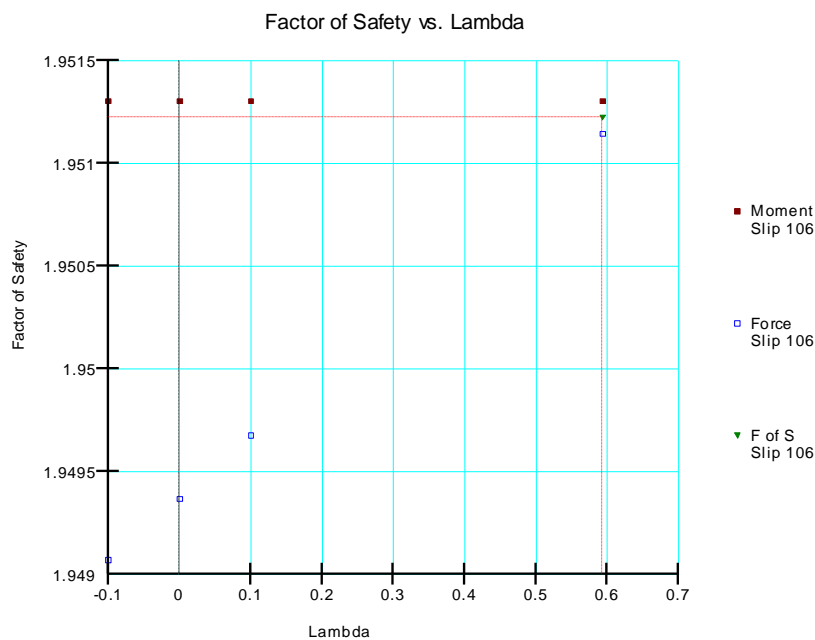
Figure 15 Talbingo Dam: Factor of Safety vs Lambda.

2.6   ACADS Talbingo Dam – Dry – Specified Slip Surface

Project File: ACADS Talbingo Dam.gsz

The model #6 is identical to model #5 with the exception is that a singular slip surface of known center and radius is analyzed in this problem.

9

2.6.1 Geometry and Material Properties
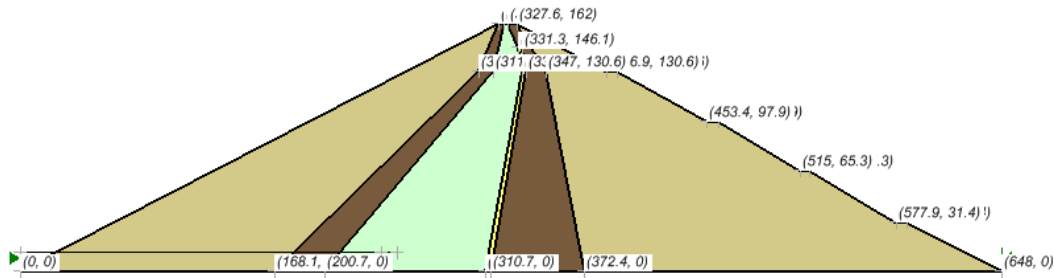
Figure 16 Talbingo Dam: Geometry

Table 12 Talbingo Dam - Specified: Slip Circle

Xc	Yc (m)	Radius (m)
100.3	291	278.8

Table 13 Talbingo Dam - Specified: Material Properties

	c (kN/m²)	φ (degrees)	γ (kN/m³)
Rock fill	0	45	20.4
Transitions	0	45	20.4
Filter	0	45	20.4
Core	85	23	18.1

2.6.2 Results and Discussions

The results of the factor of safety calculations are shown in the following table and figures. The Factor of Safety published by the ACADS study was 2.29.

Table 14 Talbingo Dam - Specified: Results

Method	Factor of Safety	
	Moment	Force
Bishop	2.207	
Janbu		1.949
Morgenstern-Price	2.299	2.299

2.299

Color	Name	Slope Stability Material Model	Unit Weight (kN/m³)	Effective Cohesion (kPa)	Effective Friction Angle (°)	Phi-B (°)
	core	Mohr-Coulomb	18.1	85	23	0
	filter	Mohr-Coulomb	20.4	0	45	0
	rock fill	Mohr-Coulomb	20.4	0	45	0
	transition	Mohr-Coulomb	20.4	0	45	0
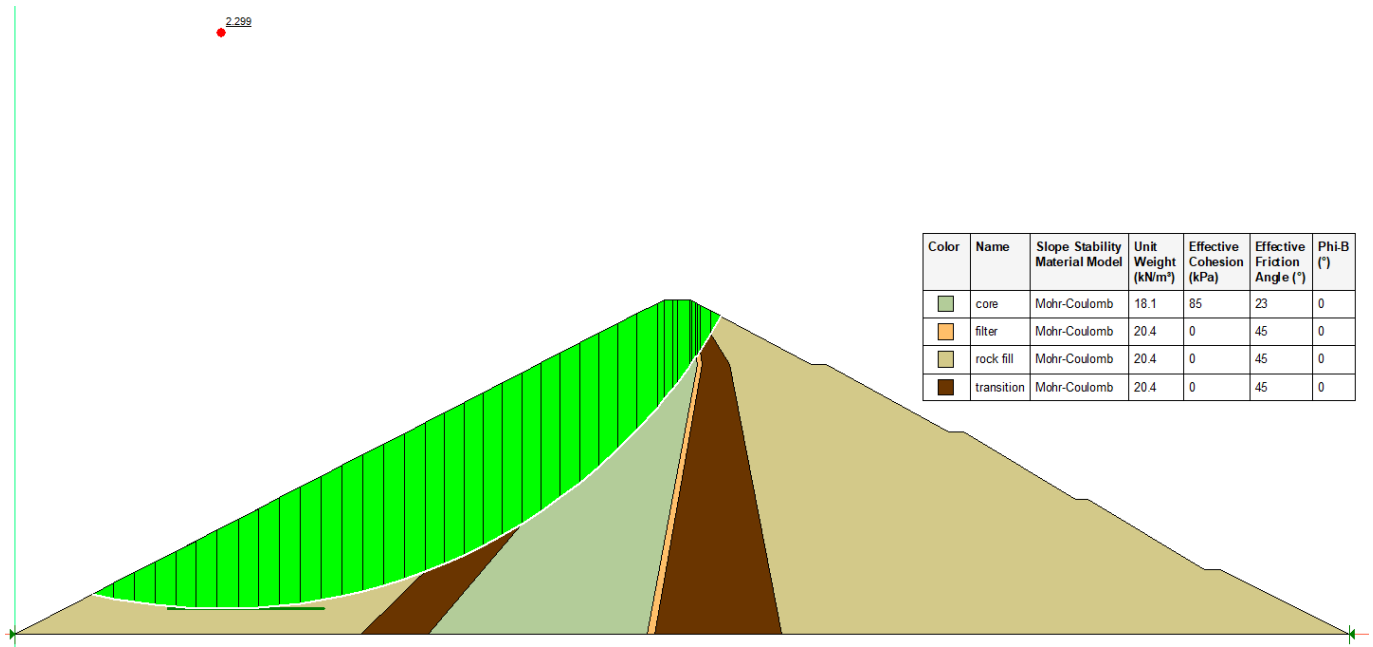
Figure 17 Talbingo Dam - Specified: Critical Slip Surface
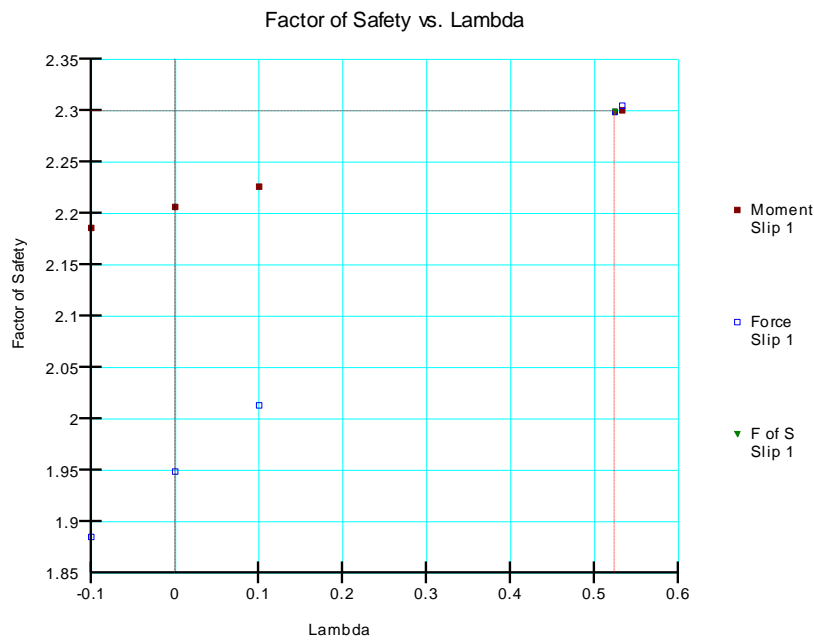
Figure 18 Talbingo Dam - Specified: Factor of Safety vs Lambda.

2.7   ACADS Weak Layer

Project File: ACADS Weak Layer.gsz

This model illustrates the analysis of a slope containing a both a piezometric surface and a weak layer. The piezometric surface is assumed to coincide with the base of the weak layer. In this case, the effects of negative pore-water pressure above the water tables were ignored. The tension crack zone is also ignored in this model.

2.7.1   Geometry and Material Properties
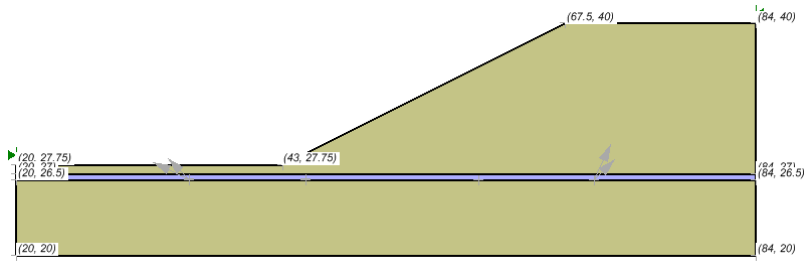
Figure 19 Weak Layer: Geometry

Table 15 Weak Layer: Material Properties

	c (kN/m²)	ϕ (degrees)	γ (kN/m³)
Soil #1	28.5	20.0	18.84
Soil #2	0	10.0	18.84

2.7.2   Results and Discussions

The results of the factor of safety calculations are shown in the following table and figures. The Factor of Safety published by the ACADS study was 1.26.

Table 16 Weak Layer: Results

Method	Factor of Safety	
	Moment	Force
Bishop	1.269	
Janbu		1.229
Morgenstern-Price	1.261	1.261

Color	Name	Slope Stability Material Model	Unit Weight (kN/m³)	Effective Cohesion (kPa)	Effective Friction Angle (°)	Phi-B (°)	Piezometric Surface
	soil_1	Mohr-Coulomb	18.84	28.5	20	0	1
	soil_2	Mohr-Coulomb	18.84	0	10	0	1
	soil_3	Bedrock (Impenetrable)					1

Figure 20 Weak Layer: Critical Slip Surface
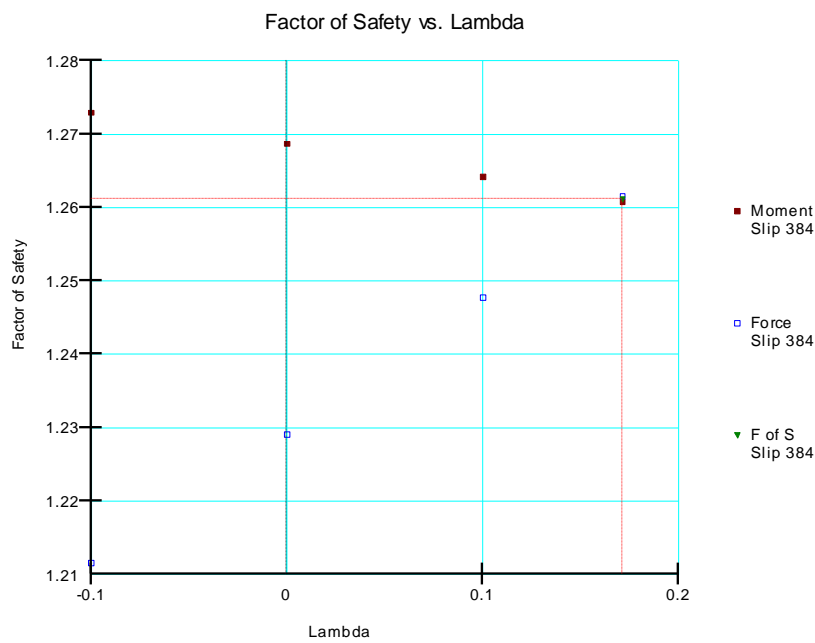
Figure 21 Weak Layer: Factor of Safety vs Lambda.

2.8   ACADS Weak Layer – Specified Slip Surface

Project File: ACADS Weak Layer.gsz

This problem is identical to preceding problem, except that the shape and location of the slip surface is fully specified.

2.8.1   Geometry and Material Properties

(67.5, 40)   (84, 40)

(20, 27.75)   (43, 27.75)
(20, 27)   (84, 27)
(20, 26.5)   (84, 26.5)

(20, 20)   (84, 20)
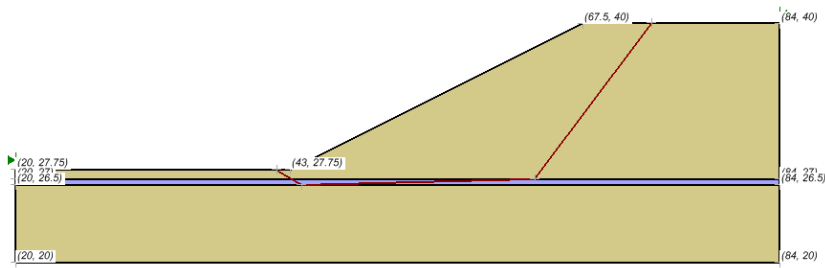
Figure 22 Weak Layer – Specified: Geometry

Table 17 Weak Layer: Failure Surface Coordinates

X (m)	Y (m)
41.85	27.75
44.00	26.50
63.50	27.00
73.31	40.00

Table 18 Weak Layer: Material Properties

	c (kN/m²)	ϕ (degrees)	γ (kN/m³)
Soil #1	28.5	20.0	18.84
Soil #2	0	10.0	18.84

2.8.2   Results and Discussions

The Factor of Safety published by the ACADS study was 1.34.

Table 19 Weak Layer - Specified: Results

Method	Factor of Safety	
	Moment	Force
Bishop	1.259	
Janbu		1.197
Morgenstern-Price	1.261	1.261

Color	Name	Slope Stability Material Model	Unit Weight (kN/m³)	Effective Cohesion (kPa)	Effective Friction Angle (°)	Phi-B (°)	Piezometric Surface
	soil_1	Mohr-Coulomb	18.84	28.5	20	0	1
	soil_2	Mohr-Coulomb	18.84	0	10	0	1
	soil_3	Bedrock (Impenetrable)					1

Figure 23 Weak Layer - Specified: Critical Slip Surface
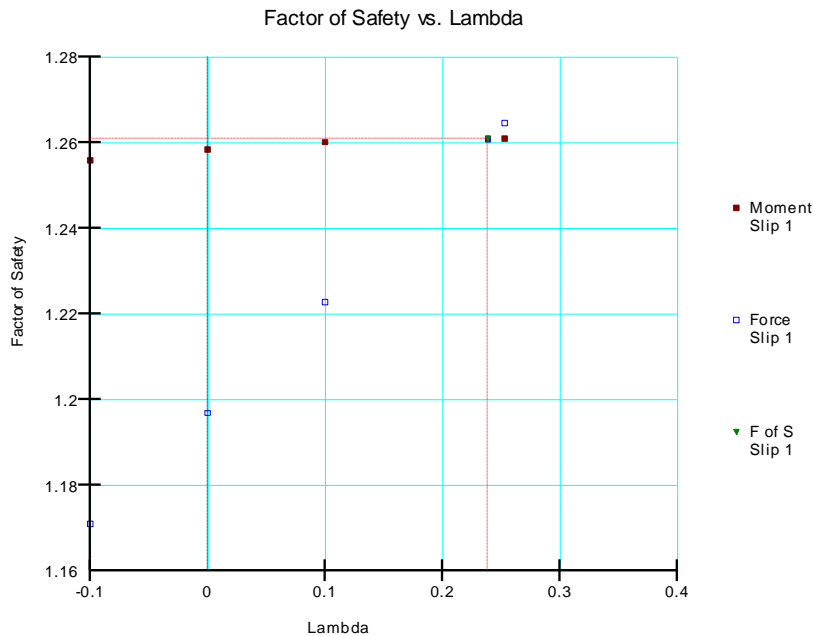
Figure 24 Weak Layer: Factor of Safety vs Lambda.

2.9   ACADS External Loading

Project File: ACADS External Load.gsz

This is a more complex example involving a weak layer, pore-water pressure and surcharge loads. The entry-exit search technique was used to locate the critical slip surface. The ACADS verification program received a wide range of answers for this problem.

2.9.1   Geometry and Material Properties

Table 20 External Loadings

X (m)	Y (m)	Normal Stress (kN/m^2)
23.00	27.75	20.00
43.00	27.75	20.00
70.00	40.00	20.00
80.00	40.00	40.00

Table 21 Data for Piezometric Surface

Pt. #	Xc (m)	Yc (m)
1	20.0	27.75
2	43.0	27.75
3	49.0	29.8
4	60.0	34.0
5	66.0	35.8
6	74.0	37.6
7	80.0	38.4
8	84.0	38.4
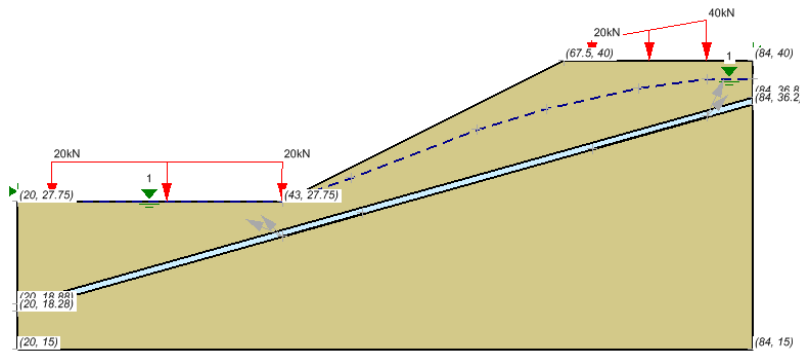
Figure 25 Geometry of the External Loading, Pore-Pressure defined by Water Table model

Table 22 Material Properties of the External Loading

	c (kN/m²)	φ (degrees)	γ (kN/m³)
Soil #1	28.5	20.0	18.84
Soil #2	0	10.0	18.84

2.9.2   Results and Discussions

The results of the factor of safety calculations are shown in the following table and figures. The Factor of Safety published by the ACADS study was 0.6878.

Table 23 Non-Homogenous Slope with Seismic Load: Results

Method	Factor of Safety	
	Moment	Force
Bishop	0.699	
Janbu		0.671
Morgenstern-Price	0.689	0.689

Color	Name	Slope Stability Material Model	Unit Weight (kN/m³)	Effective Cohesion (kPa)	Effective Friction Angle (°)	Phi-B (°)	Piezometric Surface
	soil_1	Mohr-Coulomb	18.84	28.5	20	0	1
	soil_2	Mohr-Coulomb	18.84	0	10	0	1
	soil_3	Bedrock (Impenetrable)					1

Figure 26 External Loading: Critical Slip Surface
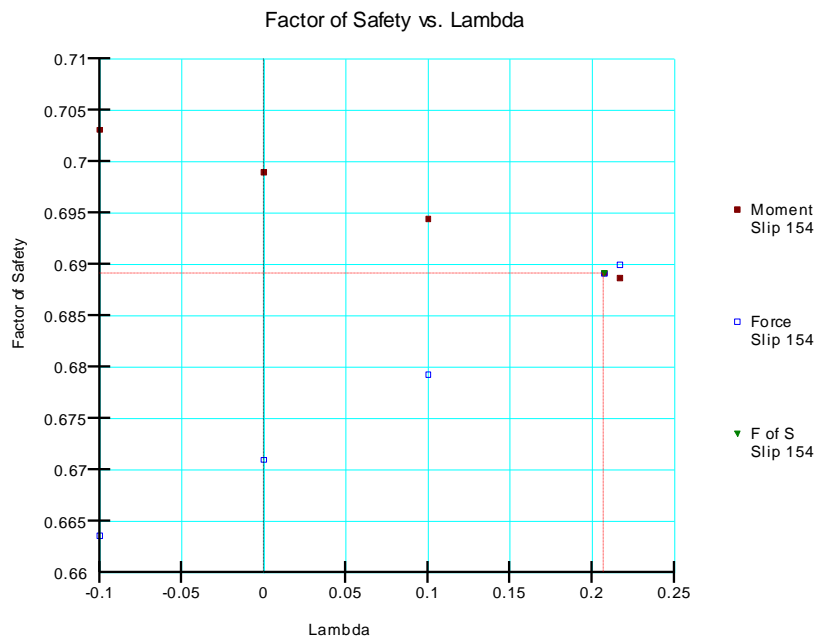
Figure 27 External Loading: Factor of Safety vs Lambda.

2.10   Lanester Embankment Verification

Project File: Lanester Embankment.gsz

17

This problem is the Lanester embankment (in France) which was built and induced to failure for testing and research purposes in 1969 (Pilot et al, 1982). A dry tension crack zone is assumed to spread over the entire modeled embankment.

2.10.1 Geometry and Material Properties

The pore-water pressures are derived from Table data, from raw data presented for this model, and interpolated across the model domain using the linear interpolation method. The location of the critical slip surface and the corresponding factor of safety are required for this model.
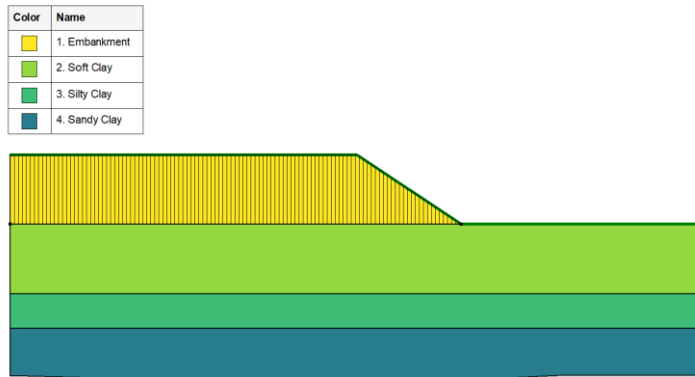
Figure 28 Geometry of the Lanester Embankment model

Table 24 Material Properties of the Lanester Embankment

	c (kN/m²)	ϕ (degrees)	γ (kN/m³)
Embankment	30	31.0	18.2
Soft Clay	4	37.0	14.0
Silty Clay	7.5	33.0	13.2
Sandy Clay	8.5	35.0	13.7

Table 25 Water Pressure Points

Pt. #	Xc (m)	Yc (m)	U kPa	Pt. .#	Xc (m)	Yc (m)	u (kPa)	Pt. #	Xc (m)	Yc (m)	u (kPa)
1	26.5	9	20	9	16	8.5	60	17	31.5	3	80
2	31.5	8.5	20	10	21	8.2	60	18	10.5	6	100
3	10.5	9.3	40	11	26.5	6	60	19	16	5	100
4	16	9.3	40	12	31.5	5	60	20	21	4.5	100
5	21	9.3	40	13	10.5	7.5	80	21	26	2.5	100
6	26.5	7.5	40	14	16	7.5	80	22	31.5	1.3	100
7	31.5	6.8	40	15	21	5.6	80	23	-	-	-
8	10.5	8.5	60	16	26	4.2	80	24	-	-	-

2.10.2 Results and Discussions

Pilot et al. (1982) reported a factor of safety of 1.13, which is close agreement with that presented in

Table 26.

Table 26 Results of the Lanester Embankment model

Method	Factor of Safety	
	Moment	Force
Morgenstern-Price	1.029	1.028
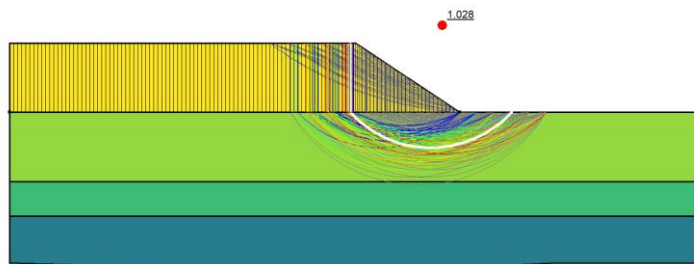
Figure 29 All slip surfaces of the Lanester Embankment model
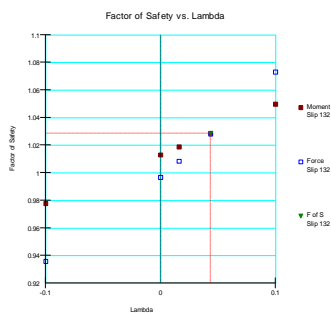
Figure 30 Factor of Safety versus Lambda (Critical Slip Surface)

2.11   Arai And Tagyo Homogeneous Slope

Project File: Arai and Tagyo - Homogeneous slope.gsz

Arai and Tagyo (1985) presented simple homogeneous soil slope with zero pore-water pressure. This model represents analysis of this particular problem and the results are provided in Table 28.

2.11.1   Geometry and Material Properties

There are no pore-water pressures input for this problem. The position of the critical slip surface, as well the calculated factor of safety is required in this analysis.
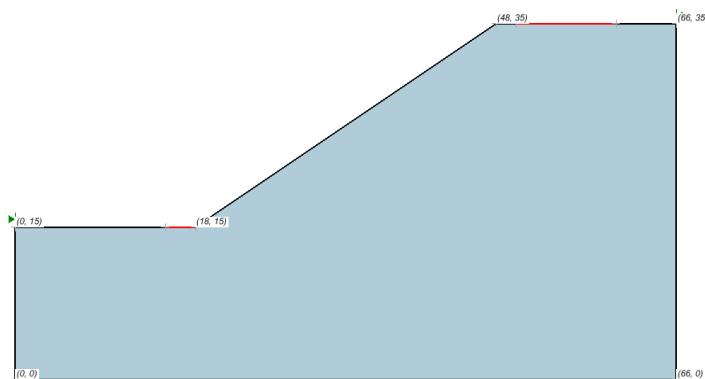
Figure 31 Geometry of the Arai and Tagyo - Homogeneous Slope Circular model

	c (kN/m²)	ϕ (degrees)	γ (kN/m³)
Soil	41.65	15.0	18.82

2.11.2   Results and Discussions

The results of the factor of safety calculations are shown in the following table and figures. The Factor of Safety published by Arai and Tagyo was 1.451.

Table 28. Arai and Tagyo – Homogeneous slope Results

Method	Factor of Safety	
	Moment	Force
Bishop	1.417	
Janbu		1.353
Morgenstern-Price	1.414	1.414

Figure 32 Arai and Tagyo – Homogeneous slope – Failure surface using the Morgenstern-Price method
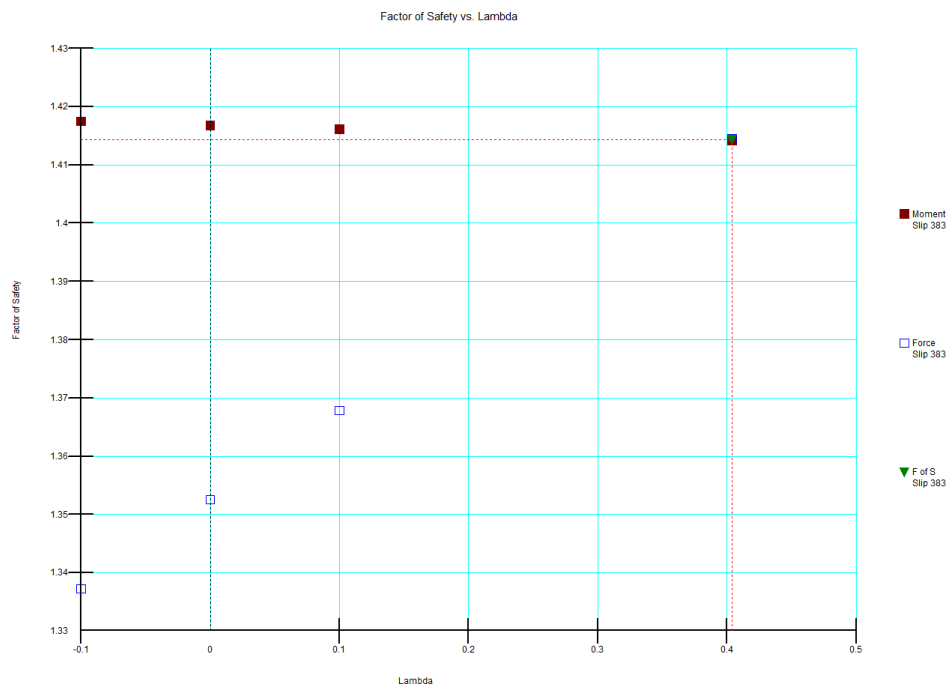
Figure 33 Arai and Tagyo – Homogeneous slope – Factor of safety vs Lambda

2.12   Arai And Tagyo Pore-Water Pressure Slope

Project File: Arai and Tagyo - Pore water pressure slope.gsz

This example 3 is from Arai and Tagyo, (1985). The model is a simple homogeneous soil slope with pore-water pressures.

2.12.1   Geometry and Material Properties

The model contains a high water table with a daylight facing water table existing along the slope. The location of the water table is shown in the below Figure 34.
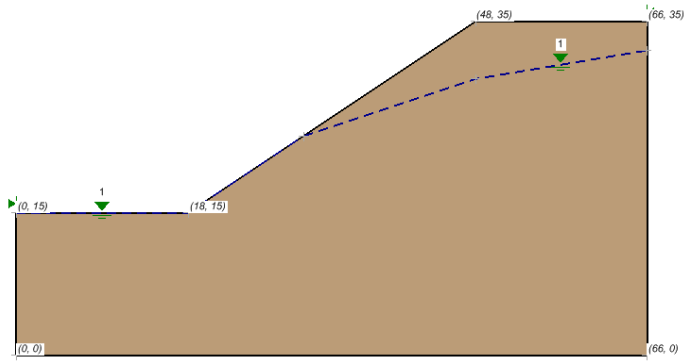
Figure 34 Geometry of the Arai and Tagyo Pore-Water Pressure Slope model

The pore-water pressures are calculated assuming hydrostatic conditions. Specific the pore-water pressures at point below the water table are calculated from the vertical distance to the water table and multiplying by the unit weight of water.

It is assumed that there is no effect of suction above the water table. The location of the vertical slip surface and the value of the factor of safety were required for this analysis.

Table 29 Material Properties of the Arai and Tagyo Pore-Water Pressure Slope model

	c (kN/m²)	φ (degrees)	γ (kN/m³)
Soil	41.65	15.0	18.82

2.12.2 Results and Discussions

The results of the factor of safety calculations are shown in the following table and figures. The Factor of Safety published by Arai and Tagyo was 1.138.

Table 30. Arai and Tagyo Results

Method	Factor of Safety	
	Moment	Force
Bishop	1.190	
Janbu		1.100
Morgenstern-Price	1.188	1.188

Color	Name	Slope Stability Material Model	Unit Weight (kN/m³)	Effective Cohesion (kPa)	Effective Friction Angle (°)	Phi-B (°)	Piezometric Surface
	Soil	Mohr-Coulomb	18.82	41.65	15	0	1
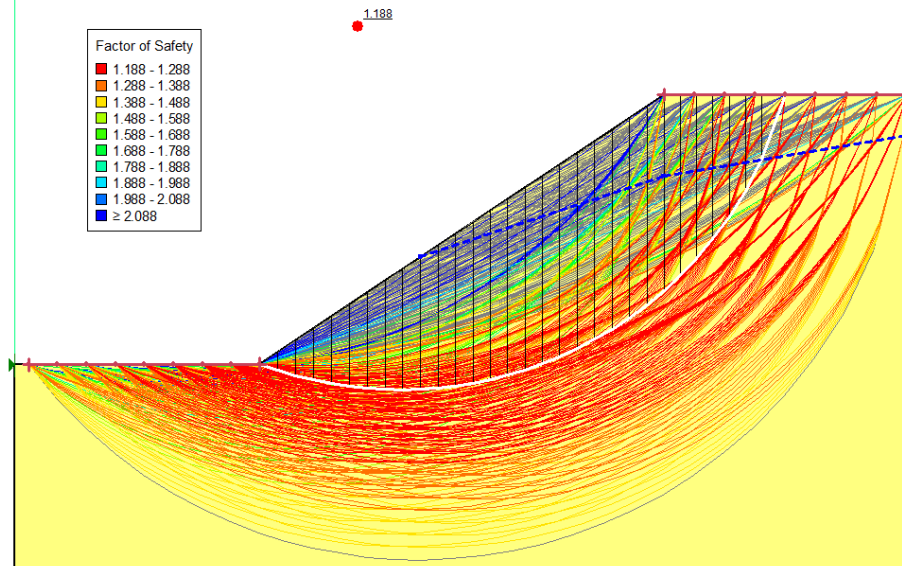
Figure 35 Arai and Tagyo – Pore water pressure slope – Failure surface using the Morgenstern-Price method
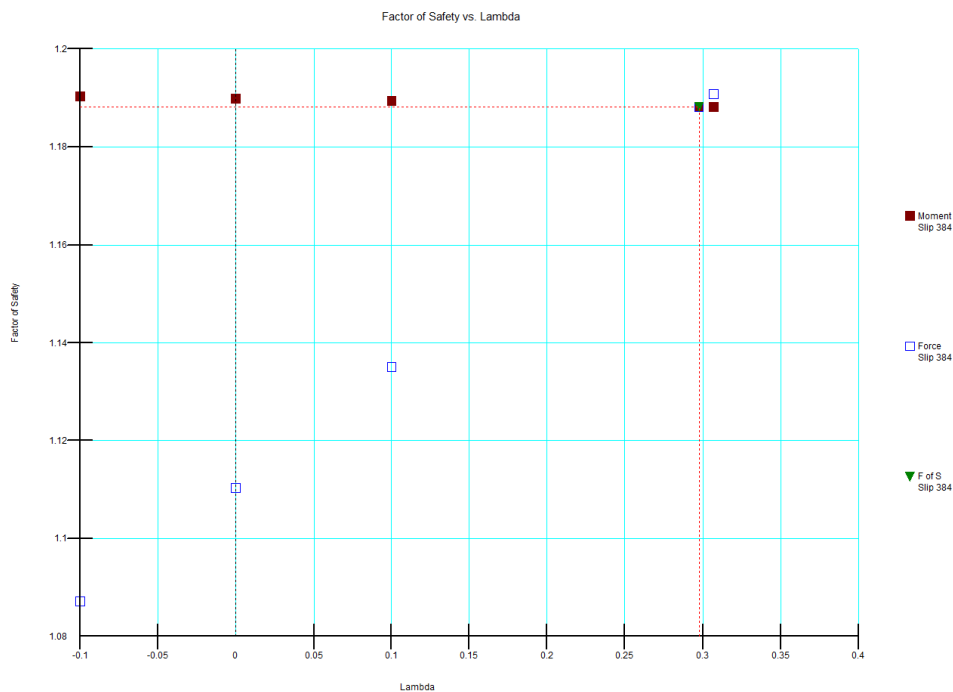
Figure 36 Arai and Tagyo – Pore water pressure slope – Factor of safety vs Lambda

2.13   Greco Layered Slope

Project File: Greco Layered Slope.gsz

This model was taken from Greco, 1996, Example # 4. It consists of a layered slope without pore-water pressures. It was originally published by Yamagami and Ueta (1988).

2.13.1 Geometry and Material Properties
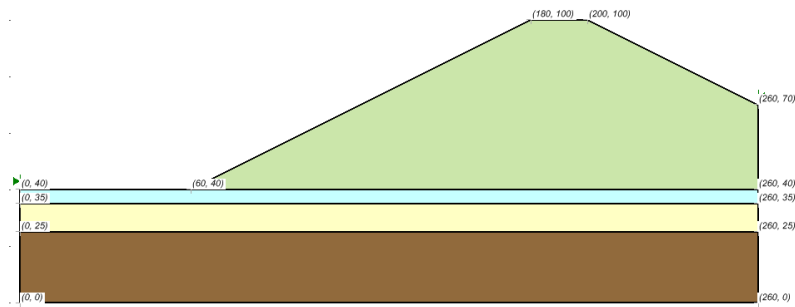
Figure 37 Geometry of the Greco Layered Structure model

Table 31 Material Properties of the Greco Layered Structure model

	c (kN/m²)	ϕ (degrees)	γ (kN/m³)
Upper Layer	49	29.0	20.38
Layer 2	0	30.0	17.64
Layer 3	7.84	20.0	20.38
Bottom Layer	0	30.0	17.64

2.13.2 Results and Discussions

The Factor of Safety published by Greco (1996) was 1.40-1.42.

Table 32 FOS Results using the entry and exit method

Method	Factor of Safety	
	Moment	Force
Bishop	1.412	
Janbu		1.275
Morgenstern-Price	1.389	1.389

Color	Name	Slope Stability Material Model	Unit Weight (kN/m³)	Effective Cohesion (kPa)	Effective Friction Angle (°)	Phi-B (°)
	1. Upper Layer	Mohr-Coulomb	20.38	49	29	0
	2. Layer 2	Mohr-Coulomb	17.64	0	30	0
	3. Layer 3	Mohr-Coulomb	20.38	7.84	20	0
	4. Bottom Layer	Mohr-Coulomb	17.64	0	30	0
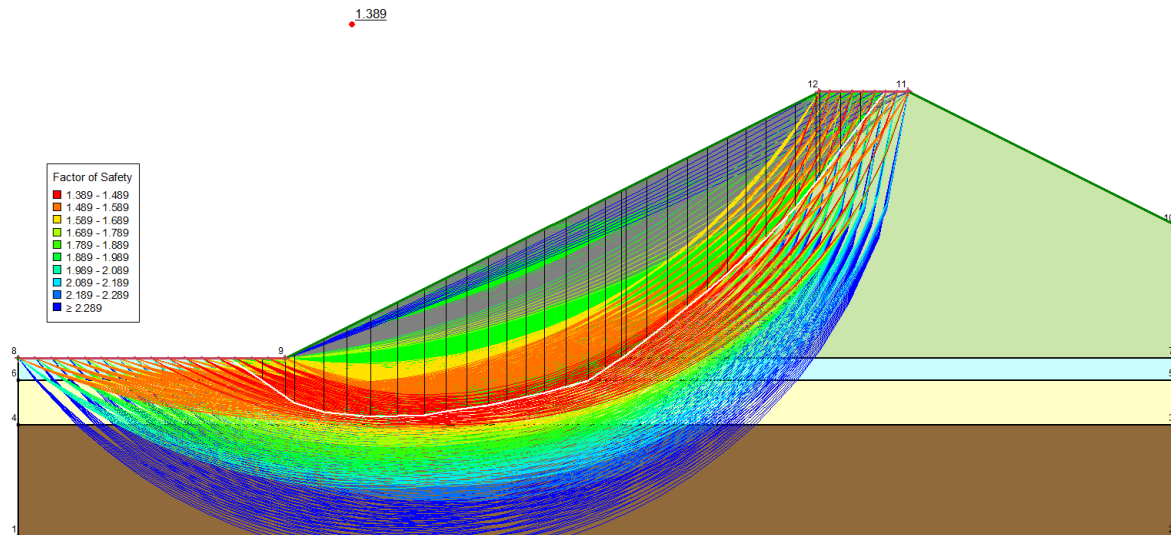
Figure 38 Greco layered slope: Critical Slip Surface
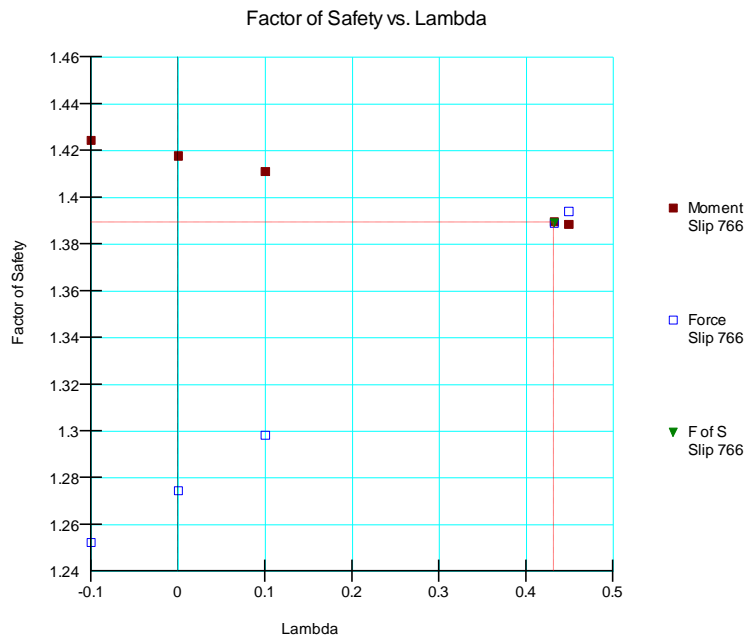
Figure 39 Greco layered slope: Factor of Safety vs Lambda.

2.14   Greco Weak Layer Slope

Project File: Greco Weak Layer Slope.gsz

This model is taken from Greco's paper (1986) (Example #5). The model was originally published by Chen and Shao (1988). It consists of a layered slope with pore-water pressures and designated by a phreatic line.

2.14.1   Geometry and Material Properties
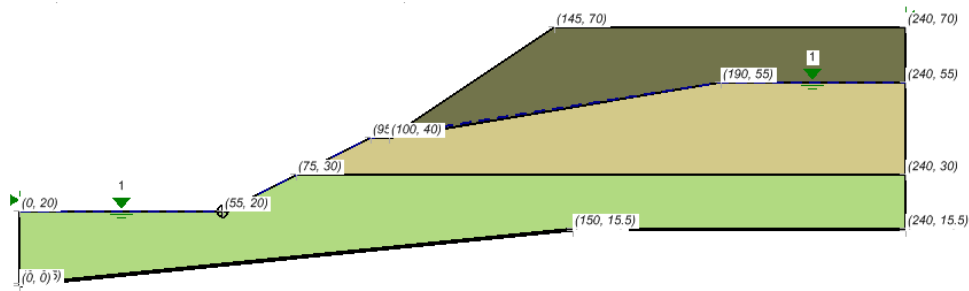
Figure 40 Geometry of the Greco Weak Layer Slope model

Table 33 Material Properties of the Greco Weak Layer Slope model

	c (kN/m²)	φ (degrees)	γ (kN/m³)
Layer 1	9.8	35.0	20.0
Layer 2	58.8	25.0	19.0
Layer 3	19.8	30.0	21.5
Layer 4	9.8	16.0	21.5

2.14.2   Results and Discussions

The Factor of Safety published by Greco (1996) was 1.08.

Table 34 FOS Results using the entry and exit method

Method	Factor of Safety	
	Moment	Force
Bishop	1.040	
Janbu		0.896
Spencer	1.054	1.054

Color	Name	Slope Stability Material Model	Unit Weight (kN/m³)	Effective Cohesion (kPa)	Effective Friction Angle (°)	Phi-B (°)	Piezometric Surface
	Layer 1	Mohr-Coulomb	20	9.8	35	0	1
	Layer 2	Mohr-Coulomb	19	58.8	25	0	1
	Layer 3	Mohr-Coulomb	21.5	19.8	30	0	1
	Layer 4	Mohr-Coulomb	21.5	9.8	16	0	1
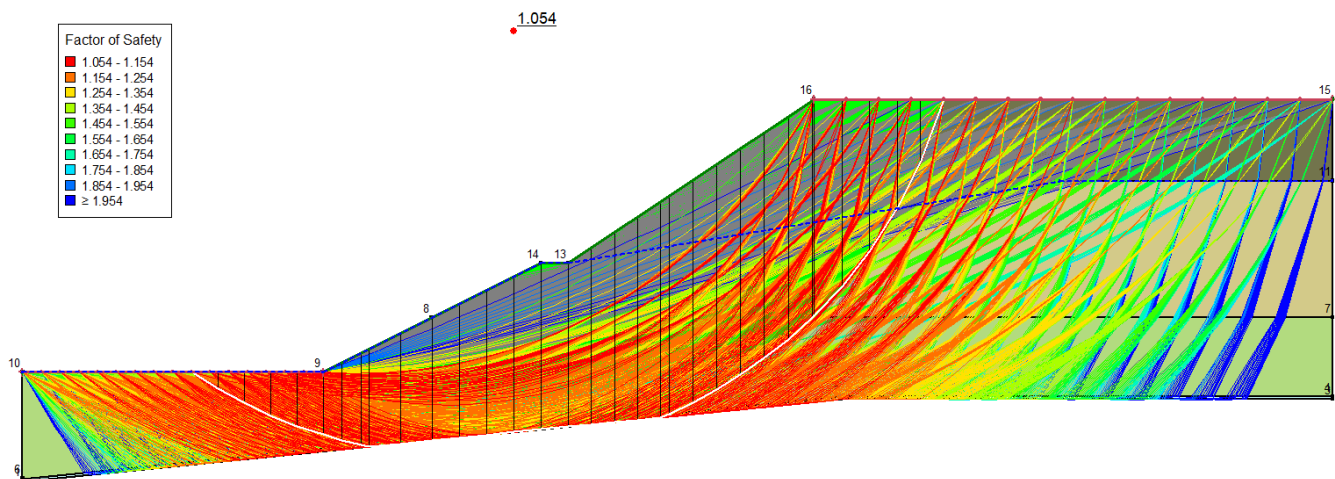
Figure 41 Greco layered slope: Critical Slip Surface

Factor of Safety vs. Lambda
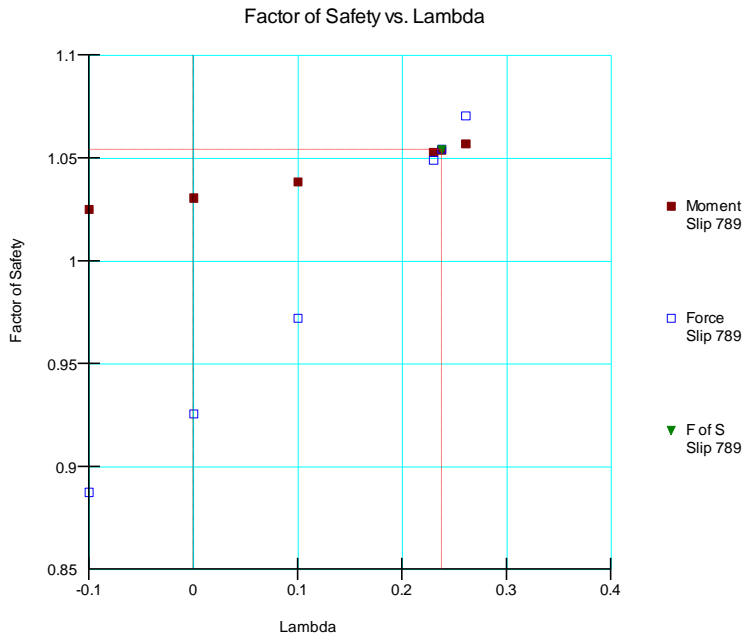
Figure 42 Greco layered slope: Factor of Safety vs Lambda.

2.15   Chen and Shao Frictionless Slope

Project File: Chen and Shao Frictionless Slope.gsz

Chen and Shao (1988) presented the problem to illustrate a plasticity solution for a weightless frictionless slope subjected to a vertical load. This problem was first solved by Prandtl (1921).

2.15.1   Geometry and Material Properties

The critical load position for the critical slip surface was defined by Prandtl and is shown in Figure 43. The critical failure surface has a theoretical factor of safety of 1.0.

The critical uniformly distributed load for failure is presented in the paper as 149.31 kN/m, with a length equal to the slope height of 10m.

NOTE:

 A "custom" interslice shear force function was used with GLE and Morgenstern-Price methods as shown in Chen and Shao (1988).

Table 35 Input data for Chen and Shao Frictionless Slope model

x	F(x)
0	1
0.3	1
0.6	0
1	0
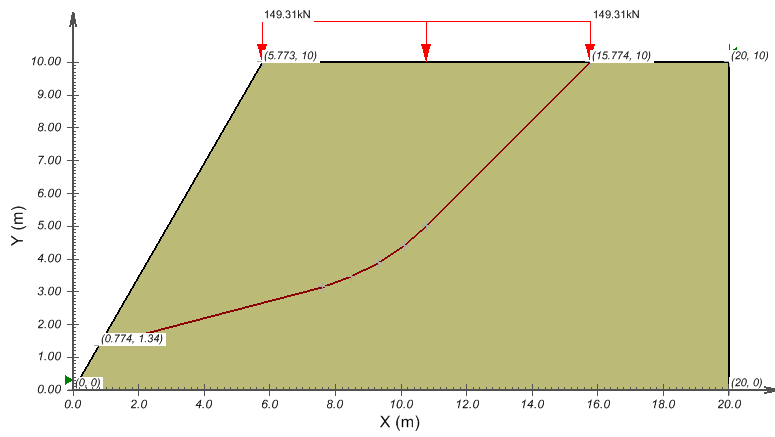
Figure 43 Geometry of the Chen and Shao Frictionless Slope model

Table 36 Material Properties of the Chen and Shao Frictionless Slope model

	c (kN/m²)	φ' (degrees)	γ (kN/m³)
Soil	49	0.0	1e-06

2.15.2 Results and Discussions

Table 37 Results of the Chen and Shao Frictionless Slope

Method	Factor of Safety
M-P	1.017
Spencer	1.036

Color	Name	Slope Stability Material Model	Unit Weight (kN/m³)	Effective Cohesion (kPa)	Effective Friction Angle (°)
	Soil	Mohr-Coulomb	1e-06	49	0
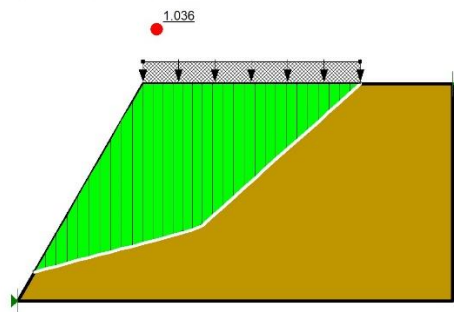
Figure 44 Chen and Shao Frictionless slope: Fully defined slip surface

28
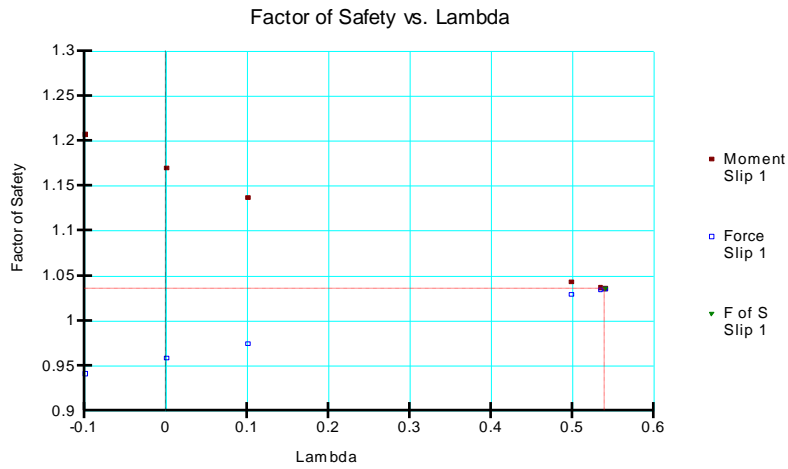
Figure 45 Chen and Shao Frictionless slope: Factor of Safety vs Lambda.

2.16   Prandtl Bearing Capacity

Project File: Prandtl Bearing Capacity.gsz

This verification test models the well-known Prandtl solution for bearing capacity on a purely cohesive soil:

$$q_c = cN_c = c(\pi + 2)$$

2.16.1   Geometry and Material Properties

The material properties are given in Table 38. For a cohesion of 20kN/m², q_c is calculated to be 102.83 kN/m. A uniformly distributed load of 102.83kN/m was applied over a width of 10m as shown in Figure 46.

Table 38 Material Properties of the Bearing Failure model

	c (kN/m²)	ϕ' (degrees)	γ (kN/m³)
Soil	20	0	1e-06
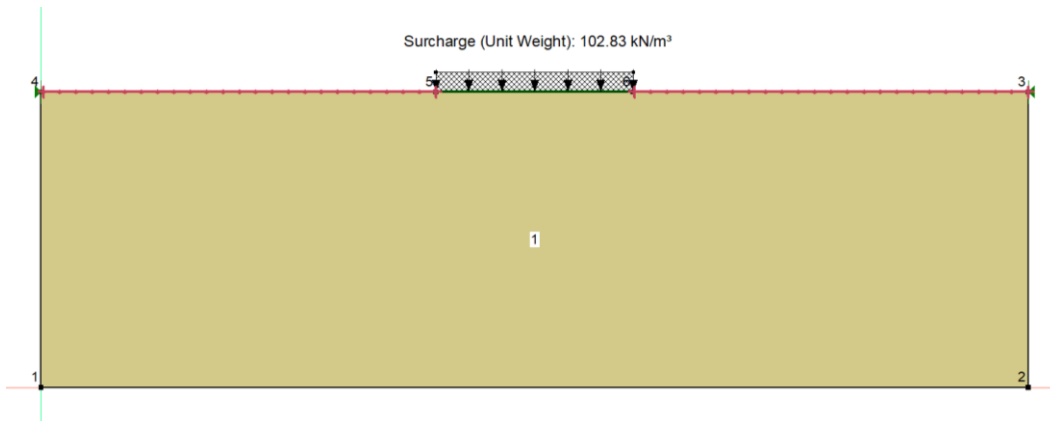
Figure 46 Geometry of the Bearing Capacity model

2.16.2   Results and Discussions

The theoretical Factor of Safety is 1.00.

Table 39 FOS Results for the Prandtl bearing capacity problem

Method	Factor of Safety (Entry and Exit)		Factor of Safety (Fully Specified)	
	Moment	Force	Moment	Force
Bishop	1.056		0.924	
Janbu		1.031		0.895
Morgenstern-Price	1.08	1.08	0.960	0.960

Color	Name	Slope Stability Material Model	Unit Weight (kN/m³)	Effective Cohesion (kPa)	Effective Friction Angle (°)	Phi-B (°)
	MC Material	Mohr-Coulomb	1e-06	20	0	0
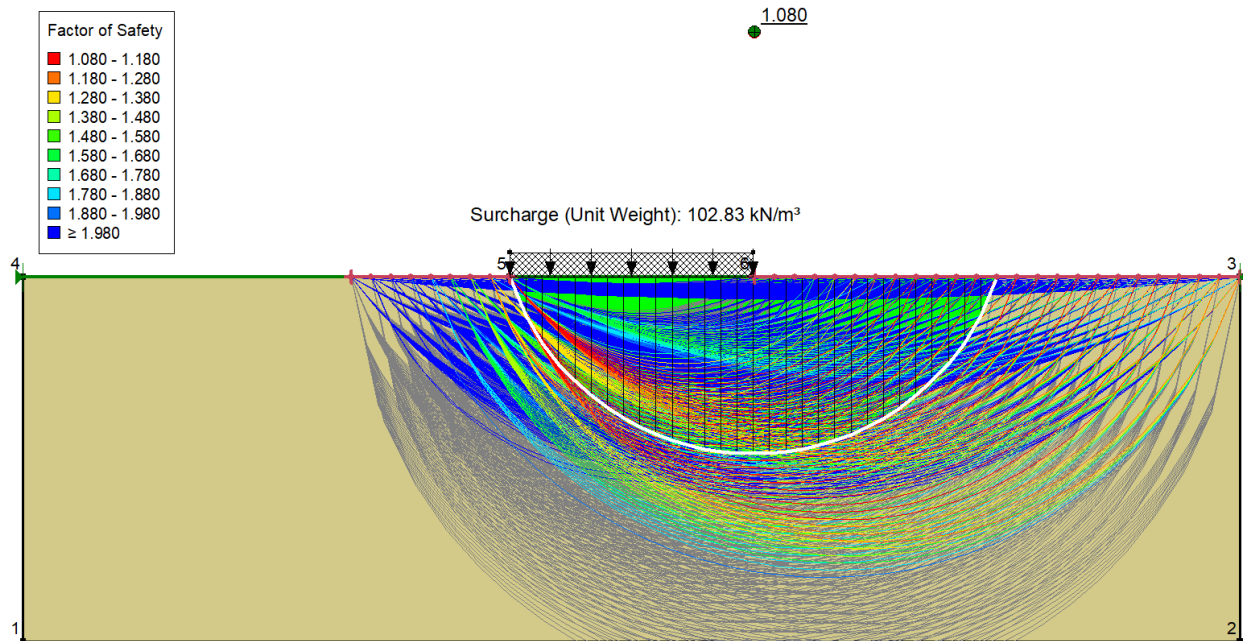
Figure 47 Presentation of the resulting factor of safety for the 'Entry and Exit' slip surface
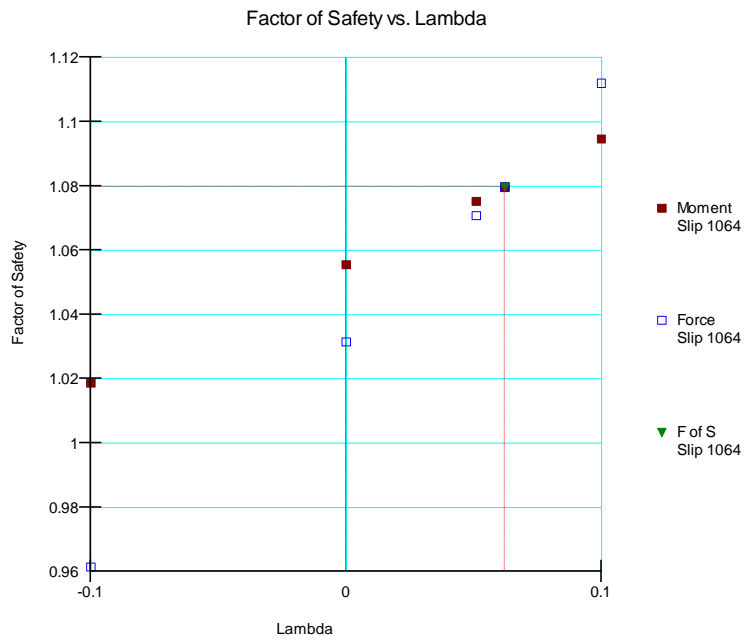
Figure 48 Factor of Safety vs Lambda: 'Entry and Exit' slip surface

Color	Name	Slope Stability Material Model	Unit Weight (kN/m³)	Effective Cohesion (kPa)	Effective Friction Angle (°)	Phi-B (°)
	MC Material	Mohr-Coulomb	1e-06	20	0	0

Figure 49 Presentation of the resulting factor of safety for the 'Fully Specified' slip surface

Factor of Safety vs. Lambda
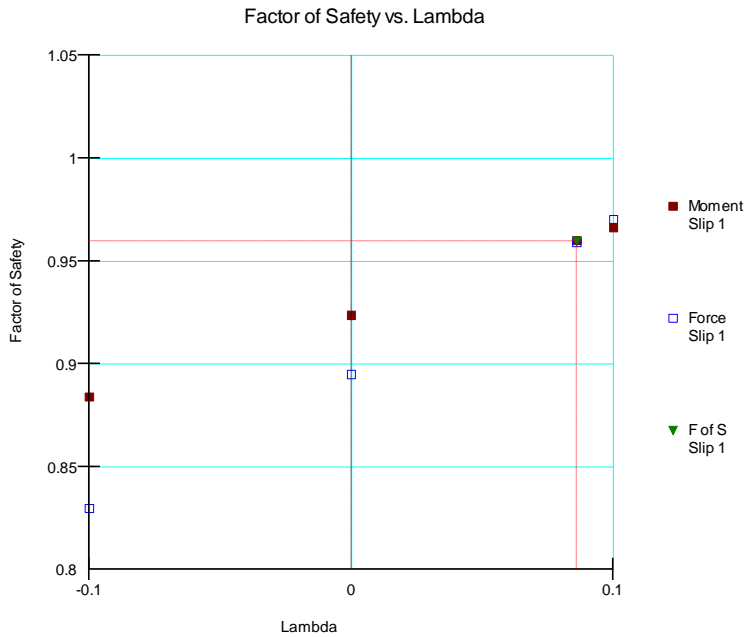
Figure 50 Factor of Safety vs Lambda: 'Fully Specified' slip surface

2.17   Chowdhury and Xu (1995)

Project File: Chowdhury and Xu statistic analysis.gsz

This set of verification problems were originally published by Chowdhury and Xu (1995). The Congress St. Cut model, which was first analyzed by Ireland (1954), contained the geometry for the first four examples. The purpose of these models is to perform a statistic analysis in which the probability of failure is calculated when the input parameters are represented in terms of means and standard deviations.

2.17.1   Geometry and Material Properties

In each of these examples 1 to 4, two sets of circular slip surfaces are considered. One set places the failure surface tangential to the lower boundary of Clay 2 layer and the second considers the slip surface tangential to the lower boundary of Clay 3. The soil models used for both clays are constant undrained shear strength.

NOTE:

Chowdhury and Xu do not consider the strength of the upper sand layer in the examples 1 to 4. As well, they use the Bishop Simplified method for all their analysis.

The unit weights for soil materials are not provided in the original paper by Chowdhury and Xu. Information also is not provided regarding the geometry of the critical slip surface.

In this example, material unit weights were selected to produce results that were similar to those published.
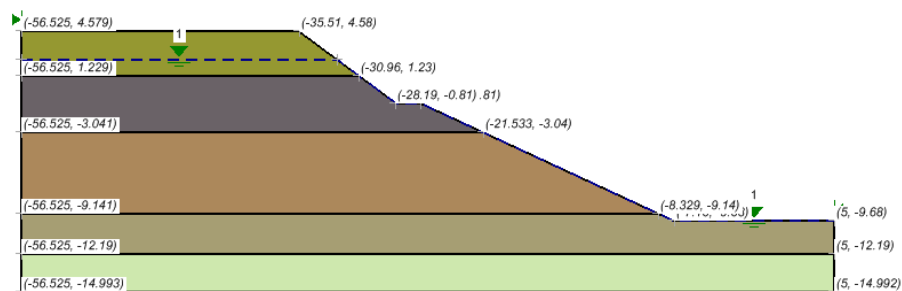
Figure 51 Geometry of the Chowdhury and Xu model

2.17.2 Example #1

Table 40 Example 1 Input Data

	Soil Layer		
	Clay 1	Clay 2	Clay 3
	c_1	c_2	c_3
Mean (kPa)	55	43	56
Stdv. (kPa)	20.4	8.2	13.2
γ (kN/m³)	21	22	22

Table 41 Results of Example 1 with Layer 2

The Factor of Safety published by Chowdhury & Xu is 1.128 based on Bishop method, and the Probability of Failure is 24.61%.

Method	Factor of Safety		PF(%)
	Moment	Force	
Morgenstern-Price	1.132	1.132	25.31

Figure 52 Factor of Safety vs Lambda, Example#1, Layer2

The Factor of Safety published by Chowdhury & Xu is 1.109 based on Bishop method, and the Probability of Failure is 27.39%.

Table 42 Results Example 1 with Layer 3

Method	Factor of Safety		PF(%)
	Moment	Force	
Morgenstern-Price	1.116	1.116	26.15
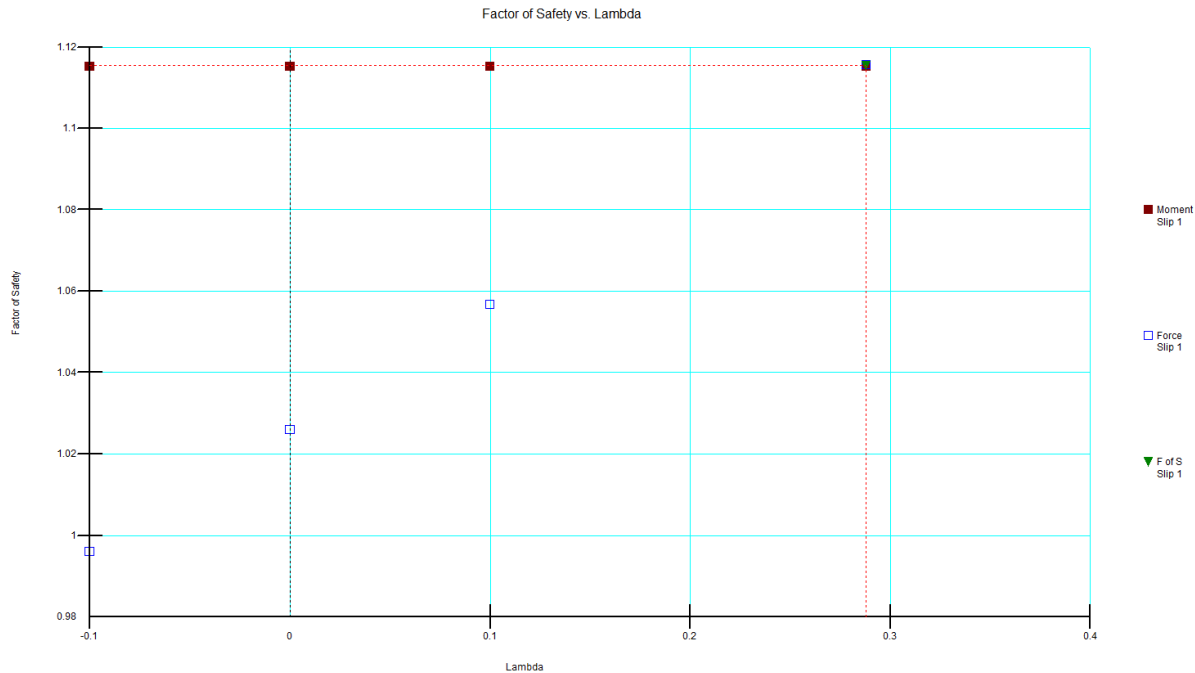
Figure 53 Factor of Safety vs Lambda, Example#1, Layer3

2.17.3 Example #2

Table 43 Example 2 Input Data

	Soil Layer		
	Clay 1	Clay 2	Clay 3
	c_1	c_2	c_3
Mean (kPa)	68.1	39.3	50.8
Standard Deviation (kPa)	6.6	1.4	1.5
γ (kN/m³)	21	22	22

The Factor of Safety published by Chowdhury & Xu is 1.109 based on Bishop method, and the Probability of Failure is 0.48%.

Table 44 Results of Example 2 with Layer 2

Method	Factor of Safety		PF(%)
	Moment	Force	
Morgenstern-Price	1.110	1.110	0.4

Figure 54 Factor of Safety vs Lambda, Example#2, Layer2

The Factor of Safety published by Chowdhury & Xu is 1.0639 based on Bishop method, and the Probability of Failure is 1.305%.

Table 45 Results of Example 2 with Layer 3

Method	Factor of Safety		PF(%)
	Moment	Force	
Morgenstern-Price	1.063	1.063	1.26
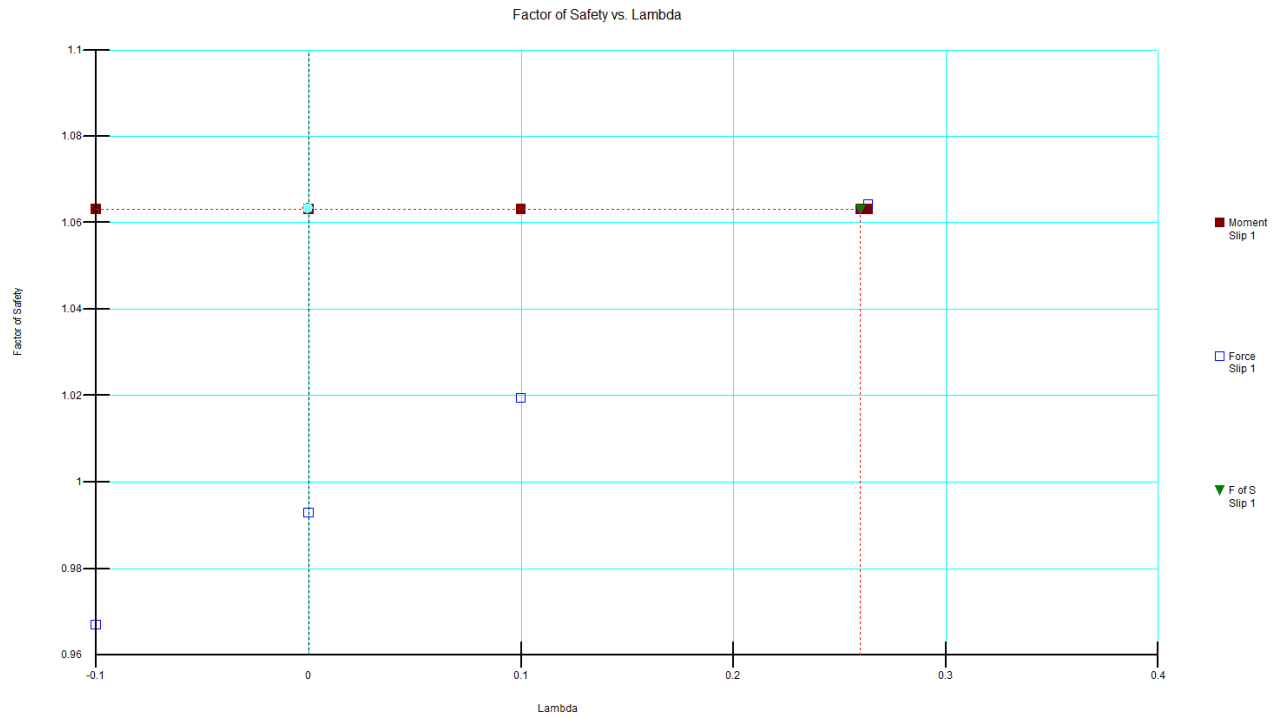
Figure 55 Factor of Safety vs Lambda, Example#2, Layer3

2.17.4 Example #3

Table 46 Example 3 Input Soil Data

	Soil Layer		
	Clay 1	Clay 2	Clay 3
	c_1	c_2	c_3
Mean (kPa)	136	80	102
Standard Deviation (kPa)	50	15	24
γ (kN/m³)	21	22	22

The Factor of Safety published by Chowdhury & Xu is 2.2343 based on Bishop method, and the Probability of Failure is 1.151%.

Table 47 Results of Example 3, Layer 2

Method	Factor of Safety		PF(%)
	Moment	Force	
Morgenstern-Price	2.248	2.248	0.04

36
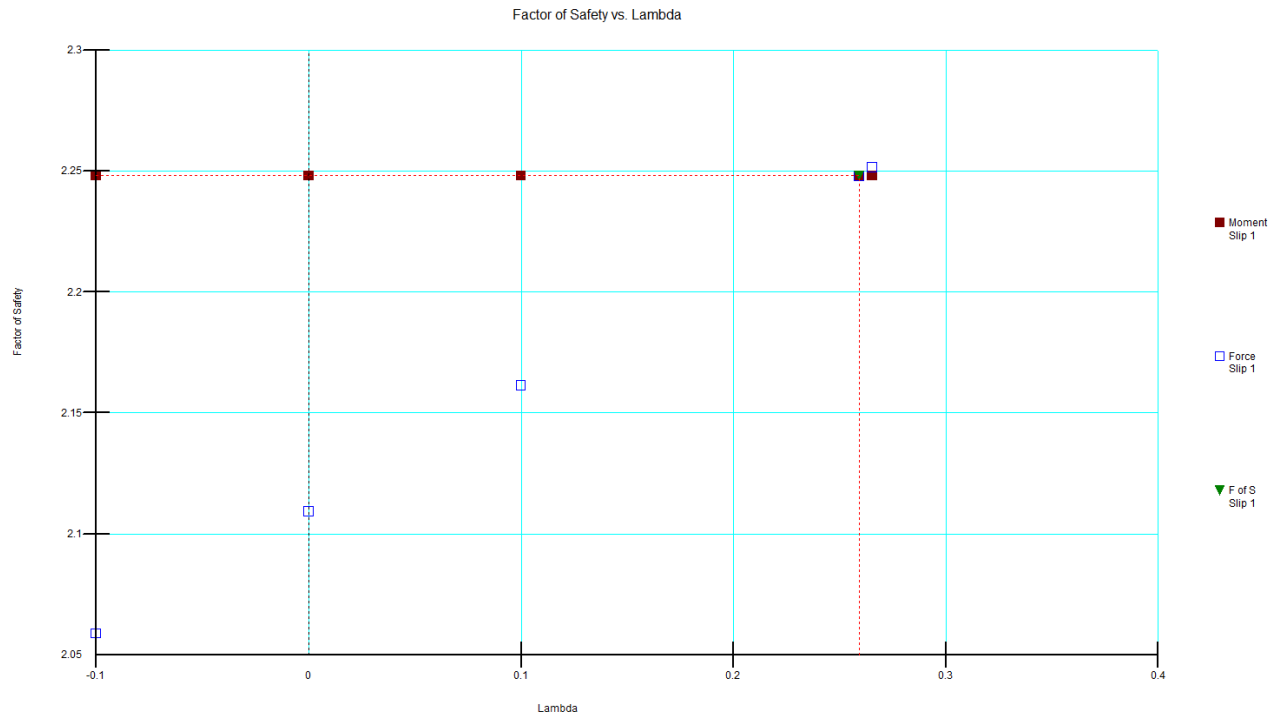
Figure 56 Factor of Safety vs Lambda, Example#3, Layer2

The Factor of Safety published by Chowdhury & Xu is 2.1396 based on Bishop method, and the Probability of Failure is 0.242%.

Table 48 Results of Example 3, Layer 3

Method	Factor of Safety		PF(%)
	Moment	Force	
Morgenstern-Price	2.138	2.138	0.02
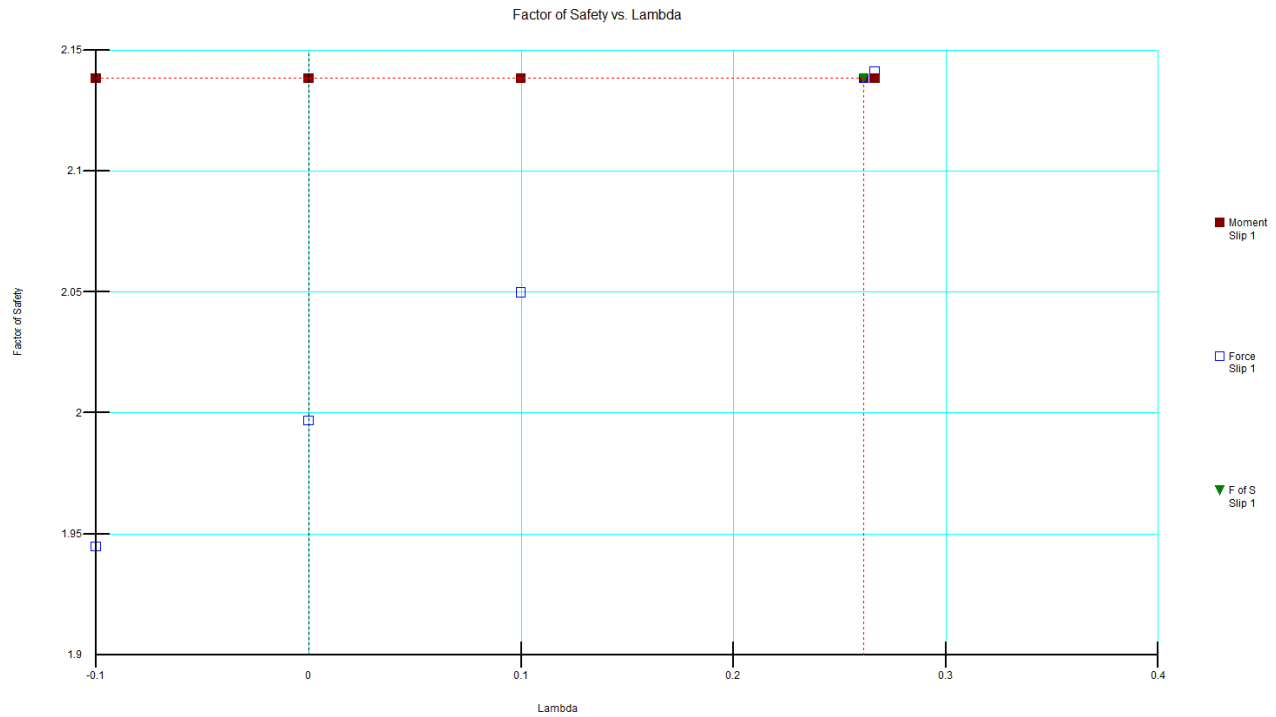
Figure 57 Factor of Safety vs Lambda, Example#3, Layer3

2.17.5 Example #4

Table 49 Example 4 Input Data

	Soil Layer					
	Clay 1		Clay 2		Clay 3	
	c_1 (kPa)	$\phi_1(^\circ)$	c_2 (kPa)	$\phi_2(^\circ)$	c_3 (kPa)	ϕ_3 $(^\circ)$
Mean (kPa)	55	5	43	7	56	8
Standard Deviation (kPa)	20.4	1	8.7	1.5	13.2	1.7
γ (kN/m₃)	17		22		22	

The Factor of Safety published by Chowdhury & Xu is 1.4239 based on Bishop method, and the Probability of Failure is 1.559%.

Table 50 Results of Example 4, Layer 2

Method	Factor of Safety		PF(%)
	Moment	Force	
Morgenstern-Price	1.422	1.422	2.36

38
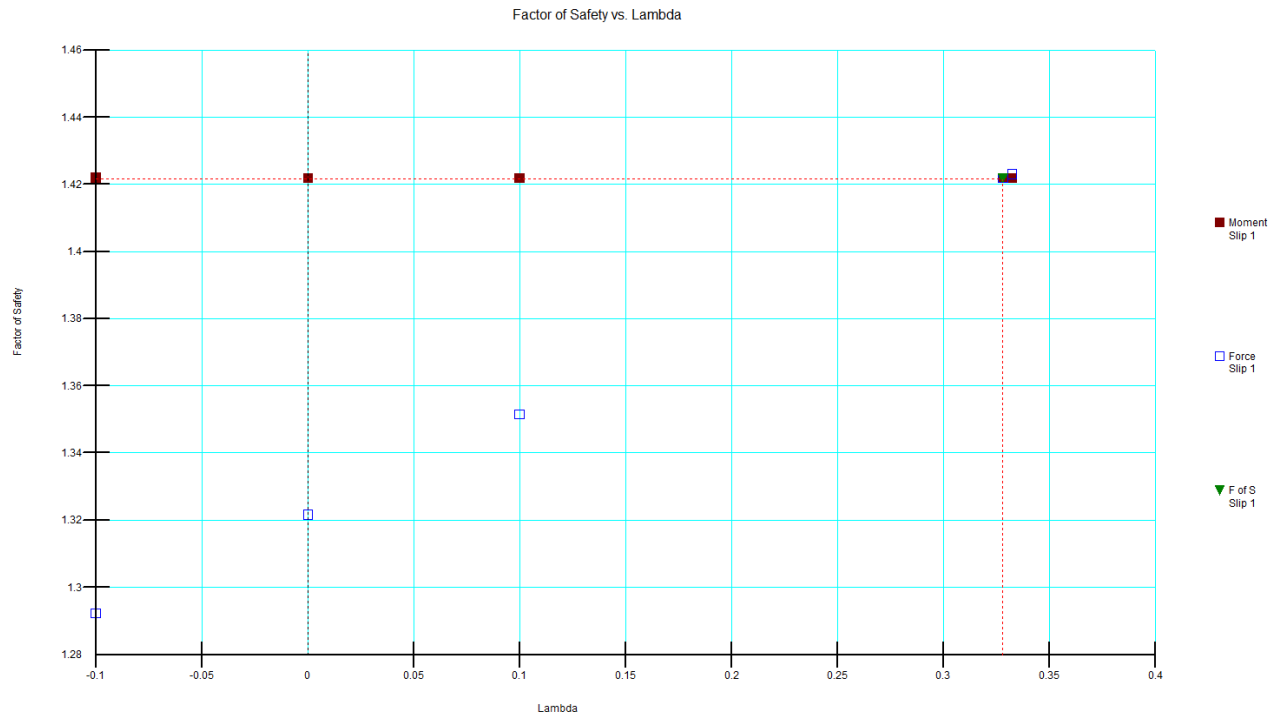
Figure 58 Factor of Safety vs Lambda, Example#4, Layer2

The Factor of Safety published by Chowdhury & Xu is 1.5075 based on Bishop method, and the Probability of Failure is 0.468%.

Table 51 Results of Example 4, Layer 3

Method	Factor of Safety		PF(%)
	Moment	Force	
Morgenstern-Price	1.504	1.504	0.54
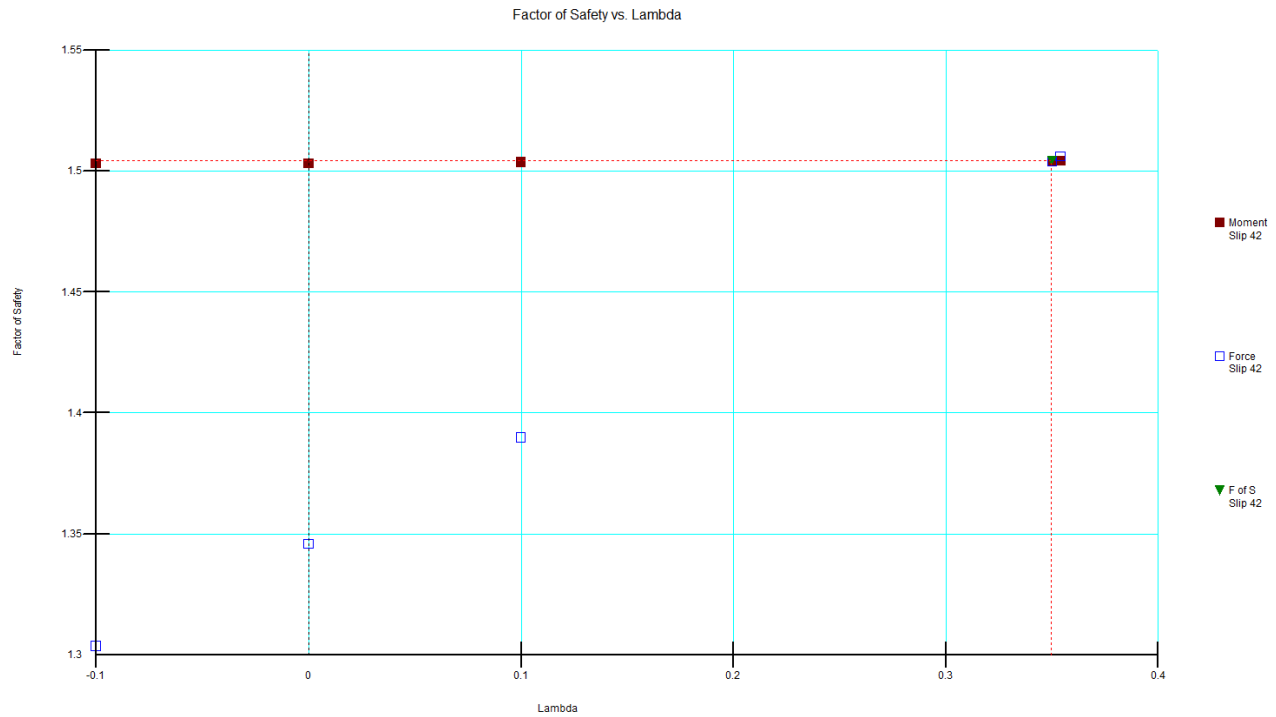
Figure 59 Factor of Safety vs Lambda, Example#3, Layer3

2.17.6 Example #5

This example illustrates the stability of an embankment on a soft clay foundation. Two circular slip surface failure conditions are again considered. First slip surface one is tangent to the interface of the embankment and the foundation and second slip surface one is tangent to the lower boundary of the soft clay foundation.

Probabilities of failure are presented in the original paper by Chowdhury and Xu (1995), which are calculated using a commonly used definition of reliability index. As well, as assumption that all factor of safety distributed.

Slope Stability makes use of the Monte Carlo technique in calculating the probability of failure. It is assumed that all input variables used in Slope Stability are normally distributed.

Table 52 Example 5 Input Data

	Soil Layer			
	Layer 1		Layer 2	
	c_1 (kPa)	$\phi(°)$	c_2 (kPa)	$\phi(°)$
Mean (kPa)	10	12	40	0
Standard Deviation (kPa)	2	3	8	0
γ (kN/m³)	20		18	

The Factor of Safety published by Chowdhury & Xu is 1.1625 based on Bishop method, and the Probability of Failure is 20.225%.

Table 53 Results of Example 5, Layer 1

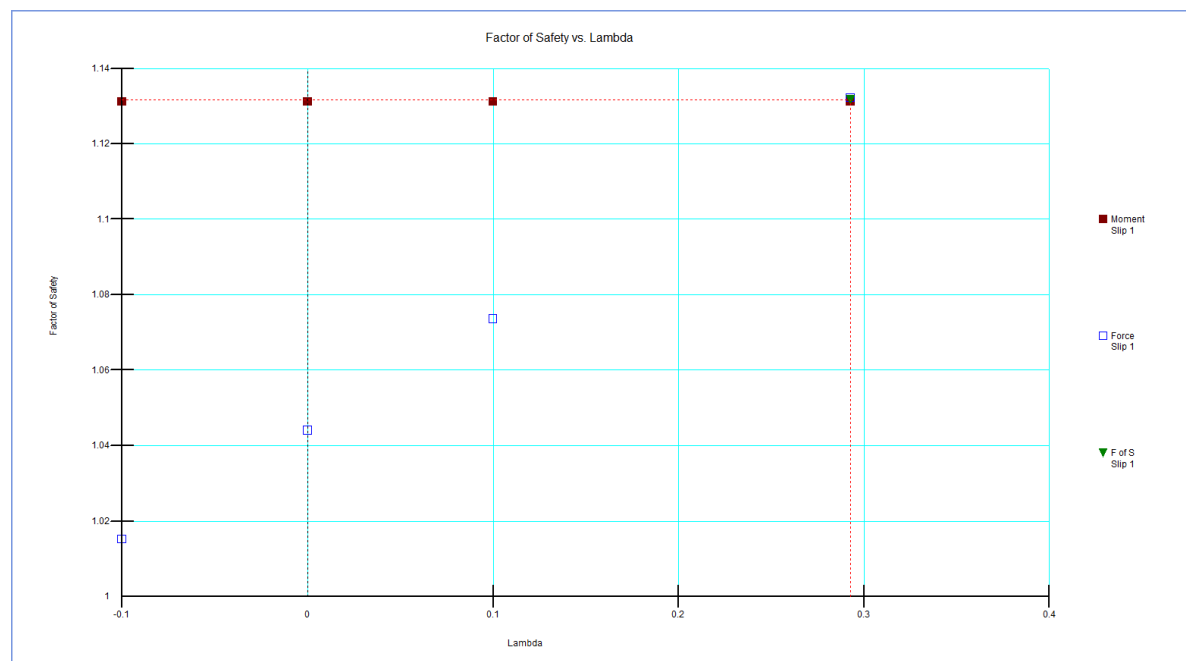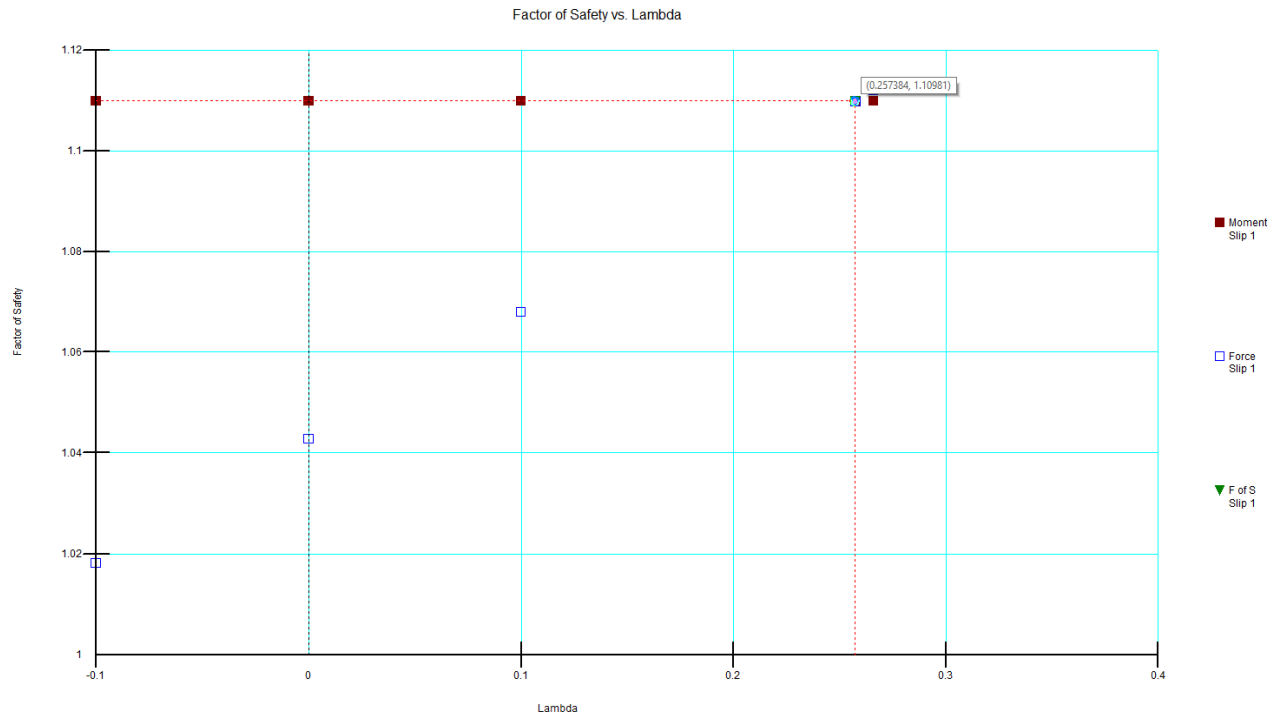| Method	Factor of Safety		PF(%)
	Moment	Force	
Morgenstern-Price	1.158	1.158	20.98

New Graph
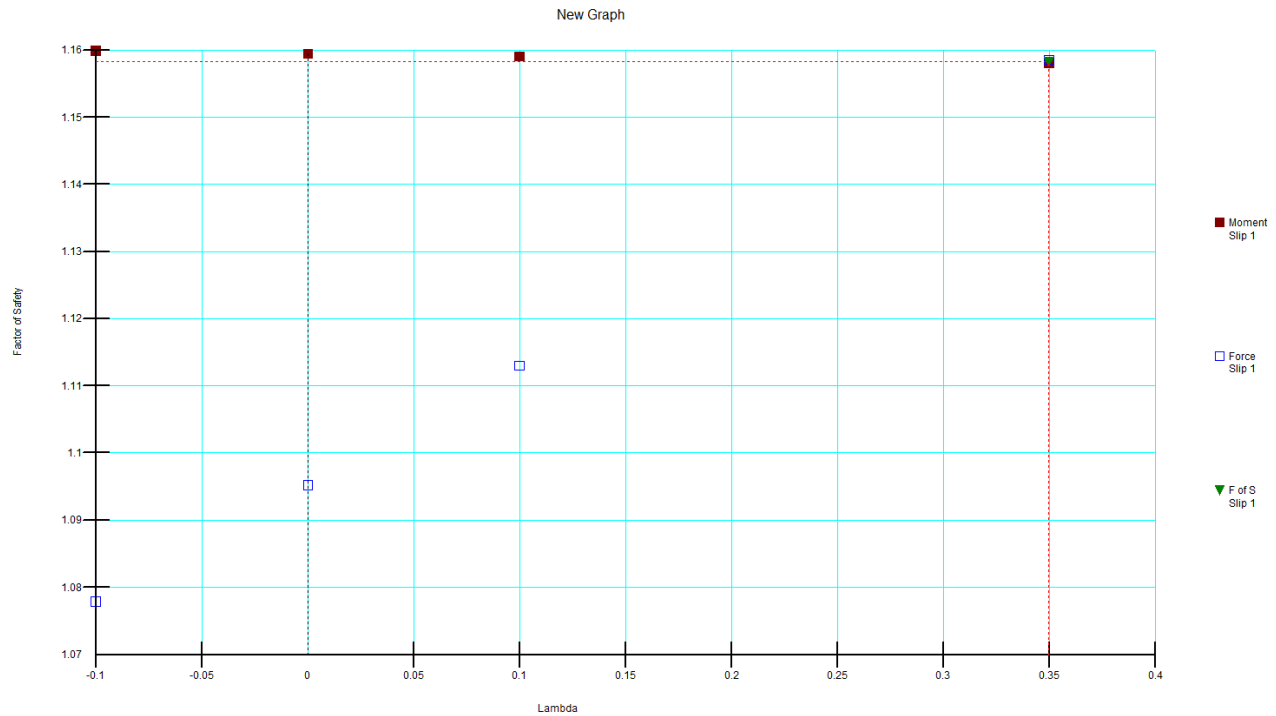
Figure 60 Factor of Safety vs Lambda, Example#5, Layer1

The Factor of Safety published by Chowdhury & Xu is 1.1479 based on Bishop method, and the Probability of Failure is 19.733%.

Table 54 Results of Example 5, Layer 2

Method	Factor of Safety		PF(%)
	Moment	Force	
Morgenstern-Price	1.178	1.178	21.39

New Graph
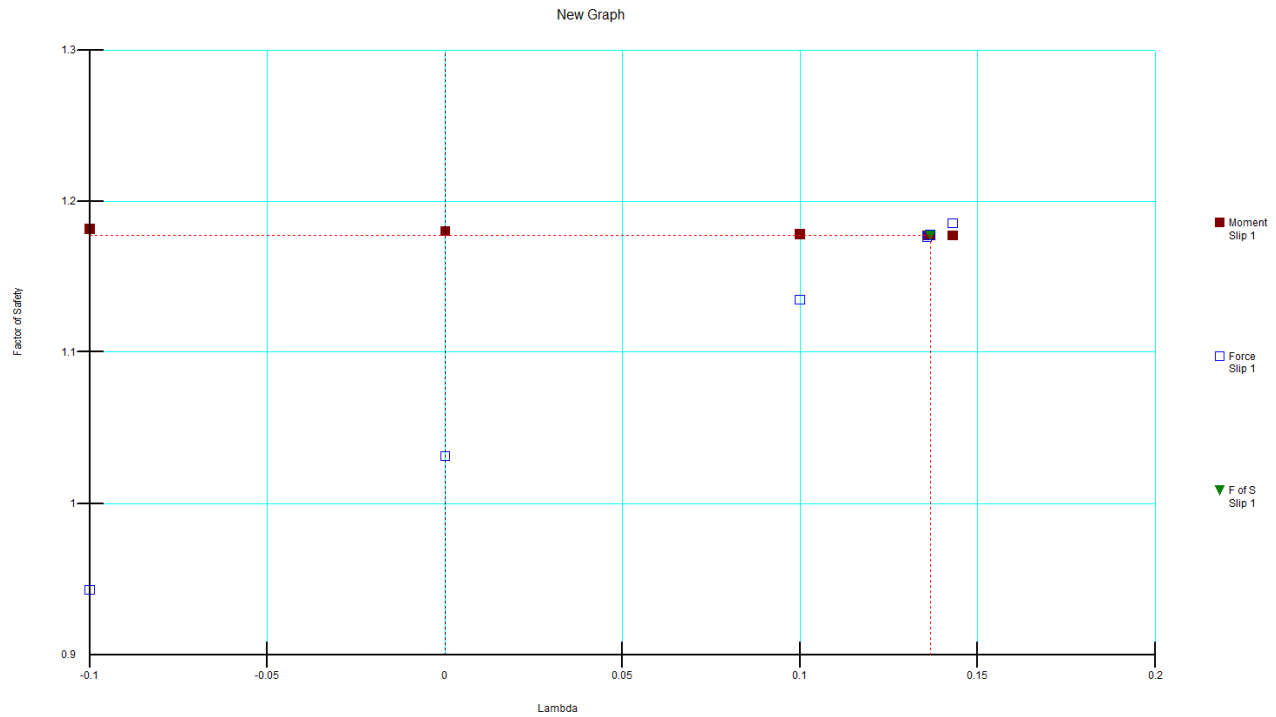
Figure 61 Factor of Safety vs Lambda, Example#5, Layer2

2.18 Borges And Cardoso – Geosynthetic Embankment #2

Project File: Borges and Cardoso - Geosynthetic embkt Case 2.gsz

This model looks at the stability of a geosynthetic-reinforced embankment placed over a soft soil. This model was original published by Borges and Cardoso (2002). This is their Case 2 example.

The model is set up as a more competent material overlaying soft clay with varying undrained shear strength. The geosynthetic has a tensile strength of 200 KN/m and a frictional resistance of 33.7 degrees. The geosynthetic is not anchored and has no adhesion.

2.18.1 Geometry and Material Properties
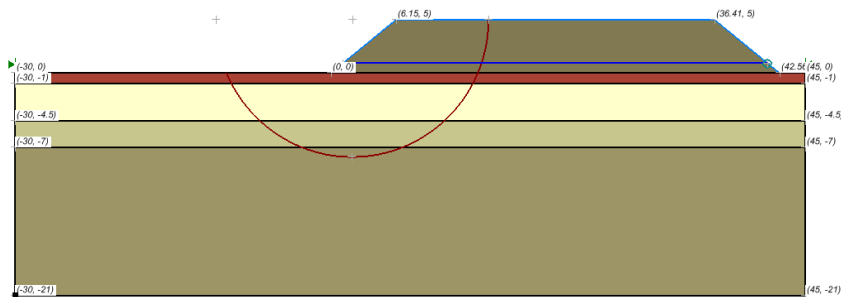
Figure 62 Geometry of Borges and Cardoso (2002) Case 2

42

Table 55 Material Properties of Borges and Cardoso (2002) Case 2

	c (kN/m²)	φ (degrees)	γ (kN/m³)
Embankment	0	35	20
	c_u top (kN/m²)	c_u bottom (kN/m²)	γ (kN/m³)
Clay 1	33	33	17
Clay 2	16	16	17
Clay 3	16	18.4	17
Clay 4	18.4	55.1	17

2.18.2   Results and Discussions

The results of the factor of safety calculations are shown in the following table and figures. The Factor of Safety published by Borges and Cardoso (2002) was 1.15.

Table 56. Borges and Cardoso (2002) –Case 2 - Results

Method	Factor of Safety	
	Moment	Force
Bishop	1.170	
Janbu		1.233
Morgenstern-Price	1.171	1.171

Figure 63 Borges and Cardoso (2002) –Case 2 – Failure surface using the Morgenstern-Price method
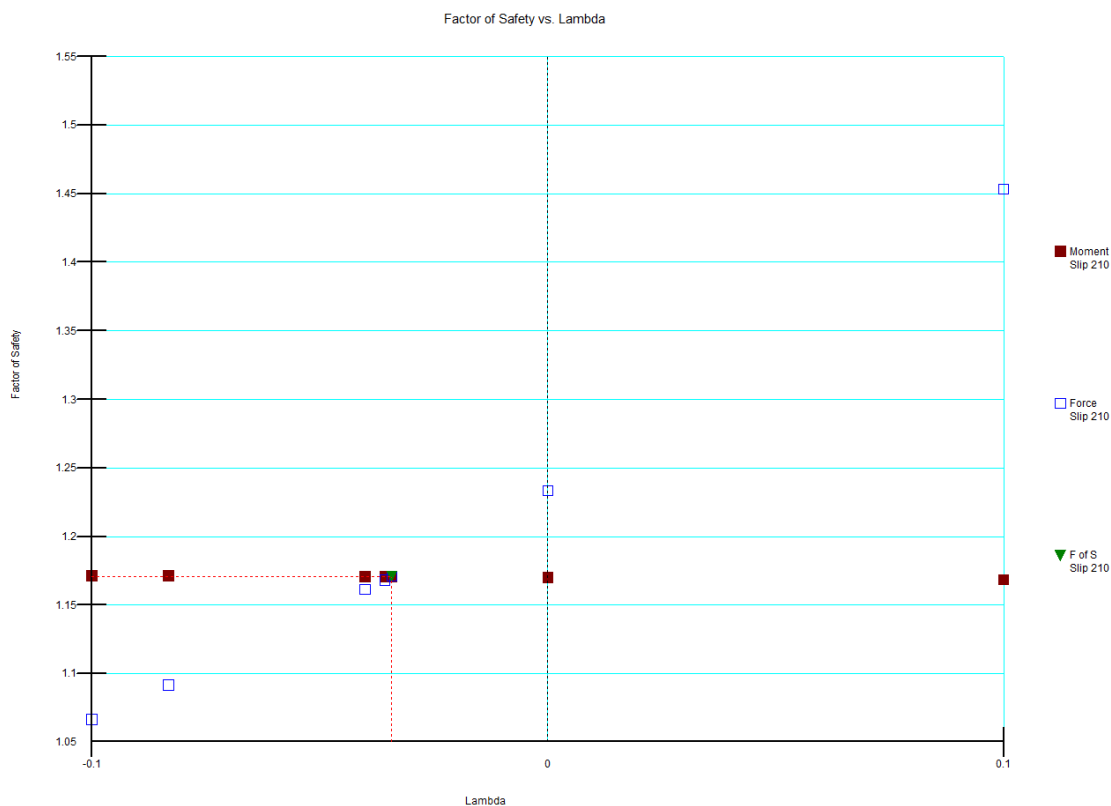
Figure 64 Borges and Cardoso (2002) –Case 2 – Factor of safety vs Lambda

2.19 Borges And Cardoso – Geosynthetic Embankment #3

Project File: Borges and Cardoso - Geosynthetic embkt Case 3.gsz

This is the case 3 example taken from Borges and Cardoso (2002). This particular model looks at the stability of a geosynthetic-reinforced embankment on soft soil for two embankment heights.

2.19.1 Geometry and Material Properties

The material properties are the same as the previous two examples. The geosynthetic in this case has the tensile strength of 200 KN/m as well as a frictional resistance of 39.6 degrees. The Bishop Simplified analysis method is used for consistency with the method used by the authors.

The two embankment materials are implemented in the model. The lower embankment material is 0 to 1 m and the upper embankment material is from 1 to 7 m or 1 to 8.75m. The geosynthetic is placed at the elevation 0.9 m, just inside on the lower embankment material.
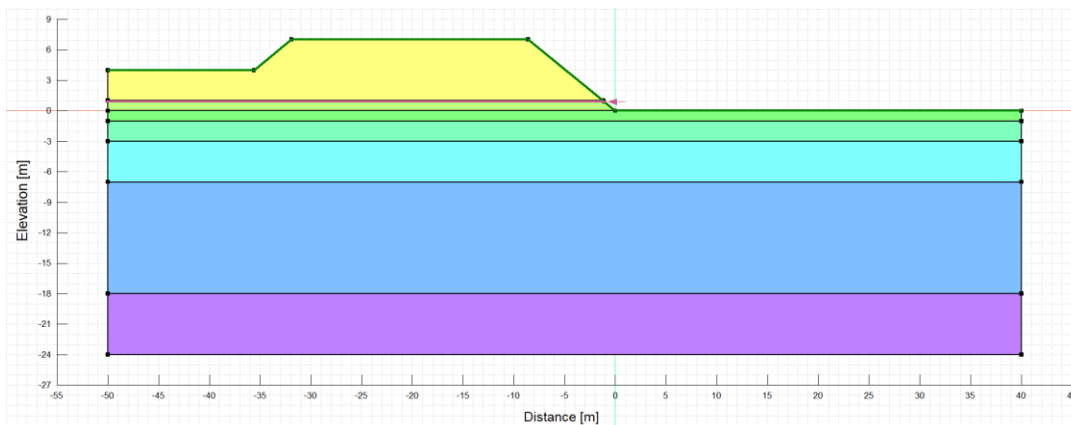
Figure 65 Geometry of Borges and Cardoso (2002) Case 3 – 7m high embankment
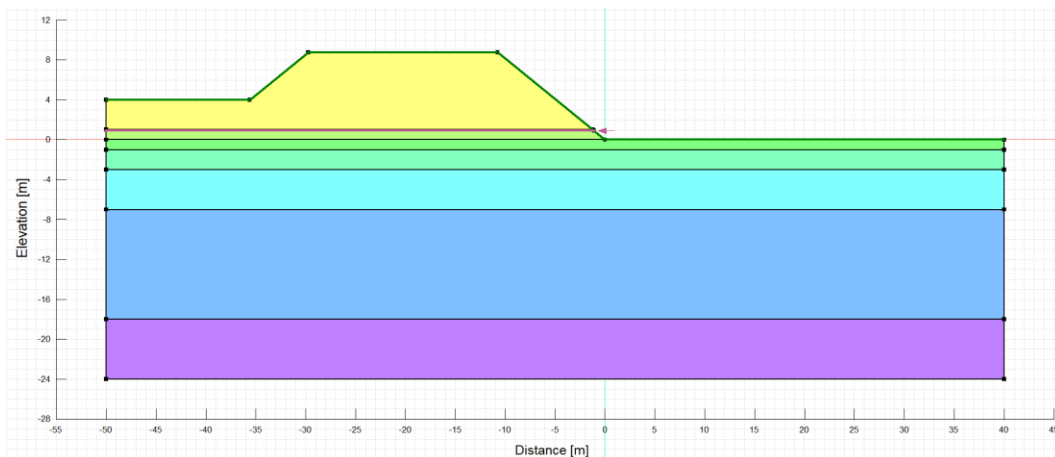
Figure 66 Geometry of Borges and Cardoso (2002) Case 3 – 8.75m high embankment

Table 57 Material Properties of Borges and Cardoso (2002) Case 3

	c (kN/m²)	ϕ (degrees)	γ (kN/m³)
Upper Embankment	0	35	21.9
Lower Embankment	0	33	17.2

Table 58 Results of Borges and Cardoso (2002) Case 3

	c_u (kN/m^2)	γ (kN/m³)
Clay 1	43	18
Clay 2	31	16.6
Clay 3	30	13.5
Clay 4	32	17
Clay 5	32	17.5

2.19.2 Results and Discussions

The results of the factor of safety calculations for the 7m high embankment are shown in the following table and figures. The Factor of Safety published by Borges and Cardoso (2002) was 1.19.

Table 59. Borges and Cardoso (2002) –Case 3 – 7m high embankment - Results

Method	Factor of Safety	
	Moment	Force
Bishop	1.230	
Janbu		1.195
Morgenstern-Price	1.230	1.230

Figure 67 Borges and Cardoso (2002) –Case 3 – 7m high embankment - Failure surface using the Morgenstern-Price method
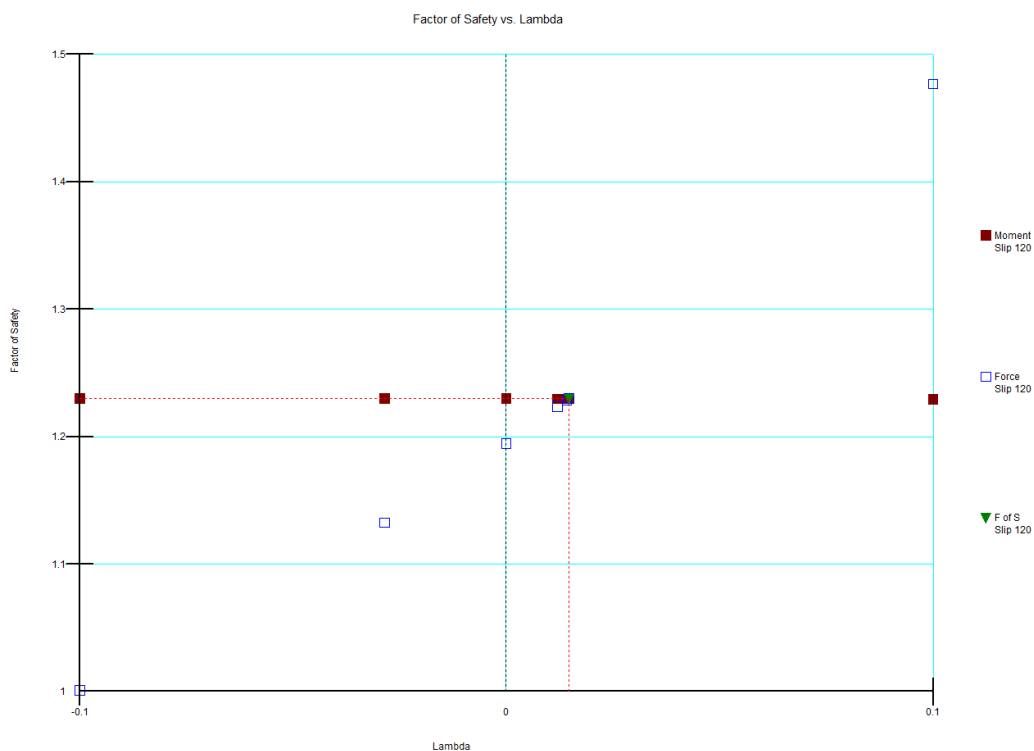
Figure 68 Borges and Cardoso (2002) –Case 3 – 7m high embankment - Factor of safety vs Lambda

The results of the factor of safety calculations for the 8.75m high embankment are shown in the following table and figures. The Factor of Safety published by Borges and Cardoso (2002) was 0.99.

Table 60. Borges and Cardoso (2002) –Case 3 – 8.75m high embankment - Results

Method	Factor of Safety	
	Moment	Force
Bishop	0.972	
Janbu		0.922
Morgenstern-Price	0.972	0.972

Figure 69 Borges and Cardoso (2002) –Case 3 – 8.75m high embankment - Failure surface using the Morgenstern-Price method
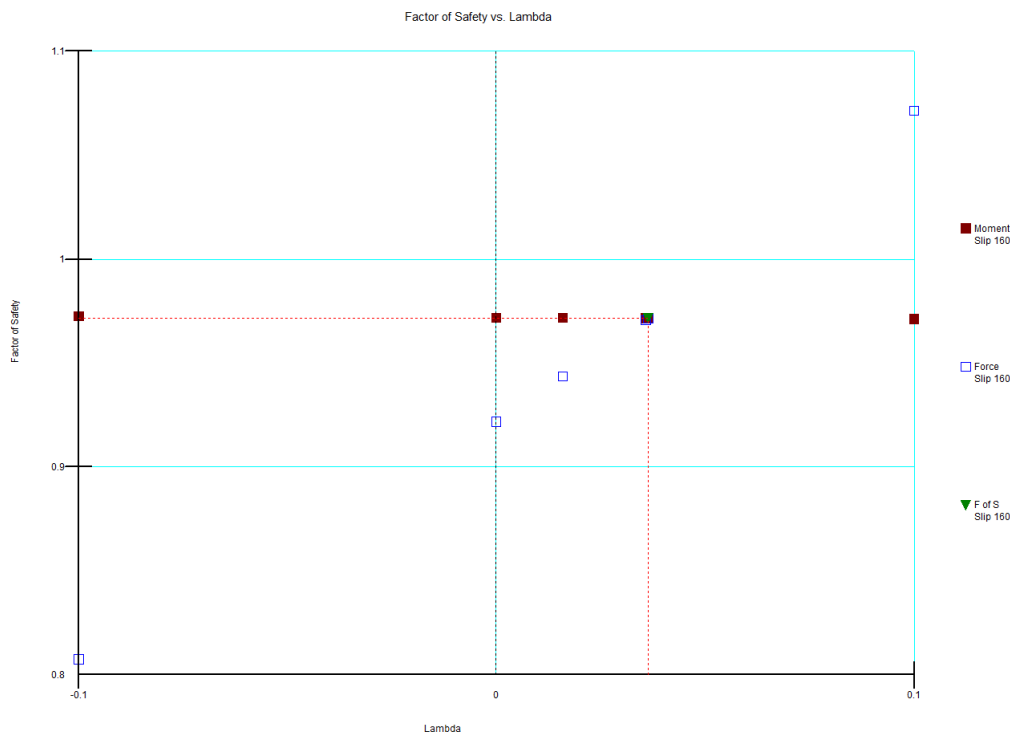
Figure 70 Borges and Cardoso (2002) –Case 3 – 8.75m high embankment - Factor of safety vs Lambda

2.20 Probabilistic - Syncrude Dyke

Project File: Probabilistic - Syncrude Dyke.gsz

El-Ramly et al (2003) published the results of a probabilistic slope stability analysis of a tailings dyke at a Syncrude mine in Alberta, Canada. The analysis did not consider spatial variation of soil properties and is therefore described as a simplified probabilistic analysis. El-Ramly et al (2003) varied both strength and pore-water pressure definitions probabilistically; however, in this analysis consideration was only given to the strength properties because El-Ramly et al. (2003) used pore pressure ratios, which are not available in GeoStudio. A Monte Carlo analysis was used to calculate the probability of failure. The input parameters were assumed normally distributed.

2.20.1 Geometry and Material Properties
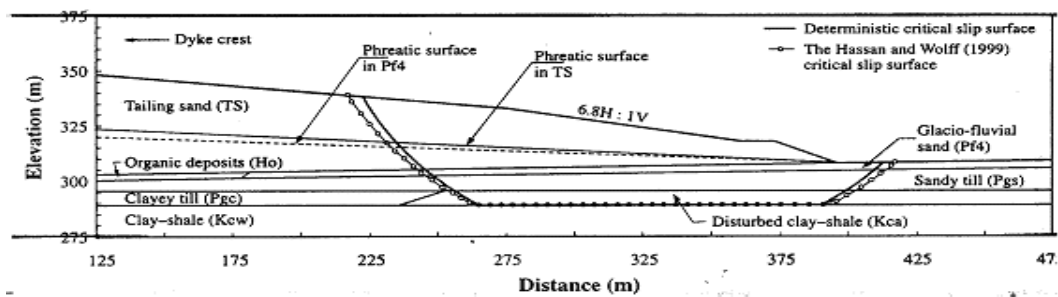
Figure 71 Original Geometry of the Syncrude Tailings Dyke model
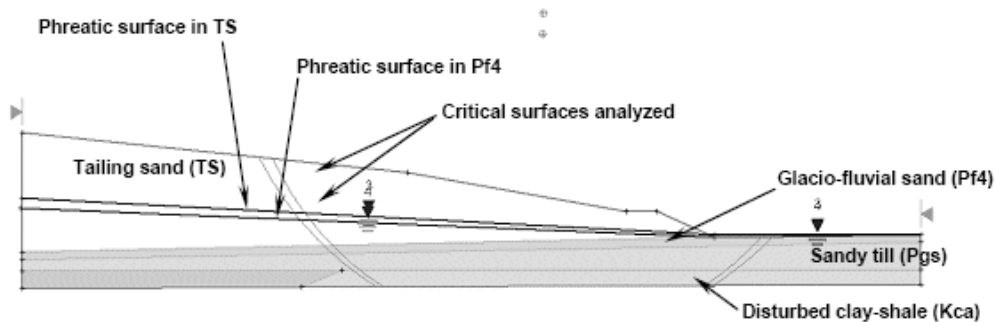
Figure 72 Piezometric Surfaces
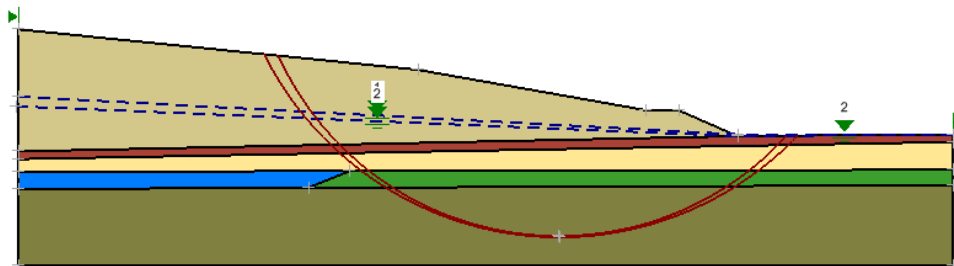
Figure 73 Geometry of the Syncrude Tailing Dyke model

Table 61 Material Properties of the Syncrude Tailing Dyke model

	c (kN/m²)	φ (degrees)	Standard Deviation of φ (degrees)	γ (kN/m³)
Tailings sand	0	34	-	20
Glacio-fluvial sand	0	34	-	17
Sandy till	0	34	2	17
Clayey Till	0	7.5	-	17
Distributed clay-shale	0	7.5	2.1	17

2.20.2 Results and Discussions

El-Ramly et al. (2003) reported a deterministic Factor of Safety of 1.31, calculated using the Bishop Method, and a probability of failure of essentially 0 (1.54E-3). The results for both slip surfaces were essentially the same.

Table 62 Probabilistic – Syncrude Dyke: Results

Method	Factor of Safety	
	Moment	Force
Bishop	1.306	

Color	Name	Slope Stability Material Model	Unit Weight (kN/m³)	Effective Cohesion (kPa)	Effective Friction Angle (°)	Piezometric Surface
	Clay Shale (Kcw)	Bedrock (Impenetrable)				2
	Clayey Till (Pgx)	Mohr-Coulomb	17	0	7.5	2
	Disturbed Clay Shale (Kca)	Mohr-Coulomb	17	0	7.5	2
	Glacio-fluvial sand (Pf4)	Mohr-Coulomb	17	0	34	2
	Sandy Till (Pgs)	Mohr-Coulomb	17	0	34	2
	Tailings Sand (TS)	Mohr-Coulomb	20	0	34	1

1.304
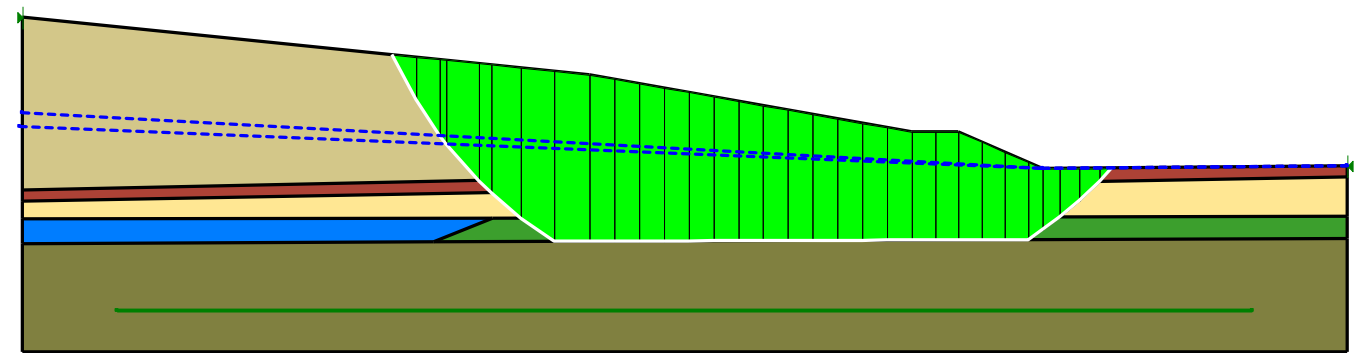
Figure 74 Probabilistic – Syncrude Dyke: Critical Slip Surface

Probability Distribution Function

⟋ P (F of S < x)

⟋ P (Failure)
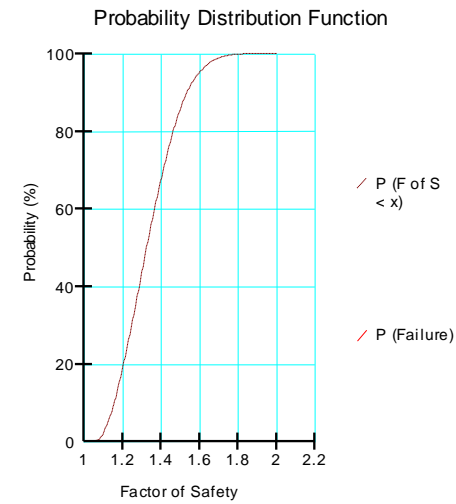
Figure 75 Probabilistic – Syncrude Dyke: Probability Distribution Function

2.21   Cannon Dam

Project File: Cannon Dam.gsz

The Cannon Dam model was published from Wolff and Harr (1987). The probabilistic analysis results from Slope Stability are compared to the results published in the paper by Wolff and Harr for a noncircular slip surfaces. Wolff and Harr (1987) used the point-estimate method for their probability analysis failure for the Cannon Dam.

The location of critical slip surface was taken from their paper. The input parameters; namely, friction angle for the Phase I and Phase II fills was calculated. The unit weights of the fills were back-calculated in order to match the factor of safety computed by Wolff and Harr. Wolff and Harr (1987) based on the stochastic properties provided in the paper originally published results that only satisfied force equilibrium.

2.21.1   Geometry and Material Properties
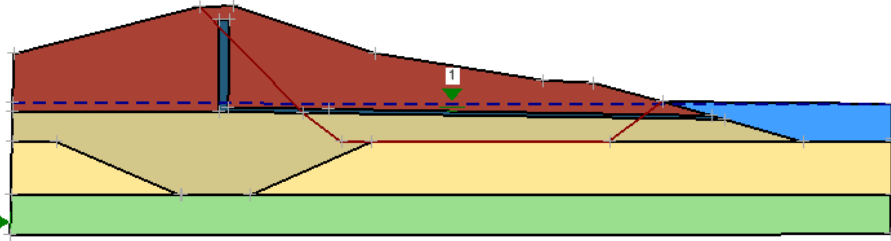
Figure 76 Geometry of the Cannon Dam model

Table 63 Material Properties of the Cannon Dam

Material	c (lb/ft^2)	Standard Deviation of c (lb/ft^2)	ϕ (degrees)	Standard deviation of ϕ (degrees)	Correlation coefficient for c and ϕ	γ (lb/ft^3)
Phase I fill	2,230	1,150	6.33	7.87	0.11	150
Phase II fill	2,901.6	1,079.8	14.8	9.44	-0.51	150
Material 3	1		50			150
Material 4	1		35			150
Spoil Fill	3,000		60			150
Filter	-		35			120

2.21.2   Results and Discussions

The results were compared to those obtained by MP method. It is assumed in the Slope Stability model that all the probabilistic input variables are normally distributed.

Table 64 Results of the Cannon Dam

	Wolff and Harr		Slope/W	
	Deterministic FOS	PF(%)	Deterministic FOS	PF(%)
MP	2.36	4.55	2.343	0.04
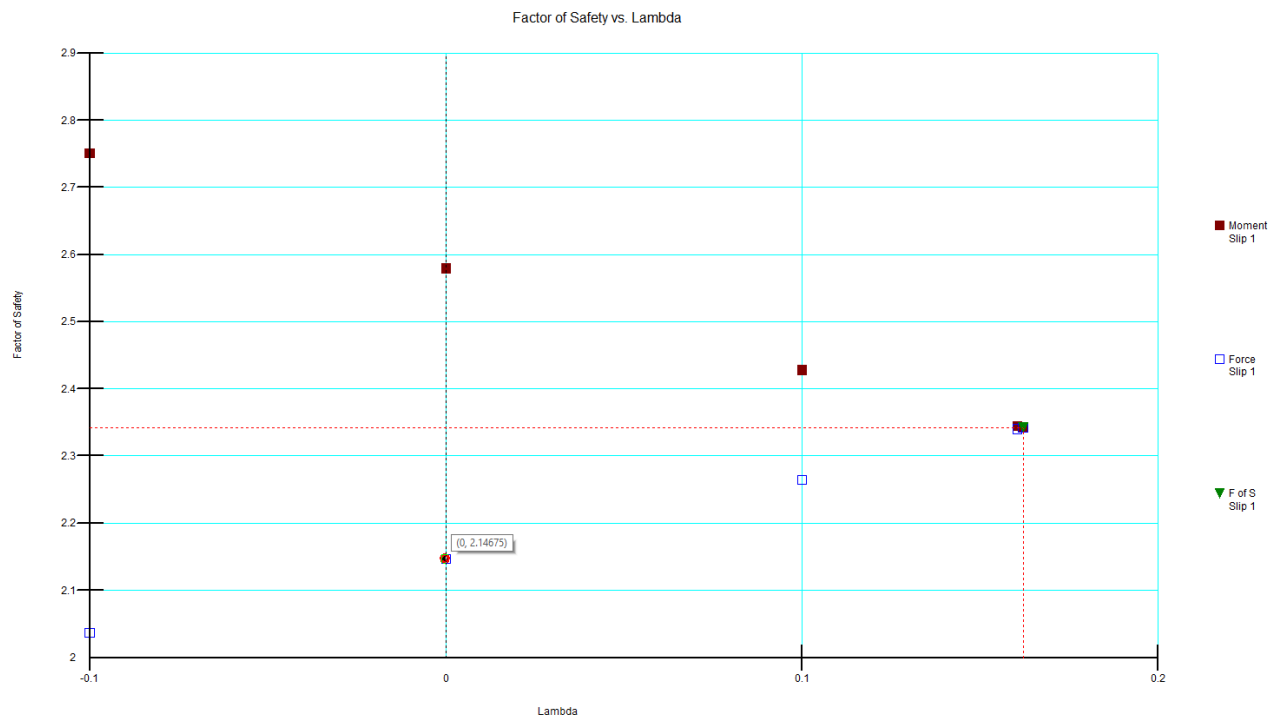
Figure 77 Canon Dam - Factor of safety vs Lambda

50

2.22   Cannon Dam #2

Project File: Cannon Dam #2.gsz

This model of the Cannon Dam in Missouri was presented by Hassan and Wolff (1999). The purpose of this verification model is to look at duplicating reliability index results for several circular failure surfaces as specified in the original paper. Hassan and Wolff (1999) presented a new reliability based approach in their paper. The cross-section of the Cannon Dam is shown below. The Bishop Simplified method of slices was used to analyze this verification problem. The present set of slip circles are those shown in

Figure 78 of the Hassan and Wolff paper and Figure 79 shows the model input parameters.

The Hassan and Wolff (1999) paper does not provided all the required input parameters. Therefore we selected values for the missing parameters that allowed to us to match the factors of safety for some of the circles slip surfaces shown in

Figure 78. The assumption is made in this analysis that all the probabilistic input variables are normally distributed for performing the Monte Carlo simulations.

The reliability indices calculated in Slope Stability are based on the mean and standard deviations of the factor of safety values calculated in the simulations. The reliability indices shown in the results section are calculated using the assumption that the factors of safety values are log-normally (Hassan and Wolff, 1999). The results obtained from Slope Stability and the results from Hassan and Wolff are shown in Table 66.

2.22.1   Geometry and Material Properties
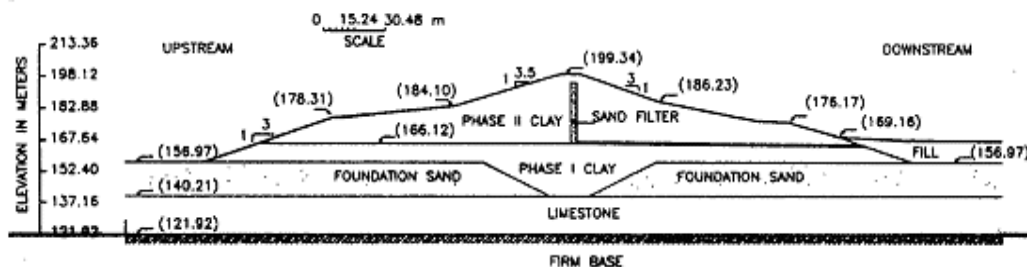
Figure 78 Hassan and Wolff's Geometry
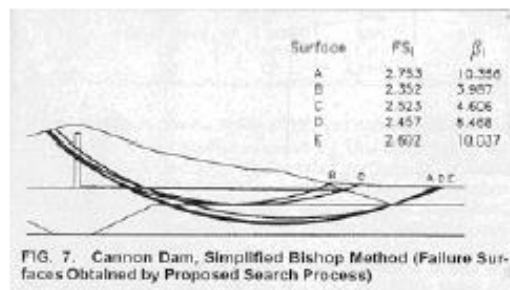
51
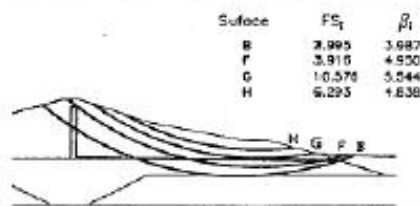
Figure 79 Hassan and Wolff (1999) paper
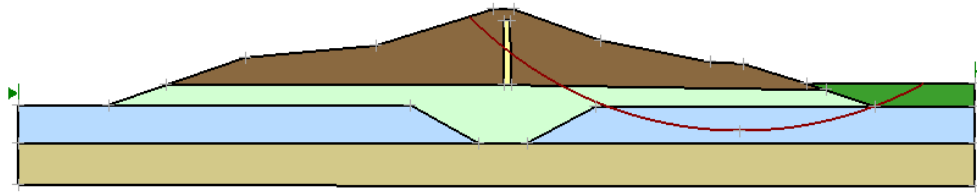
Figure 80 Geometry of VS_35_1_Fig7_Surface A - Cannon Dam #2

Table 65 Material Properties of the Cannon Dam #2

Material	c (lb/ft^2)	Standard Deviation of c (lb/ft^2)	ϕ (degrees)	Standard deviation of ϕ (degrees)	Correlation coefficient for c and ϕ	γ (lb/ft^3)
Phase I clay fill	117.79	58.89	8.5	8.5	0.1	22
Phase II clay fill	143.64	79	15	9	-0.55	22
Sand Filter	0	-	35	-	-	22
Foundation sand	5	-	18	-	-	22
Spoil fill	5	-	35	-	-	25

2.22.2   Results and Discussions

Table 66 Results of the Cannon Dam #2

Surface	Hanssan and Wolff		SLOPE/W	
	Deterministic FOS	Reliability Index	Deterministic FOS	Reliability Index (lognormal)
Figure7 A	2.551	10.953	2.560	11.428
Figure7 B	2.820	4.351	2.806	3.353
Figure7 C	2.777	4.263	2.771	3.246
Figure7 D	2.583	11.092	2.589	11.632
Figure7 E	2.692	10.281	2.703	10.719
Figure8 B	2.672	4.858	2.673	3.936
Figure8 F	3.598	5.485	3.586	4.469
Figure8 G	6.074	5.563	6.069	5.128
Figure8 H	11.230	6.394	11.583	4.309

2.23   Li and Lumb – Reliability Index

Project File: Li and Lumb - Reliability Index.gsz

Li and Lumb (1987) and Hassan and Wolff (1999) presented the results of an analysis that involved calculation of the reliability index of the deterministic global circular surface and the minimum reliability index value obtained from an analysis of multiple slip surfaces. The Bishop Simplified method of analysis was used. A Monte Carlo analysis was used which assumes that all input probability variables are normally distributed. The reliability

52

indices are calculated on the assumption that the factors of safety values are distributed log normal. This interpretation is consisted with the original analysis presented by Hassan and Wolff (1999). Separate reliability indices are calculated for the minimum deterministic critical slip surface, as well as the critical probabilistic slip surface.

2.23.1 Geometry and Material Properties

The geometry is presented in Figure 81 and the material properties are presented in Table 67.
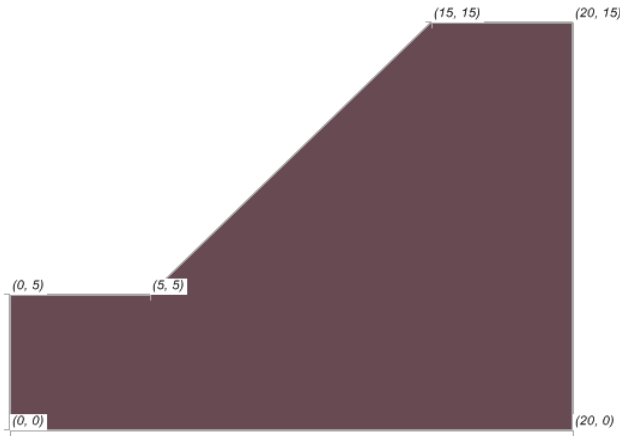
Figure 81 Li and Lumb (1997): Geometry

Table 67 Li and Lumb (1987): Material Properties

Property	Mean Value	Standard deviation
c (kN/m²)	18	3.6
φ (degrees)	30	3
γ (kN/m³)	18	0.9
R_u	0.2	0.02

2.23.2 Results and Discussions

GeoStudio calculates and presents the reliability index (see the Figures):

$$\beta = \frac{\mu - 1}{\sigma}$$

where μ is the mean factor of safety and σ is the standard deviation. Hassan and Wolff (1999) calculated and presented the lognormal reliability index:

$$\beta_{ln} = \frac{ln\left[\frac{\mu}{\sqrt{1 + V^2}}\right]}{\sqrt{ln(1 + V^2)}}$$

where V is the coefficient of variation of Factor of Safety calculated as s/m. Note that the minimum reliability index and its lognormal variant are not necessarily in agreement.

Hassan and Wolff (1999) reported the critical deterministic Factor of Safety was 1.334 and the corresponding lognormal reliability index was 2.336. GeoStudio calculated a Factor of Safety of 1.343 and reliability index of 2.051, which corresponds to lognormal reliability index of 2.32. The results agree with Hassan and Wolff (1999).

Hassan and Wolff (1999) reported that the minimum lognormal reliability index was 2.293, which corresponded to a Factor of Safety of 1.190. GeoStudio calculated a minimum reliability index of 2.04, which corresponds to a

lognormal reliability index of 2.32 and a factor of safety of 1.354. The results do not agree with Hassan and Wolff (1999); however, they have been verified by other means.
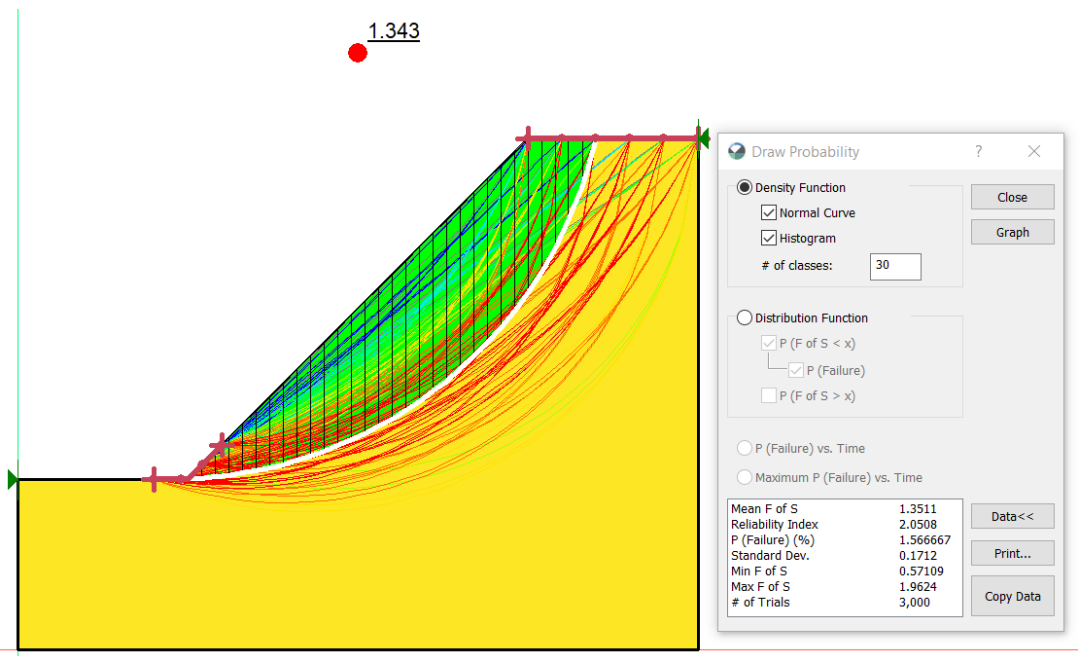
Figure 82 Li and Lumb: Probabilistic results for the deterministic slip surface
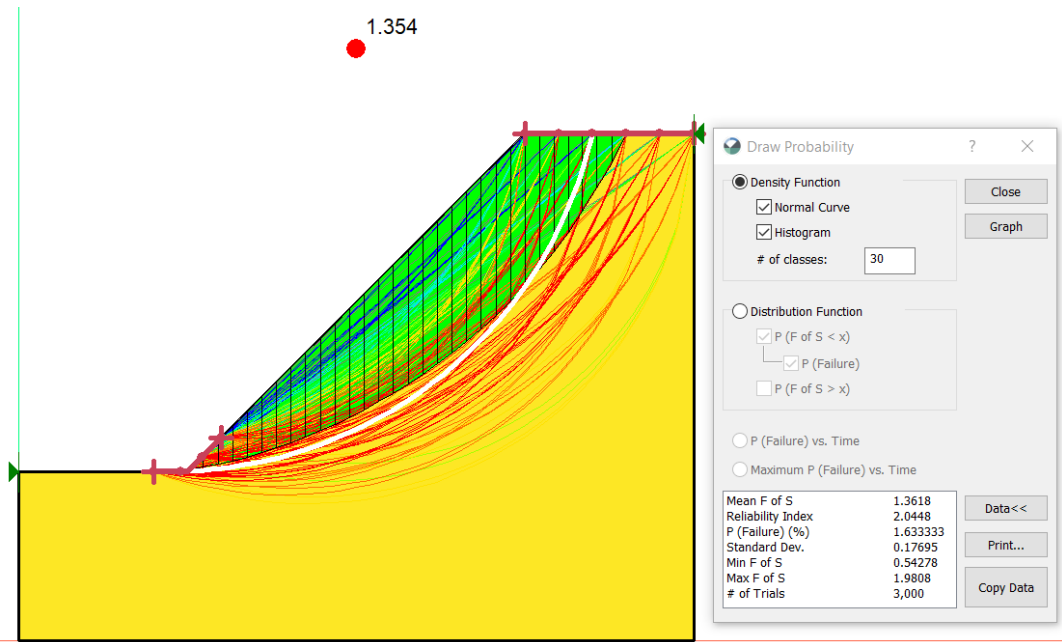
Figure 83 Li and Lumb: Probabilistic results for the slip with the minimum reliability index

2.24   Tandjiria – Geosynthetic Reinforced Embankment

Project File: Tandjiria Geosynthetic Reinforced Embankment.gsz

This model was presented by Tandjiria (2002) to examine the stability of a geosynthetic-reinforced embankment on soft soil. This problem considers the embankment stability when it consists of sand or an undrained clay fill

with water filled tension cracks, and ultimately determines the required reinforcement force to yield a factor of safety of 1.35.

Both circular and noncircular critical slip surfaces were examined for both the sand and clay embankments. In each case, the embankment was first analyzed without reinforcement and the critical slip surfaces determined. The critical slip surface was used in a secondary analysis for each case, where geosynthetic reinforcement was added at the base of the embankment. The reinforcement forces determined by Tandjiria (2002) were used to determine the associated factor of safety.

2.24.1   Geometry and Material Properties
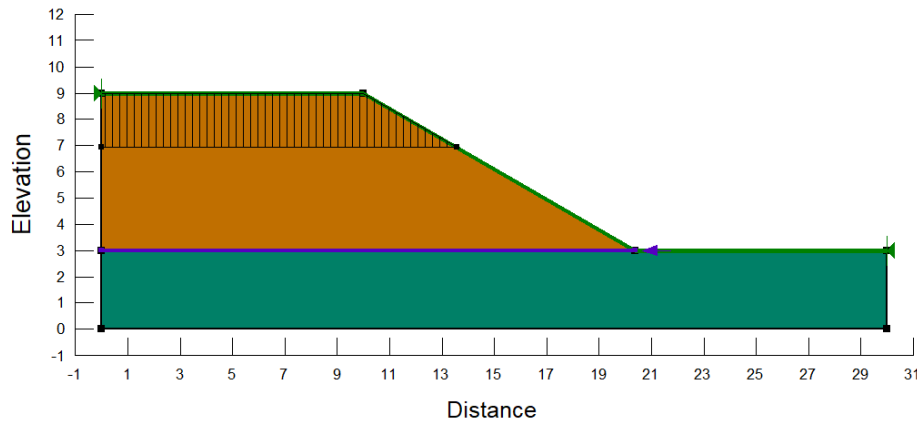
Figure 84 Clay Fill Embankment with Tension Cracks and Reinforcement

Table 68 Material Properties

	c_u/c (kN/m²)	ϕ (degrees)	γ (kN/m³)
Clay Fill Embankment	20	0	19.4
Sand Fill Embankment	0	37	17.0
Soft Clay Foundation	20	0	19.4

2.24.2   Results and Discussions

Tandjiria (2002) found the following deterministic Factor of Safeties for the embankments without reinforcement, using the Spencer Method. The results for both circular and noncircular slip surfaces were essentially the same.

Table 69 Results for clay and sand embankments with no reinforcement

Material	Slip Surface Shape	Factor of Safety	
		Tandjiria (2002)	SLOPE/W
Clay	Circular	0.981	0.982
Clay	Noncircular	0.941	0.937
Sand	Circular	1.219	1.216
Sand	Noncircular	1.192	1.186

There were small differences between the results for the reinforcement analyses. These were due to the different slip surface definition. Instead of setting the slip surface as the exact same shape as those published by Tandjiria (2002), SLOPE/W searched for the circular and noncircular slip surfaces. Additionally, the exact details of the reinforcement force application were not provided. Thus, slight differences in the reinforcement definition can explain differences in Factor of Safety.

Material	Slip Surface Shape	Reinforcement Force (kN)	Factor of Safety	
			Tandjiria (2002)	SLOPE/W
Clay	Circular	170	1.35	1.416
Clay	Noncircular	190	1.35	1.366
Sand	Circular	45	1.35	1.369
Sand	Noncircular	56	1.35	1.352
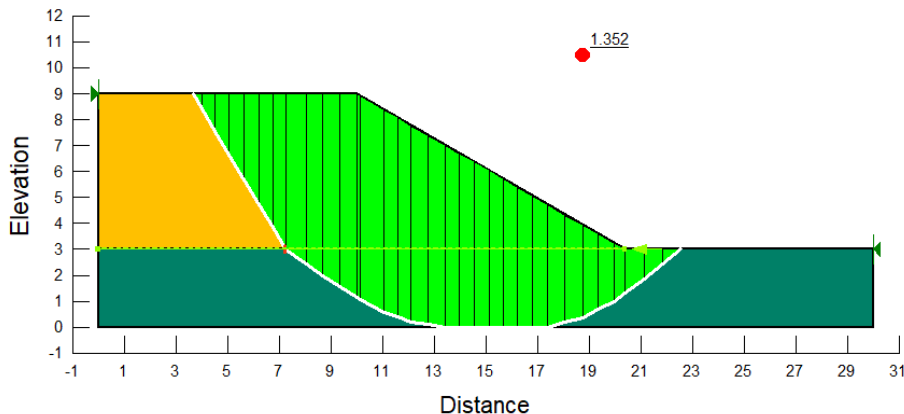
Figure 85 Results of the sand embankment with reinforcement and a noncircular slip surface

2.25   Baker and Leschinsky – Earth Dam

Project File: Baker and Leschchinsky - Earth Dam.gsz

This model was original published by Baker and Leshchinsky (2001). It was presented to illustrate the use of safety maps as practical tools for slope stability analysis.

2.25.1   Geometry and Material Properties

The geometry of the model can be seen in Figure 86. The model consists of a clay core with granular fill surrounding the core. The model has a solid base.

A dry tension crack is placed at the top of the model to stimulate a 5m thick crack layer. All trial slip surfaces must be plotted on the dam to obtain a safety map of regional safety factors of safety. Noncircular slip surfaces and corresponding factor of safety are also required in this analysis.

Color	Name	Unit Weight (kN/m³)	Effective Cohesion (kPa)	Effective Friction Angle (°)
⬜	Clay Core	20	20	20
⬜	Granular Fill	21.5	0	40
⬜	Hard Base	24	200	45
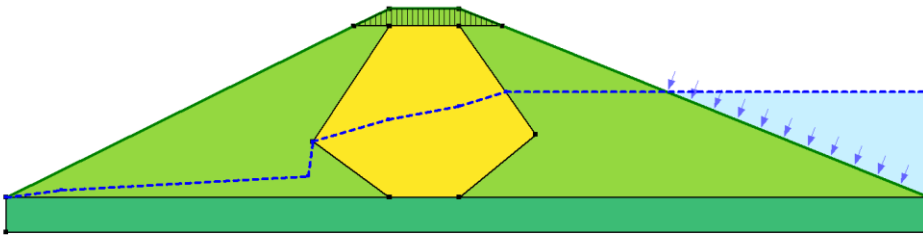
Figure 86 Geometry of the Baker and Leshchinsky Earth Dam model

Table 71 Material Properties of the Earth Dam Circular model

	c (kN/m²)	ϕ (degrees)	γ (kN/m³)
Clay core	20	20	20
Granular Fill	0	40	21.5
Hard Base	200	45	24

2.25.2 Results and Discussions

Baker and Leshchinsky (2001) reported a factor of safety of 1.91, which is in very close agreement with that presented in Table 72.

Table 72 Results – Non-circular failure surface using optimization

Method	Factor of Safety	
	Moment	Force
Spencer	1.868	1.868
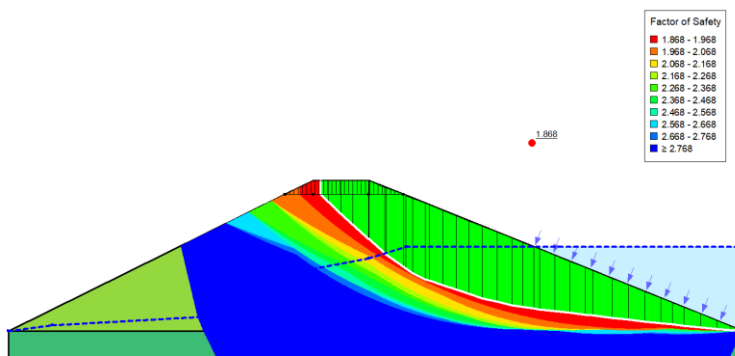
Figure 87 Safety Map of the Baker and Leshchinsky Earth Dam Model
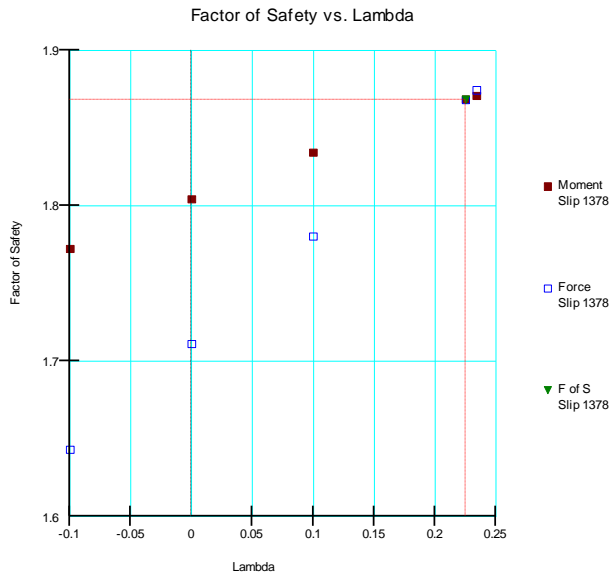
Figure 88 Factor of Safety versus Lambda (Critical Slip Surface)

2.26   Baker – Planar Homogeneous

Project File: Baker - Planar Homogeneous.gsz

This model is original published by Baker (2001) and looks at the factor of safety of planar slip surfaces. The results are compared at various failure plane angles. The slope presented is homogenous and dry.

2.26.1   Geometry and Material Properties

The geometry can be seen in Figure 89. In this case, there are two tests that must be run on this slope. The first test is that the plot of factors of safety versus *x*-coordinate are required for all critical failure planes passing through the toe of the slope.

Subsequently, the critical circular slip surfaces in Zone A must determined at which point the safety factors versus *x*-coordinate for Zone A must be plotted. A method of locating the factor of safety as a function of the failure plane angle is presented.

Color	Name	Slope Stability Material Model	Unit Weight (kN/m³)	Effective Cohesion (kPa)	Effective Friction Angle (°)	Phi-B (°)
☐	MC Material	Mohr-Coulomb	20	30	30	0
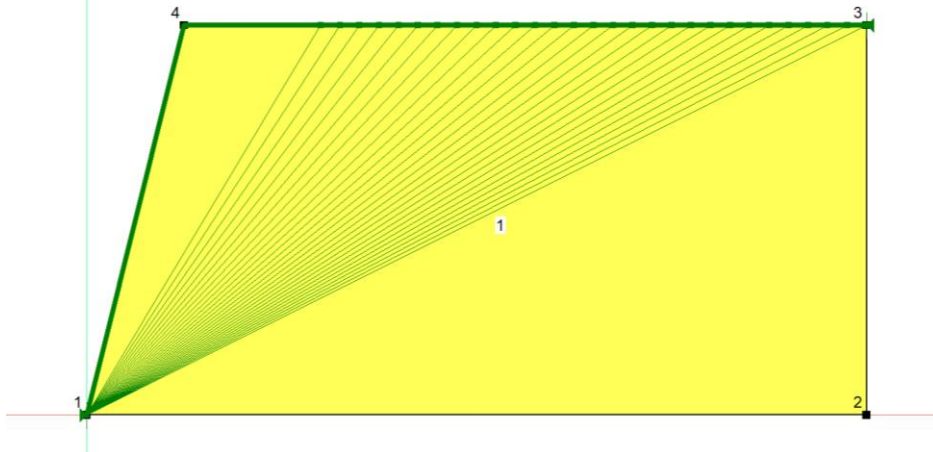
Figure 89 Geometry of the Baker (2001) - Planar Homogeneous Slope

Table 73 Material Properties of the Baker (2001) - Planar Homogenous Slope

	c (kN/m²)	φ (degrees)	γ (kN/m³)
Material	30	30	20
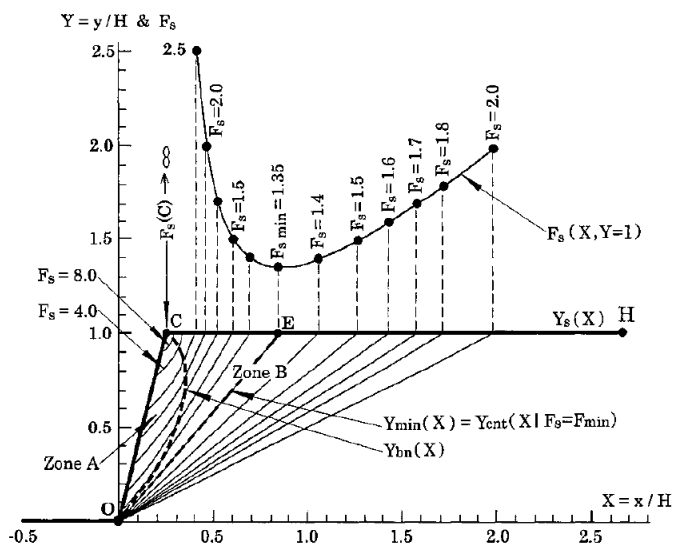
Figure 90 Baker's (2001) Distribution

59

2.26.2   Results and Discussions

(a) x/H = 2

(b) x/H = 1.75

(c) x/H = 0.85 – critical slip surface

(d) x/H = 0.6
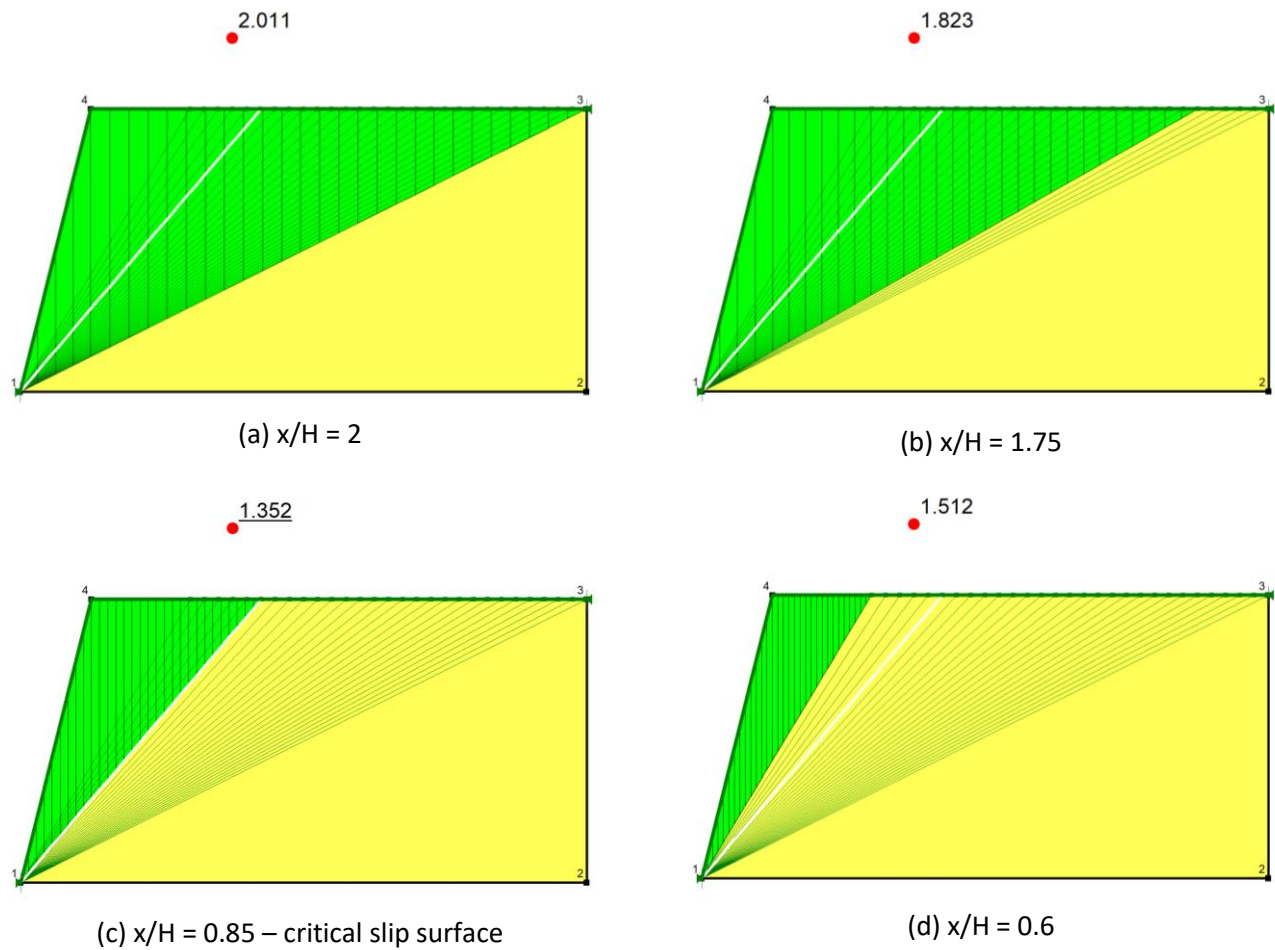
Figure 91 FOS results for four slip surfaces
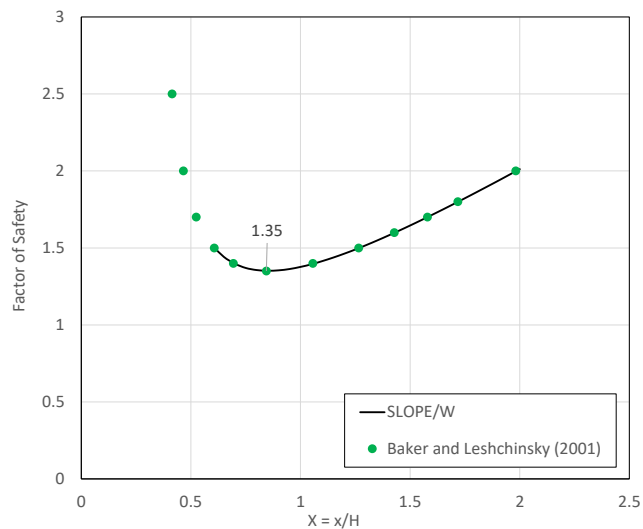
Figure 92 Comparison between SLOPE/W results and Baker and Leshchinsky (2001)

2.27   Sheahan – Amhearst Soil Nails

Project File: Sheahan Amhearst Soil Nails.gsz

This problem, published by Sheahan (2003), examines the Amhearst test wall, which failed due to over excavation. This wall includes two rows of soil nails in undrained, homogeneous clay.

2.27.1 Geometry and Material Properties

The geometry of the analysis is shown in Figure 93 and the material properties are provided in Table 74. The shotcrete plate on the soil nails has a weight of 14.6 kN/m, which was included as a point load at the top of the wall face. The soil nail definition is provided in Figure 94.
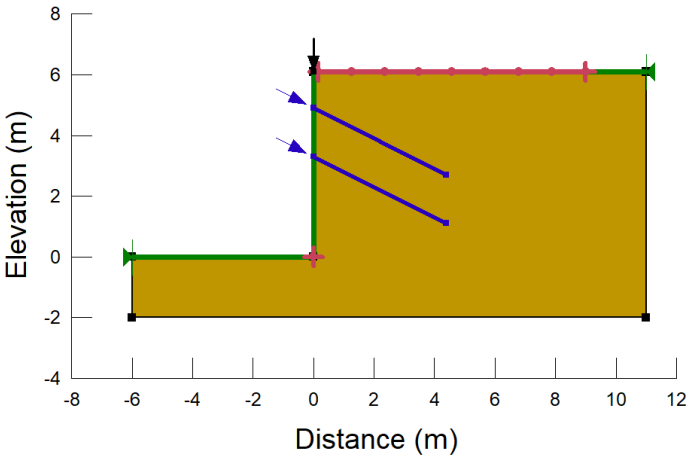
Figure 93 Geometry of the Sheahan Amhearst Soil Nails Model

Table 74 Material Properties of the Sheaham Amhearst Soil Nails model

Material	c (kN/m²)	γ (kN/m³)
Amherst Clay	25	18.9

Figure 94 Soil Nail Definition

2.27.2 Results and Discussions

Sheahan (2003) found a deterministic Factor of Safety of 0.887 for the Amhearst test wall using the Janbu Simplified Method. The results were essentially the same in SLOPE/W, as provided in Table 75 and illustrated in Figure 95.

Table 75 Results –Amhearst Soil Nails

Method	Factor of Safety	
	Moment	Force
Bishop	0.869	
Janbu		0.883
Morgenstern-Price	0.869	0.869
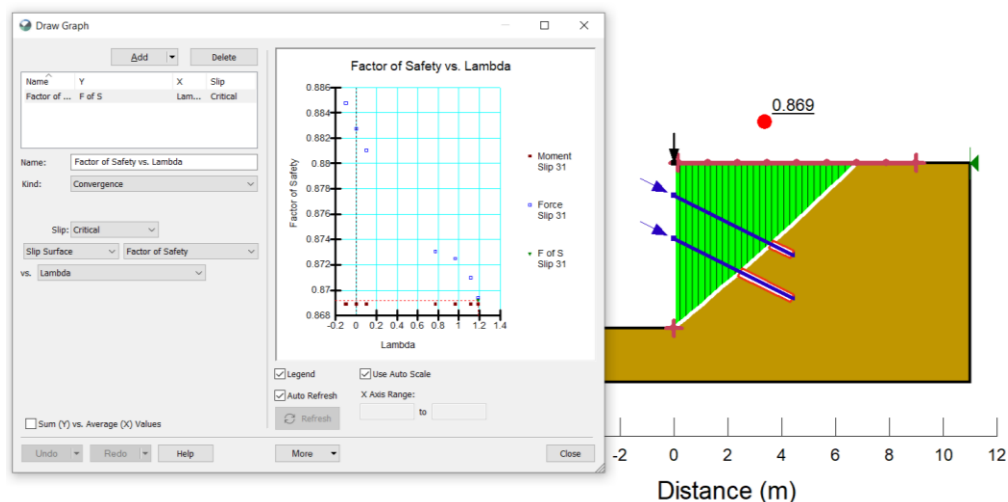
Figure 95 Results - Amhearst Soil Nails

2.28 Sheahan – Clouterre Test Wall

Project File: Sheahan Clouterre Test Wall.gsz

This problem was presented by Sheahan (2003) and it examines the Clouterre Test Wall. The test wall was constructed using Fontainebleu sand and failed by backfill saturation. The test was carried out as part of the French national project on soil nailing. The factor of safety is calculated for six different plane angles ranging from 45 to 70 degrees.

2.28.1 Geometry and Material Properties

The geometry and material properties are presented in Figure 96 and Table 76, respectively. The test wall was reinforced using seven rows of soil nails. The shotcrete plate weight was modeled as point load acting on the wall face. The soil nail parameters are presented in Table 77. The nails start at an elevation of 1.5 m and are spaced at 1 m in the vertical direction.
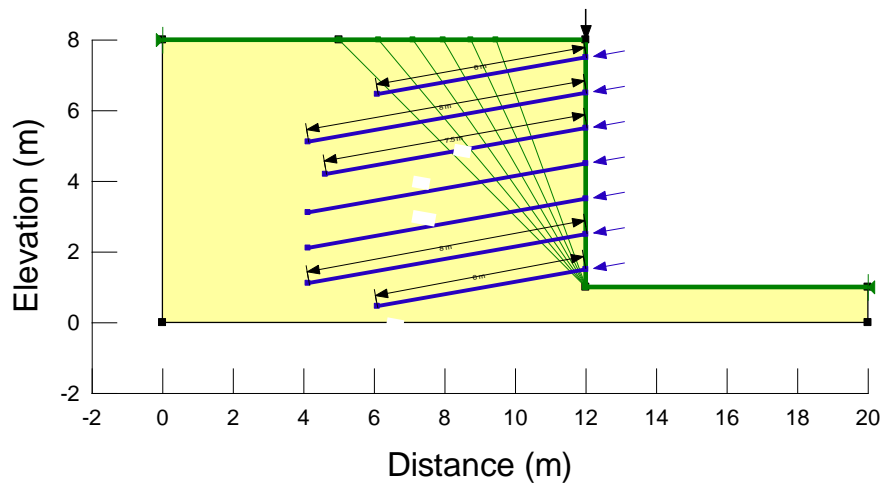
Figure 96 Geometry of the Sheahan Clouterre Test Wall model

Table 76 Material Properties of the Sheahan Clouterre Test Wall model

Material	c (kN/m²)	φ (degrees)	γ (kN/m³)
Fontainebleau Sand	3	38	20

Table 77 Soil Nail Properties

Type	Out-of-plane Spacing (m)	Tensile Strength (kN)	Bond Strength (kN)
Passive	1.5	15	7.5

2.28.2 Results and Discussions

Results for the Sheahan (2003) Clouterre Test wall are presented in Figure 97 and Table 78, respectively.
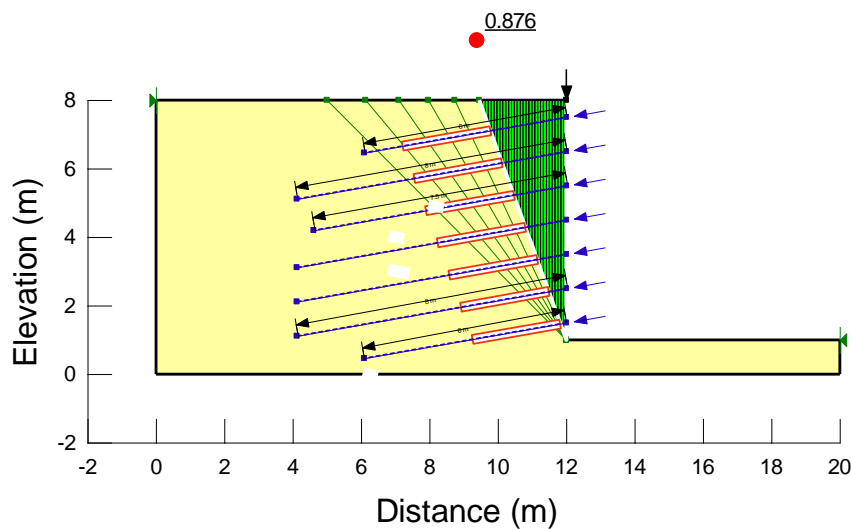
Figure 97 Results using the Janbu Simplified method

Table 78 Results for different slope angles of the failure surface

Slope Angle	Factor of Safety	
	Sheahan	SLOPE/W
45	1.176	1.159
50	1.070	1.051
55	0.989	0.971
60	0.929	0.917
65	0.893	0.880
70	0.887	0.876

2.29 Snailz – Reinforced Slope

Project File: Snailz - Reinforced Slope.gsz

This model was taken from the SNAILZ reference manual (http://www.dot.ca.gov/hq/esc/geotech). The model has two materials and is a slope reinforced with a soldier pile tieback wall. Imperial units are used for this model.

2.29.1 Purpose

The purpose of this model is to determine the factor of safety for a given slip surface.

2.29.2 Geometry and Material Properties

There are two different types of reinforcements in this model. Each of the two rows of soil nails has different bar diameters, which results in different tension capabilities. The soldier piles are modeled using a micro-pile in Slope Stability.
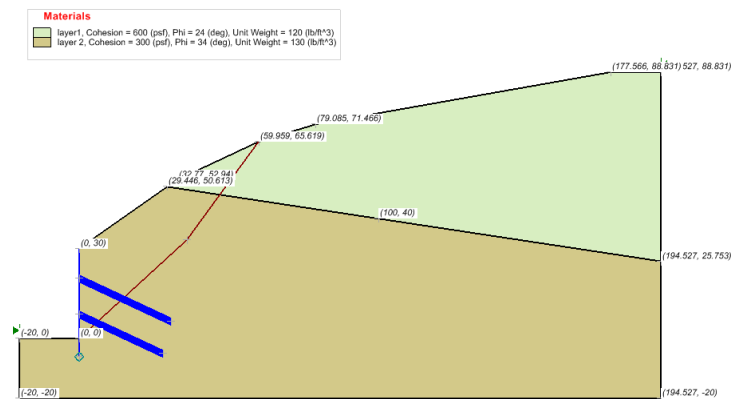
Figure 98 Geometry of the Snailz Reinforced Slope model

Table 79 Material Properties of the Snailz Reinforced Slope

Material	c (psf)	φ (degrees)	γ (pcf)
Layer 1	600	24	120
Layer 2	300	34	130

Table 80 Soil Nail Properties (Active)

	Out-of-plane Spacing (m)	Tensile Strength (lb)	Plate Strength (kN)	Bond Strength (kN)

Anchor: top now	8	120344.9	120344.9	13571.68
Anchor: bottom row	8	164217.3	164217.3	13571.68
Micro-pile (active)	1	Pile shear strength: 5900 lb.		

2.29.3 Results and Discussions

Factor of Safety vs. Lambda

Legend: ■ Moment Slip 1, □ Force Slip 1, ▼ F of S Slip 1
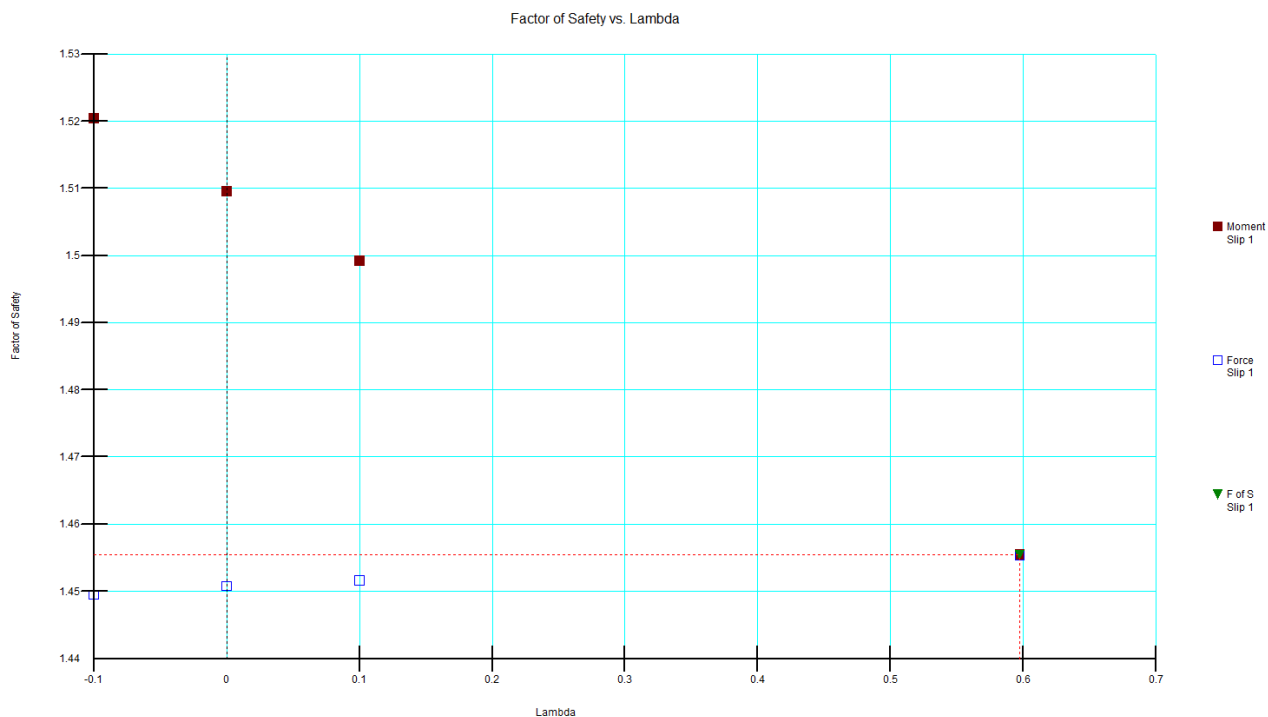
Figure 99 Factor of Safety vs Lambda, Snailz – Reinforced Slope

Table 81 Results of the Snailz Reinforced Slope

Method	Factor of Safety	
	SNAILZ	SLOPE/W
MP	1.52	1.455

2.30 Snailz – Geotextile Layers

Project File: Snailz - Geotextile Layers.gsz

This problem is taken from the SNAILZ reference manual. It examines a slope, which has been reinforced with geotextile layers extending to different depths into the slope. It should be noted that SNAILZ models the geotechnical characteristics with soil nails as having the same parameters as it would have if it were not equipped with geotextile reinforcement.

The problem at hand involves two layers with multiple reinforcement parameters. In this model, each horizontal reinforcement consists of parallel rows varying in length, tensile capacity and bond strength. The rows are all evenly spaced at 1.8 ft, except for row 14, which is spaced 1.8 ft. The problem at hand considers rows that are evenly spaced. The rows are numbered starting at the crest. The factor of safety is required for the two failure surfaces given in Figure 100.

2.30.1 Geometry and Material Properties
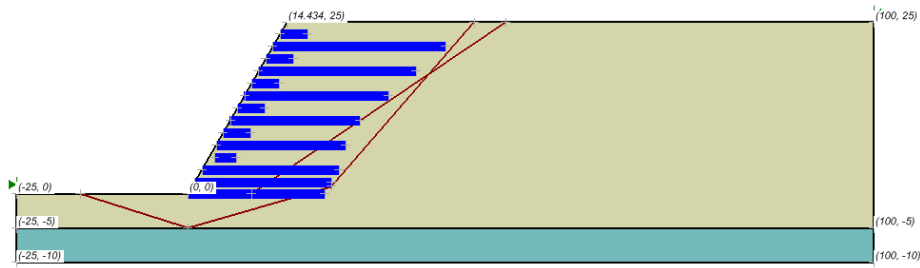
Figure 100 Geometry of the Snailz Geotextile Layers model

Table 82 Material Properties of the Snailz Geotextile Layers

Material	c (psf)	φ (degrees)	γ (pcf)
Layer 1	600	24	120
Layer 2	300	34	130

Table 83 Results for the Snailz Geotextile Layers

	Out-of-plane Spacing (ft)	Tensile Strength (lb)	Plate Strength (lb)	Bond Strength (lb/ft)	Length (ft)
Rows: 1,3,4,7, 9,11	1	1103	1103	1206.37	4
Rows: 12, 13, 14	1	2212	2212	1206.37	20
Rows: 8	1	1103	1103	965.096	19
Rows: 6	1	1103	1103	732.822	21
Rows: 4	1	1103	1103	482.548	23
Rows: 2	1	1103	1103	241.274	25
Rows: 10	1	1103	1103	1206.31	19

2.30.2   Results and Discussions
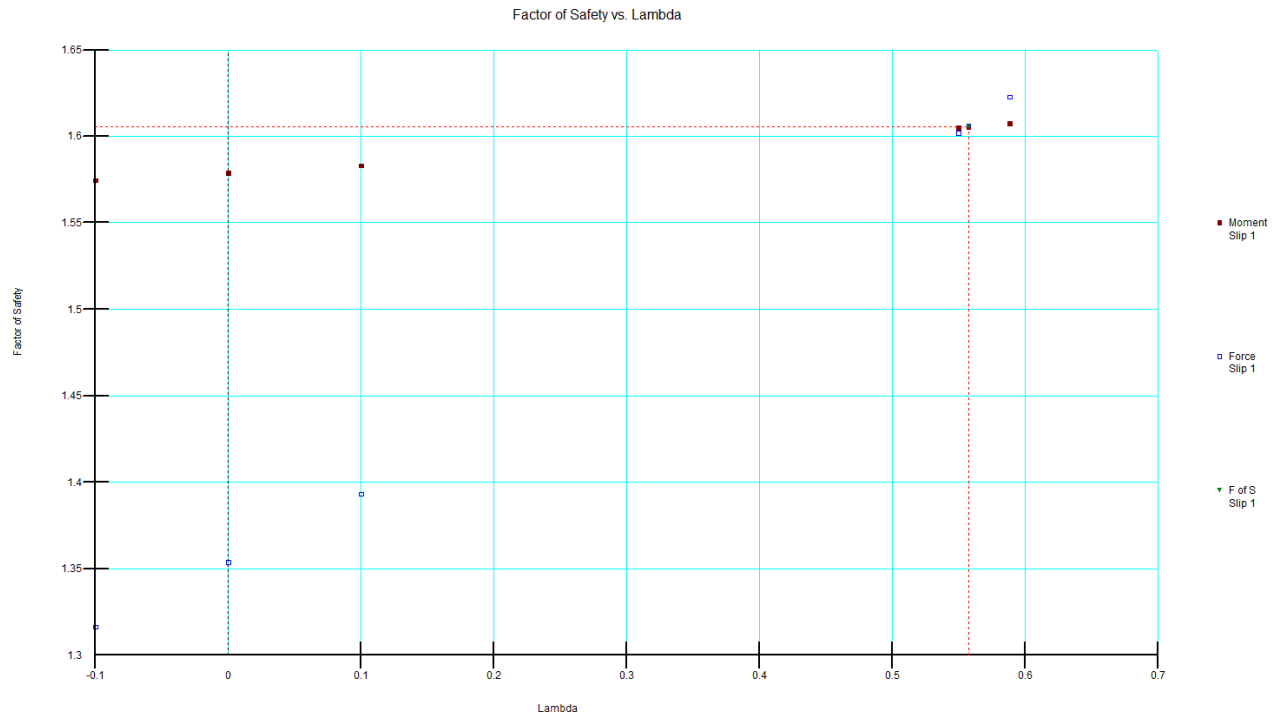
Figure 101 Factor of Safety vs Lambda, Snailz – Geotextile Layers

Table 84 Results for Case (0, -15)

Method	Factor of Safety		
	SNAILZ	SLOPE/W	
		Moment	Force
Janbu	1.46		1.354
MP		1.606	1.606

2.31   Zhu – Four Layer Slope

Project File: Zhu - Four Layer Slope.gsz

This model was presented by Zhu (2003). The problem consists of four soil layers with a designated slip surface, using a number of different methods. The multiple layers slope is analyzed using circular slip surfaces.

Tension cracks are placed through the top layer and the slope is assumed to be subjected to earthquake conditions with a seismic coefficient of 0.1.

2.31.1 Geometry and Material Properties
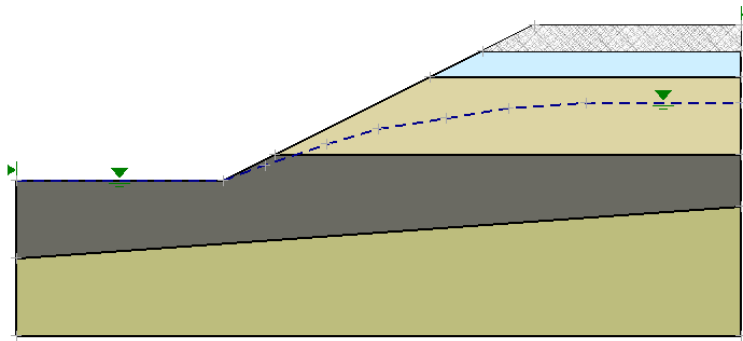
Figure 102 Geometry of the Zhu Four Layer Slope model

Table 85 Material Properties of the Zhu Four Layer Slope

Material	c (kN/m²)	φ (degrees)	γ (kN/m³)
Layer 1 (top)	20	32	18.2
Layer 2	25	30	18.0
Layer 3	40	18	18.5
Layer 4 (bottom)	40	28	18.8

2.31.2 Results and Discussions

Table 86 Zhu – Four Later Slope: Results

Method	Factor of Safety	
	SLOPE/W	Zhu
Bishop	1.284	1.278
Corp#2	1.368	1.377
Janbu	1.115	1.112
Lowe-Karafiath	1.283	1.290
Spencer	1.299	1.293
Morgenstern-Price	1.310	1.303

Factor of Safety vs. Lambda
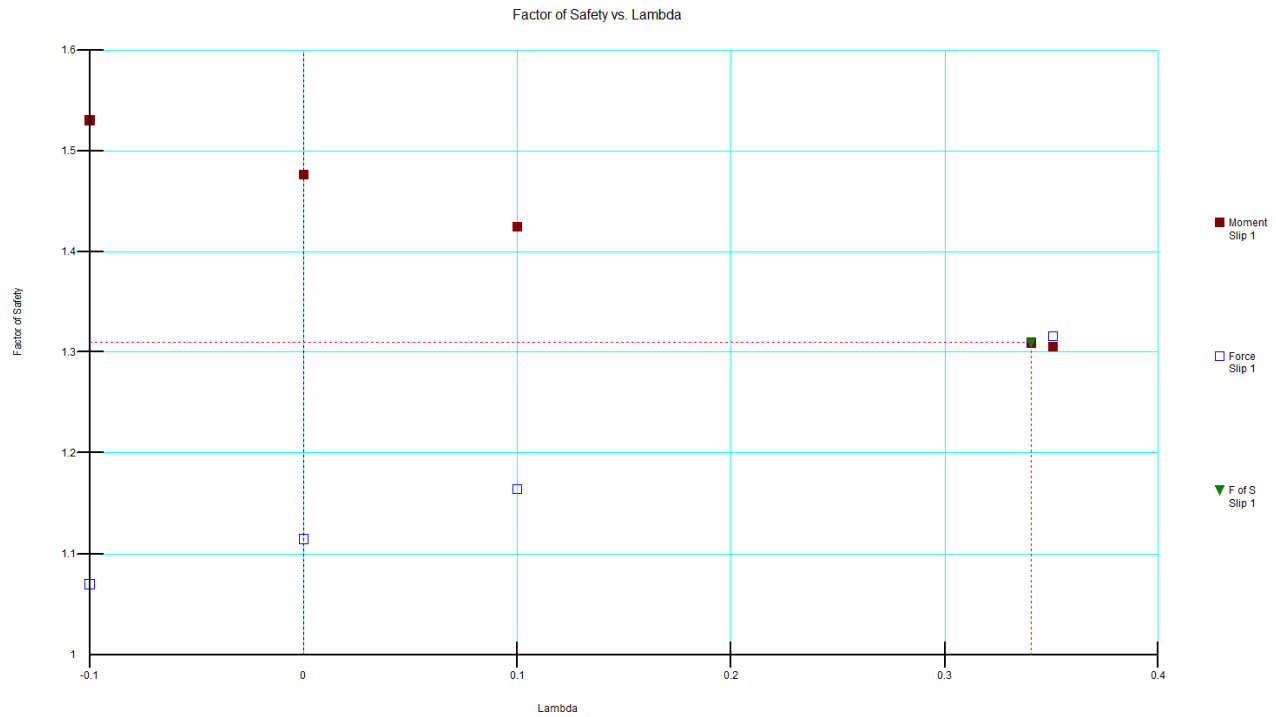
Figure 103 Factor of Safety vs Lambda, Zhu – Four Layer Slope

2.32   Zhu And Lee – Heterogeneous Slope

Project File: Zhu and Lee - Heterogeneous Slope.gsz

Zhu and Lee (2002) presented this model to analyze a heterogeneous slope under wet and dry conditions. Four different slip surfaces were analyzed for each of these conditions, two circular slip surface analysis are presented here.

A dry tension crack was placed at the top of the slope and the factor of safety was required for eight separate cases, four distinct slip surfaces under dry conditions, and four distinct slip surfaces when a water table was included (Table 2).

2.32.1   Geometry and Material Properties
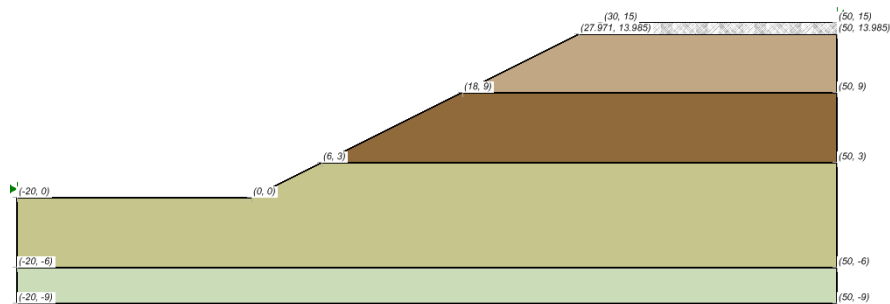
Figure 104 Geometry of the Zhu and Lee Heterogenous Slope model

Table 87 Material Properties of the Zhu and Lee Heterogenous Slope model

Material	c (kN/m²)	φ (degrees)	γ (kN/m³)
Layer 1 (top)	20	18	18.8

69

Layer 2	40	22	18.5
Layer 3	25	26	18.4
Layer 4 (bottom)	10	12	18.0

Table 88 Water Table Geometry wet condition

Coordinates	Arc
(0, -20)	
(0,0)	
(6,3)	
	(100568, 5.284)
	(25.314, 9.002)
	(39.149, 10.269)
(50,10.269)	

2.32.2 Results and Discussions

Table 89 Surface 1 Circular, shallow

Method	Factor of Safety	
	Zhu & Lee	Slope/W
M-P (dry)	2.035	2.017
M-P (wet)	1.559	1.533
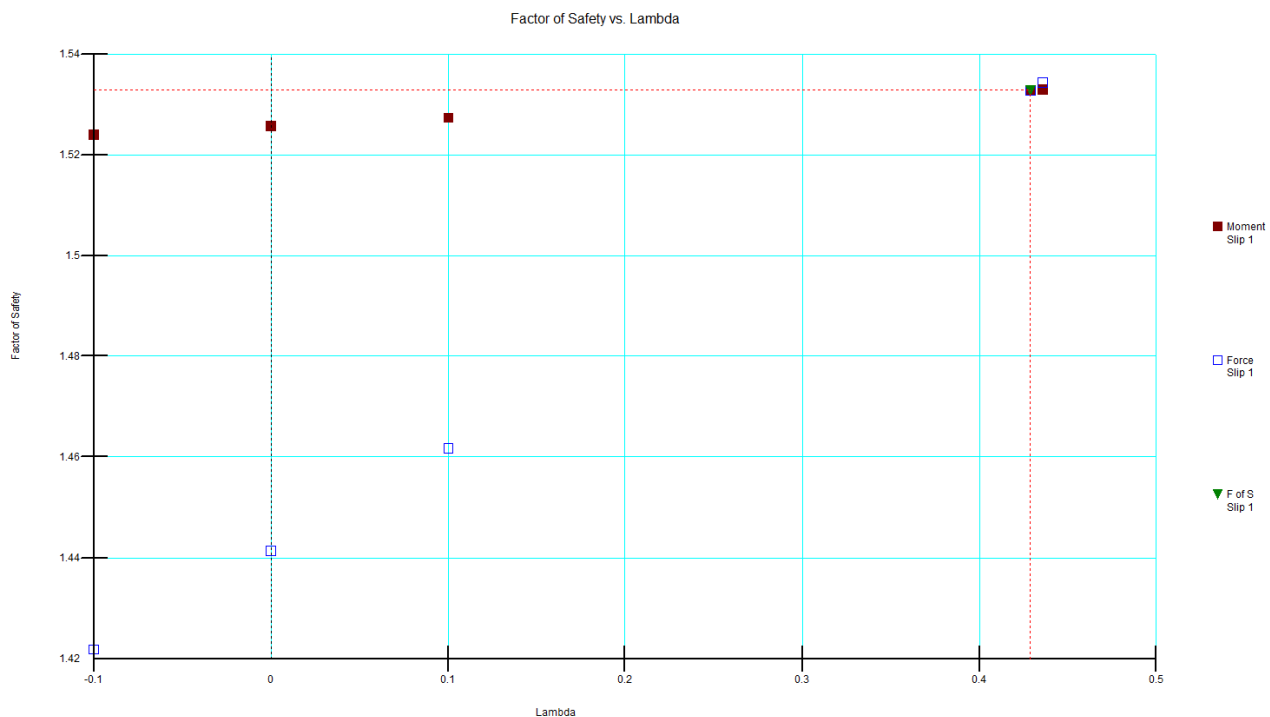
Figure 105 Factor of Safety vs Lambda, Zhu And Lee – Heterogeneous Slope

Table 90 Results Surface 3 Circular, deep Grid search

Method	Factor of Safety	
	Zhu & Lee	Slope/W
M-P (dry)	1.823	1.783
M-P (wet)	1.197	1.166

2.33   Priest – Rigid Blocks

Project File: Priest - Rigid Blocks.gsz

This model was presented by Priest (1993) for the analysis of rigid blocks. It also contains a sensitivity analysis on various parameters. The model presents a homogeneous slope undergoing failure along a specified noncircular surface. In this case the slope has a tension crack, which is 15m deep at the crest.

2.33.1   Purpose

The purpose of this analysis is to determine a factor of safety for the block.

2.33.2   Geometry and Material Properties

A water table is also present in this analysis. Water fills the tension crack 25% at the line of failure.

The water table is also assumed to be horizontal until it passes the intersection between the tension crack and the failure plane. The water table then dips steeply and linearly approaches the toe.
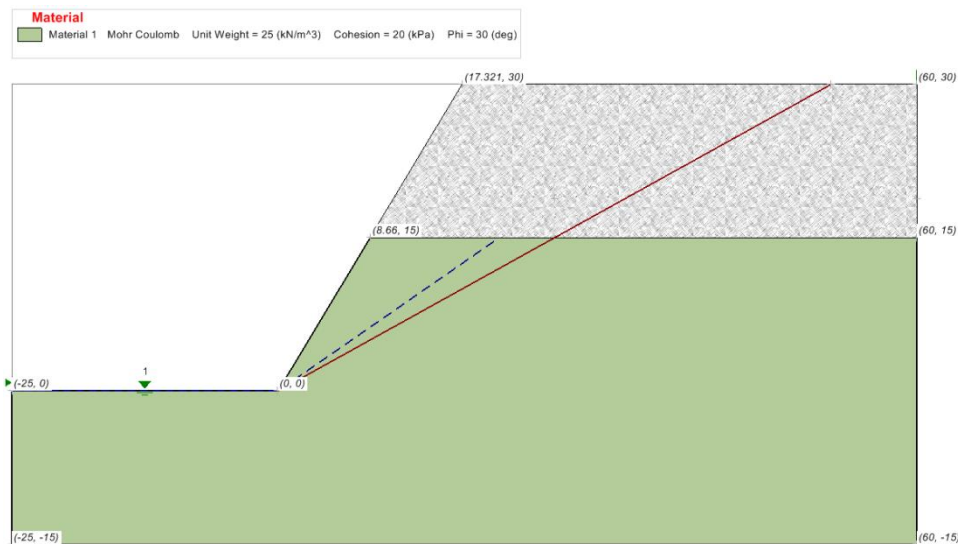
Figure 106 Geometry of the Priest Rigid Block Model (VS_53)

Table 91 Material Properties of the Priest Rigid Block model

Material	c (kN/m²)	ϕ (degrees)	γ (kN/m³)
Material 1	20	30	25

71

2.33.3 Results and Discussions
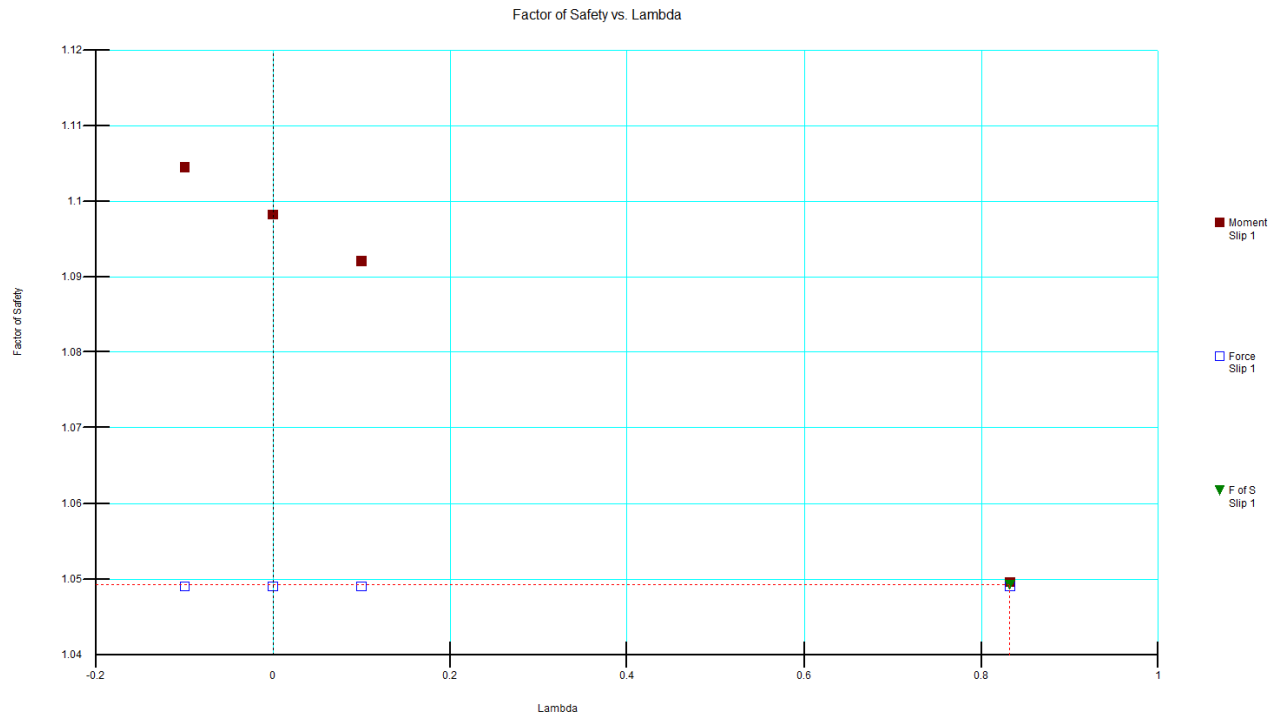
Figure 107 Factor of Safety vs Lambda, Priest - Rigid Blocks

Table 92 Results of the Priest Rigid Block model

Method	Factor of Safety	
	Priest	SLOPE/W
Janbu Simplified	1.049	1.049
MP		1.049

2.34 Yamagami – Stabilizing Piles

Project File: Yamagami Stabilizing Piles.gsz

Yamagami et al. (2000) presented a design method for slope stabilizing piles. This model was used to demonstrate the stability without and with the piles installed in the paper. It was a homogeneous slope. The piles were spaced 1 m in the out-of-plane direction. The shear strength of pile was 10.7 kN independent on the calculated factor of safety of slope.

2.34.1 Geometry and Material Properties
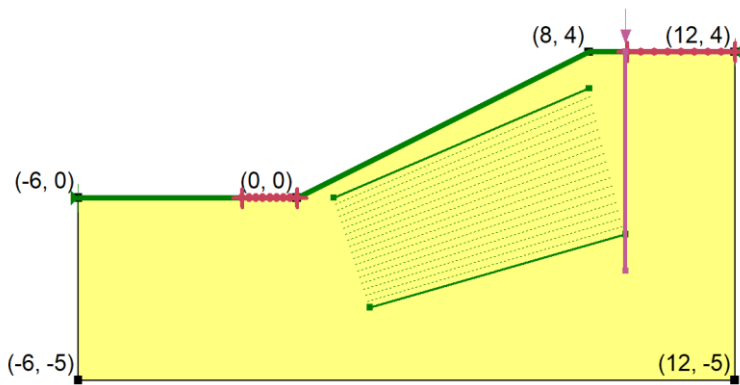
Figure 108 Yamagmi: Geometry, with piles installed

Table 93 Yamagmi: Material Properties

Material	c (kPa)	φ (degrees)	γ (kN/m³)
Material 1	4.9	10	15.68

2.34.2 Results and Discussions

The results of the analyses are shown in the following table and figures. The Factor of Safety results published in the paper without and with the piles were 1.1 and 1.2 using Bishop's method.

Table 94 Results Yamagmi without pile – Factor of safety results

Method	Factor of Safety	
	Moment	Force
Bishop	1.102	
Janbu		1.000
Spencer	1.100	1.100
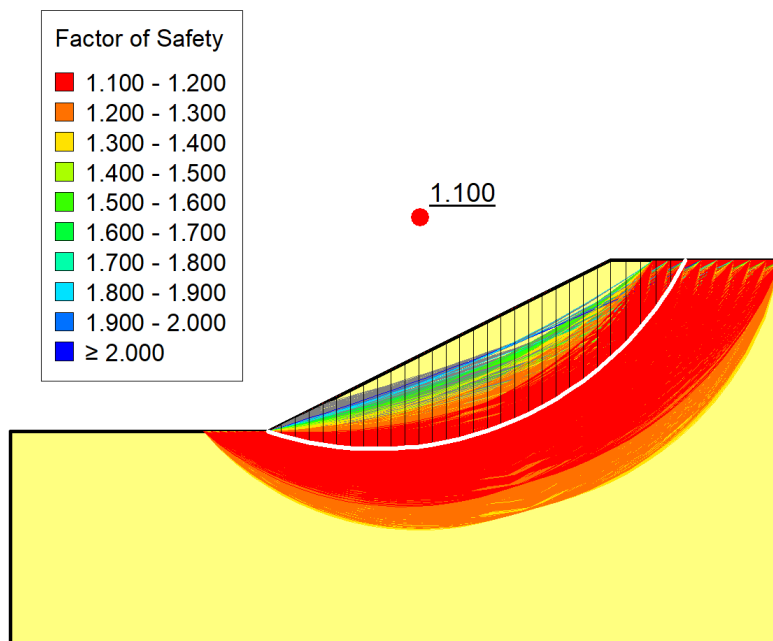
Figure 109 Yamagmi without pile – Critical slip surface
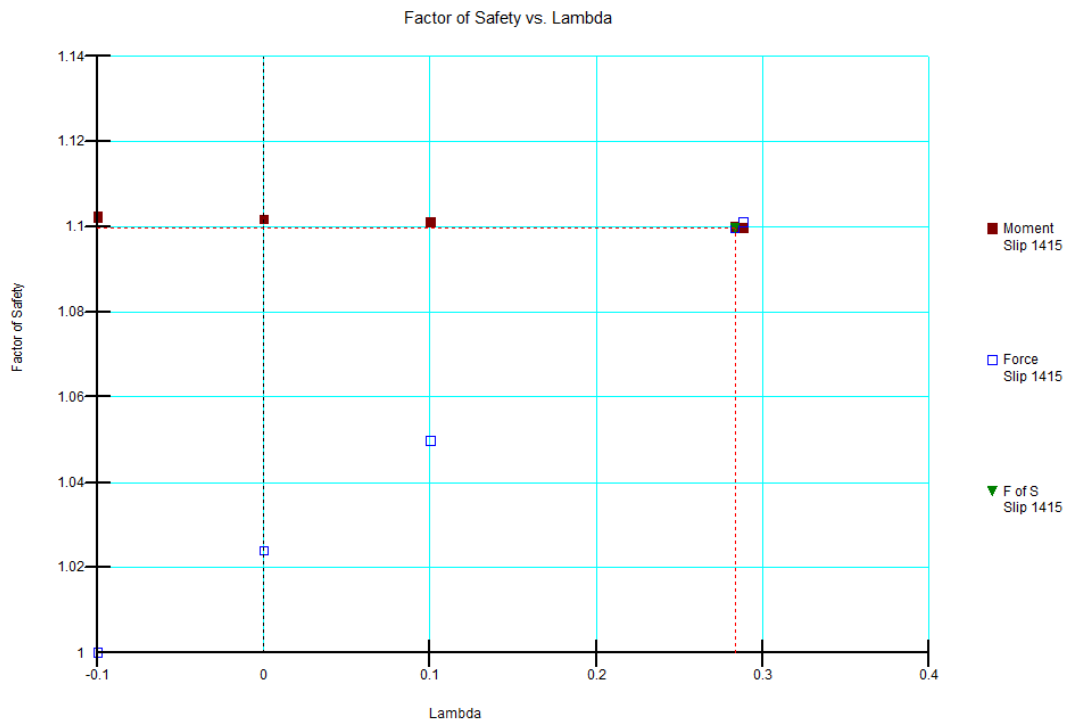
Figure 110 Yamagmi without pile - Factor of safety calculations

Table 95 Results Yamagmi with pile – Factor of safety results

Method	Factor of Safety	
	Moment	Force
Bishop	1.223	
Janbu		1.156
Spencer	1.226	1.226
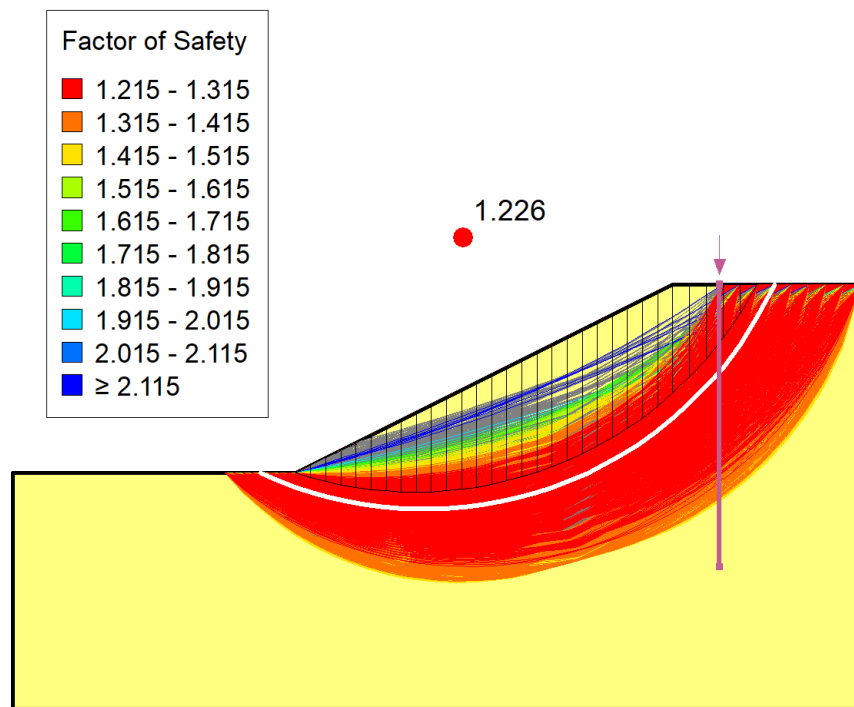
Figure 111 Yamagmi with pile – Critical slip surface

Factor of Safety vs. Lambda
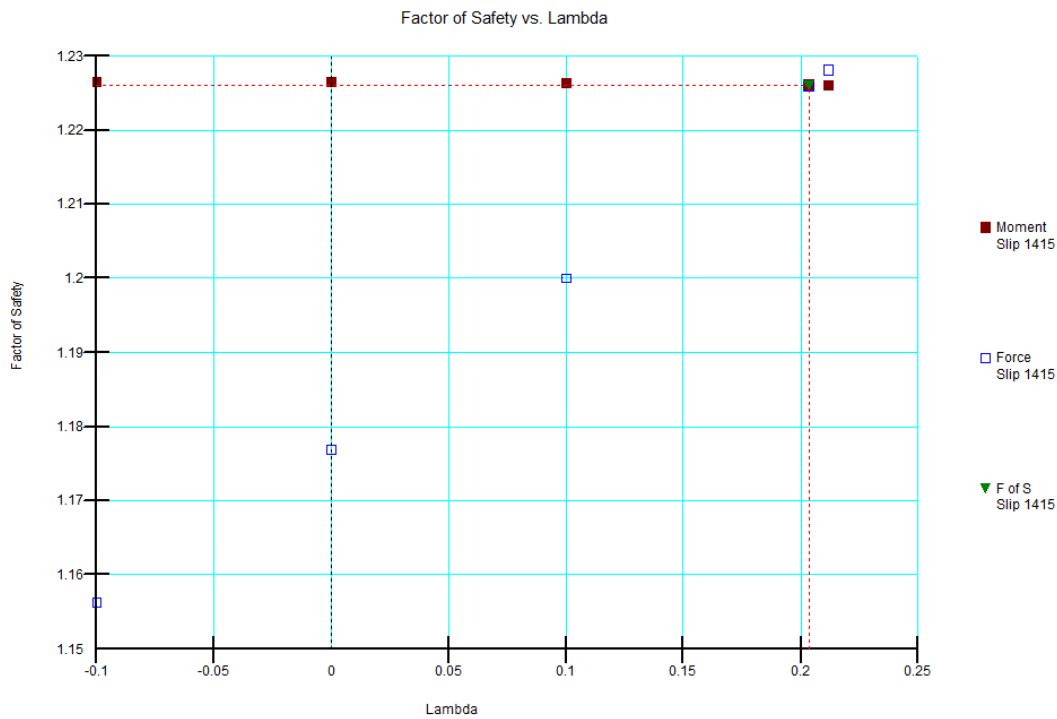
Figure 112 Yamagmi with pile - Factor of safety calculations

2.35   Pockoski and Duncan – Tie-Back Wall

Project File: Pockoski and Duncan - Tie-Back Wall.gsz

This is the fourth test slope analysis provided by Pockoski and Duncan (2000). This model analyzes a tie-back wall in a layered soil. The purpose of the model is to determine the location of critical failure surface and the factor of safety. A piezometric surface traverses along the ground surface in front of the wall, vertically upward at the toe, and then horizontal through the Cohesive Fill. Three identical rows of active grouted tie back reinforcement are installed at about 20 degrees from the horizontal.

2.35.1   Geometry and Material Properties

Color	Name	Slope Stability Material Model	Unit Weight (pcf)	Effective Cohesion (psf)	Effective Friction Angle (°)	Piezometric Surface
	Cohesive Fill (CF)	Mohr-Coulomb	114.7	0	30	1
	Glaciomarine Deposits (GD)	Mohr-Coulomb	147.1	1,500	0	1
	Granular Fill (GF)	Mohr-Coulomb	120.4	0	30	1
	Lower Marine Clay (LM)	Mohr-Coulomb	117.8	1,085	0	1
	Middle Marine Clay (MM)	Mohr-Coulomb	117.8	960	0	1
	OC Crust (OC)	Mohr-Coulomb	117.8	2,485	0	1
	Organic Silt (OS)	Mohr-Coulomb	110.2	900	0	1
	Upper Marine Clay (UM)	Mohr-Coulomb	117.8	1,670	0	1

Figure 113 Geometry of the Pockoski and Duncan Tie Back Wall model

75

Table 96 Material Properties of the Pockoski and Duncan Tie Back Wall model

Layer	c (psf)	φ (degrees)	γ (pcf)
Granular Fill (GF)	0	30	120.4
Cohesive Fill (CF)	0	30	114.7
Organic Silt (OS)	900	0	110.2
OC Crust (OC)	2485	0	117.8
Upper Marine Clay (UM)	1670	0	117.8
Middle Marine Clay (MM)	960	0	117.8
Lower Marine Clay (LM)	1085	0	117.8
Glaciomarine Deposits (GD)	1500	0	147.1

Table 97 Grouted Tieback Properties all rows

Tensile Cap. (lbs)	Plate Cap. (lbs)	Bond Strength (lb/ft)	Bond Length (ft)	Out-of-Plane Spacing (ft)
247343	247343	4000	40	4

2.35.2 Results and Discussions

Pockoski and Duncan (2000) reported a Factor of safety of 1.14 using the Spencer method. Factor of safety values were also presented for GOLD-NAIL and SNAL (Wedge method – noncircular) of 1.19 and 1.03, respectively.
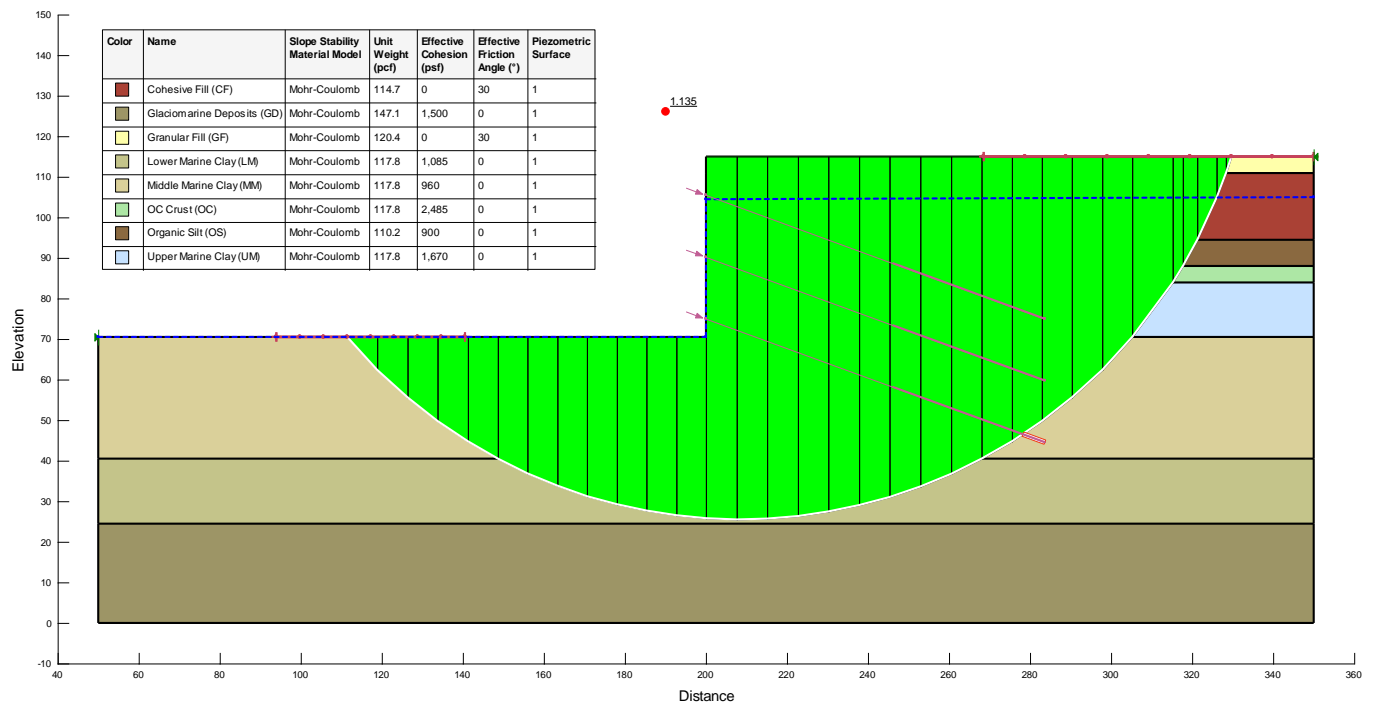
Figure 114 Critical slip surface and factor of safety.
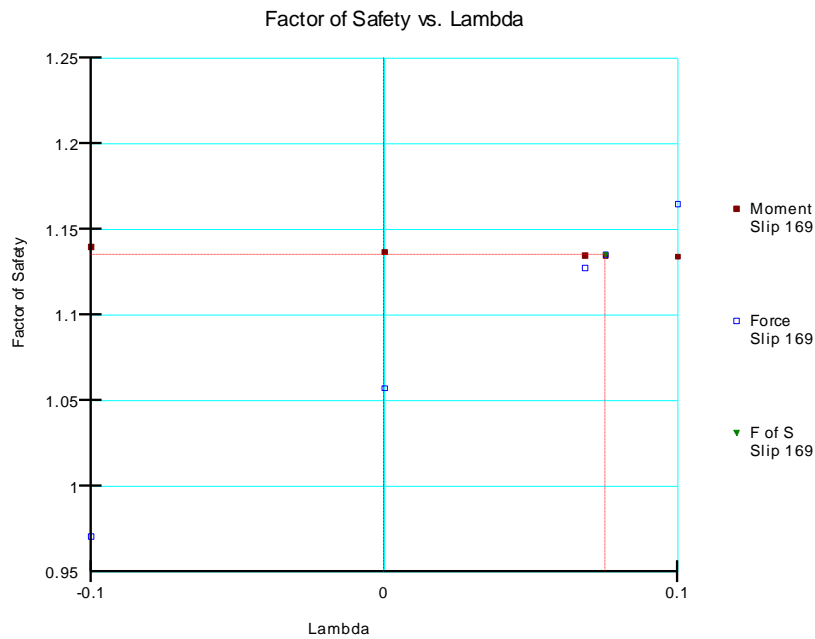
Figure 115 Factor of Safety vs Lambda: Pockoski and Duncan – Tie-Back Wall

2.36   Pockoski and Duncan - Reinforcement

Project File: Pockoski and Duncan - Reinforcement.gsz

This is the fifth test slope provided by Pockoski and Duncan (2000). This scenario varies the effect of the reinforcement. The analysis represents a tie back wall and homogeneous sand.

2.36.1   Geometry and Material Properties

A single row of active grouted tieback support is installed. A single piezometric surface defines the pore-water pressures.

Color	Name	Slope Stability Material Model	Unit Weight (pcf)	Effective Cohesion (psf)	Effective Friction Angle (°)
	Sand	Mohr-Coulomb	120	0	30
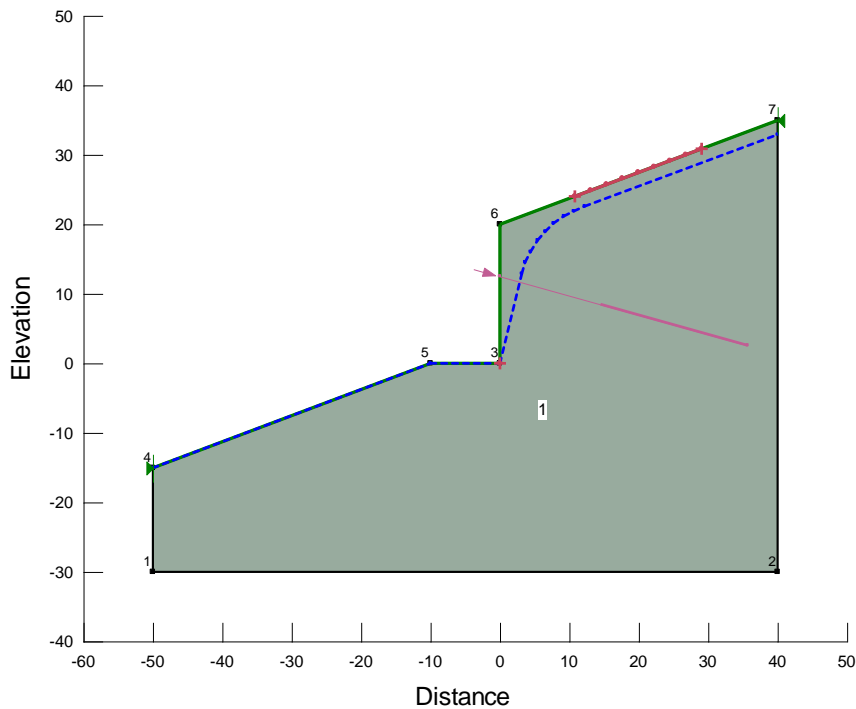
Figure 116 Geometry of the Reinforcement model

Table 98 Material Properties of the Pockoski and Duncan Reinforcement model

Material	c (psf)	φ (degrees)	γ (pcf)
Sand	0	30	120

Table 99 Soil Nail Properties

Tensile Cap. (lbs)	Plate Cap. (lbs)	Bond Strength (lb/ft)	Bond Length (ft)	Out-of-Plane Spacing (ft)
184077	184077	5000	22	8

2.36.2 Results and Discussions

Table 100 Results Circular

Method	UTEXAS	SLOPE/W	WINSTABL
Bishop	0.56	0.53	0.74
Janbu	0.64	0.58	0.76
Lowe-Karafiath	0.76	0.59	
Spencer	0.65	0.57	0.59

2.37 Pockoski and Duncan – Soil Nails

Project File: Pockoski and Duncan - Soil Nails.gsz

This is the seventh test slope providing by Pockoski and Duncan (2000). This model analyzes a soil nailed wall in homogenous clay. There are five parallel soil nails that reinforce the wall. Each row has identical strength

characteristics. There is a dry tension crack down to the first nail. Two uniformly distributed loads of 500 lb/ft and 250 lb/ft are applied on the high bench. The purpose of the model is to calculate the critical slip surface (through the toe) as well as the factor of the safety.

2.37.1 Geometry and Material Properties
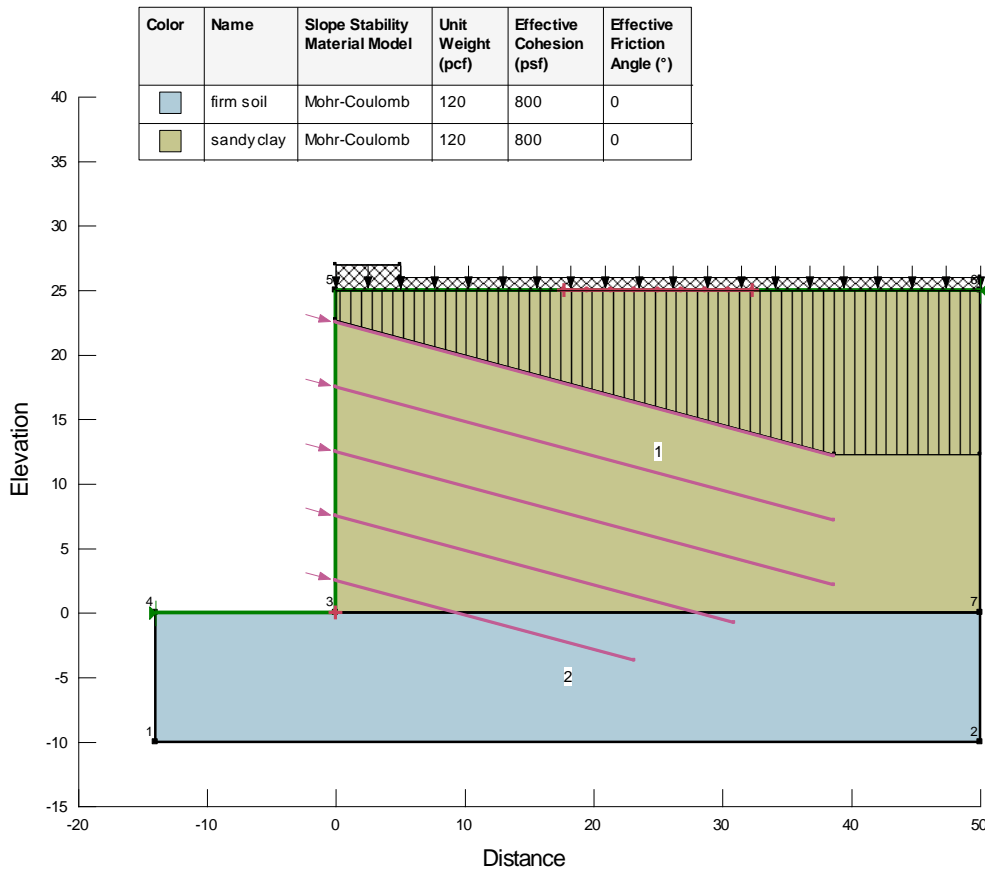
Figure 117 Geometry of the Pockoski and Duncan Soil Nails model (VS_60)

Table 101 Material Properties of the Pockoski and Duncan Soil Nails model

Material	c (psf)	φ (degrees)	γ (pcf)
Sand	800	0	120

Table 102 Soil Nail Properties

Tensile Cap. (lbs)	Bond Strength (lb/ft)	Out-of-Plane Spacing (ft)
47123.89*	1508*	5

*A reduction factor of 1.818 and 2.0 were applied to the tensile capacity and bond strength, respectively.

2.37.2 Results and Discussions

Table 103 Results: Pockoski and Duncan – Soil Nails

Method	UTEXAS4	SLOPE/W	WINSTABL
Bishop Simplified	1.00	0.995	1.06
Spencer	1.02	1.00	0.99

Color	Name	Slope Stability Material Model	Unit Weight (pcf)	Effective Cohesion (psf)	Effective Friction Angle (°)
	firm soil	Mohr-Coulomb	120	800	0
	sandy clay	Mohr-Coulomb	120	800	0
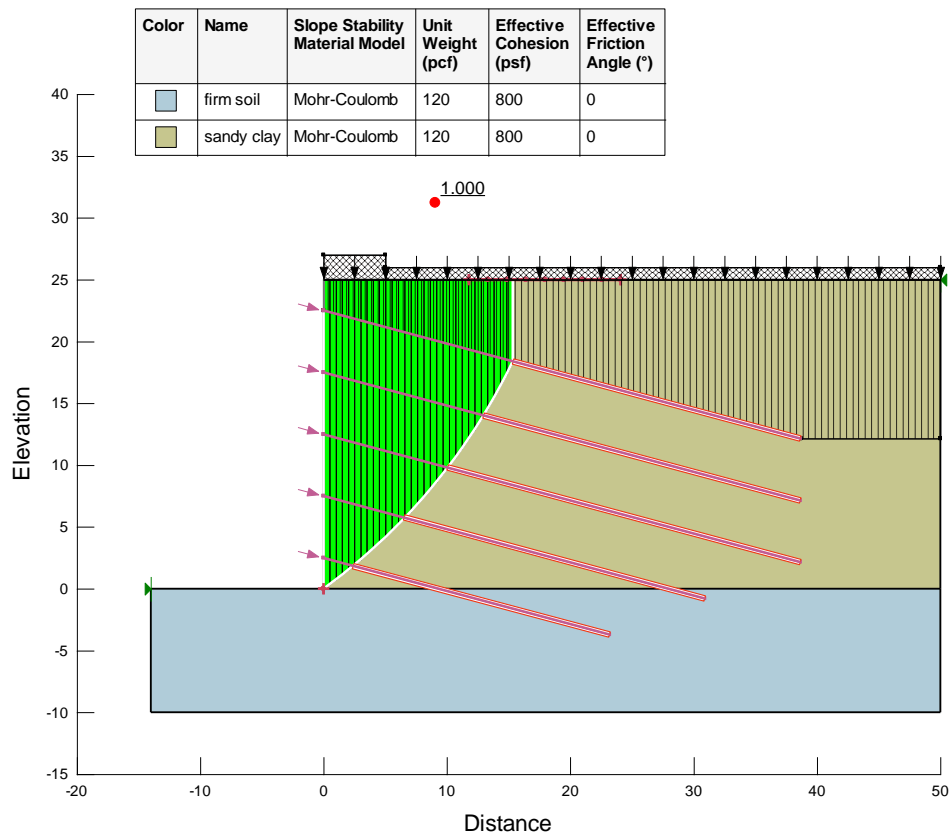
Figure 118 Critical slip surface and factor of safety (Spencer).
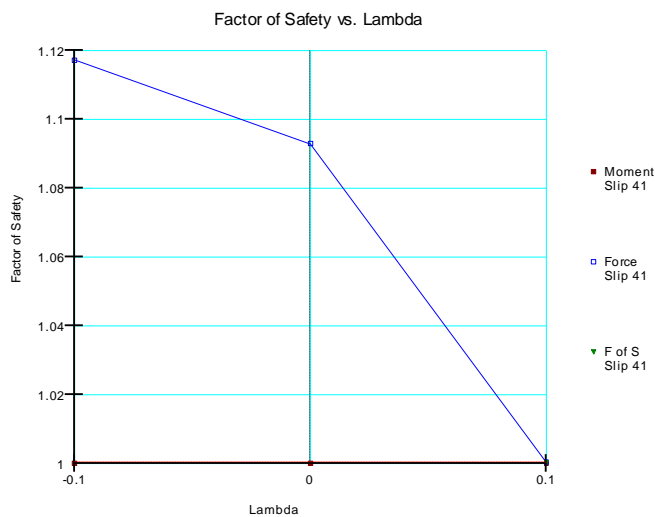
Figure 119 Factor of Safety vs Lambda: Pockoski and Duncan – Soil Nails

2.38 Loukidis – Seismic Coefficient

Project File: Loukidis - Seismic Coefficient.gsz

This model was published by Loukidis et al. (2003) and provides a method for determining the critical seismic coefficient k_c. The seismic coefficient determined corresponds a factor of safety of 1.0. This is their first example.

2.38.1 Purpose

The purpose of this verification problem is to reproduce a safety factor of 1 using Spencer's method and the seismic coefficients presented in the Loukidis et al. paper (2003).

2.38.2 Geometry and Material Properties

A simple homogenous earth slope is subjected to seismic loading. circular surfaces are considered in the analysis and all slip surfaces must pass through the toe of the slope. Two independent pore-water pressures conditions are given consideration:

- Dry slope, and

- R_u of 0.05.
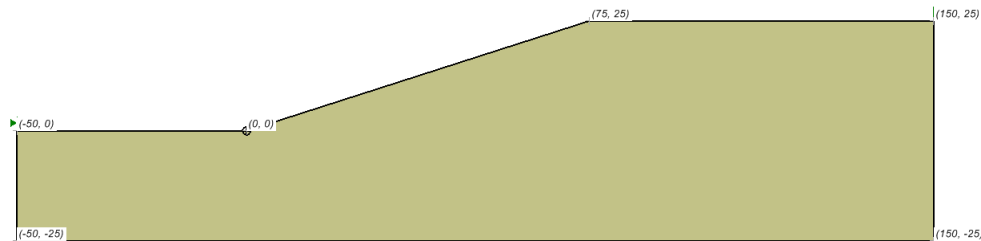
Figure 120 Geometry of the Loukidis Seismic Coefficient model

Table 104 Seismic Coefficients

Dry Slope	0.432
R_u = 0.5	0.132

2.38.3 Results and Discussions

Table 105 Results Dry Slope (k_c = 0.432)

Type	Spencer	Bishop Simplified
Circular (Grid Search)	1.001	0.993

Table 106 Results R_u = 0.5 (k_c = 0.132)

Type	Spencer	Bishop Simplified
Circular (Grid Search)	1.001	0.988

2.39 Loukidis – Seismic Coefficient #2

Project File: Loukidis - Seismic Coefficient#2.gsz

This is the second example problem presented by Loukidis et al., 2003. The effect of the critical seismic coefficient is examined in this example. This model analyzes a layered dry slope under seismic loading conditions.

2.39.1 Purpose

The purpose of the model is to bring the Spencer's factor of safety to 1.0 using the author's presented seismic coefficient of 0.115. The Loukidis analysis was for the case of a log-spiral surface.

2.39.2   Geometry and Material Properties

This problem is analyzed in Slope Stability by using a Entry and Exit search technique with optimization. The critical slip surface in this case passes through the material boundary on the slope between the middle and lower layers.
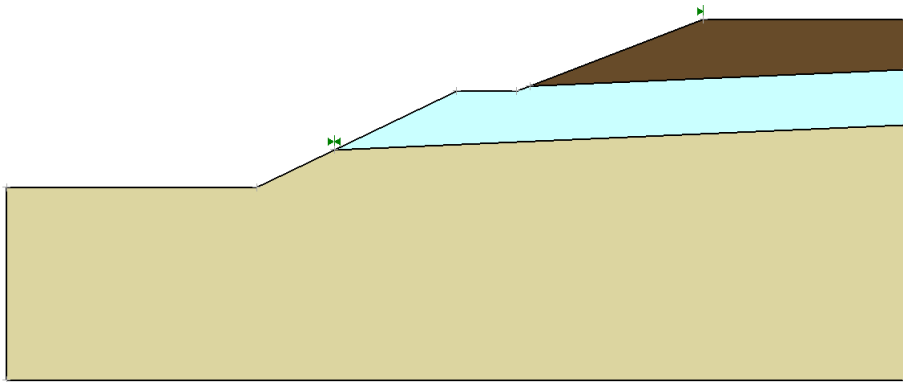
Figure 121 Geometry of the Loukidis Seismic Coefficient model

Table 107 - Material Properties of the Loukidis Seismic Coefficient model

Layer	c (kN/m²)	ϕ (degrees)	γ (kN/m³)
Top	4	30	17
Middle	25	15	19
Bottom	15	45	19

2.39.3   Results and Discussions
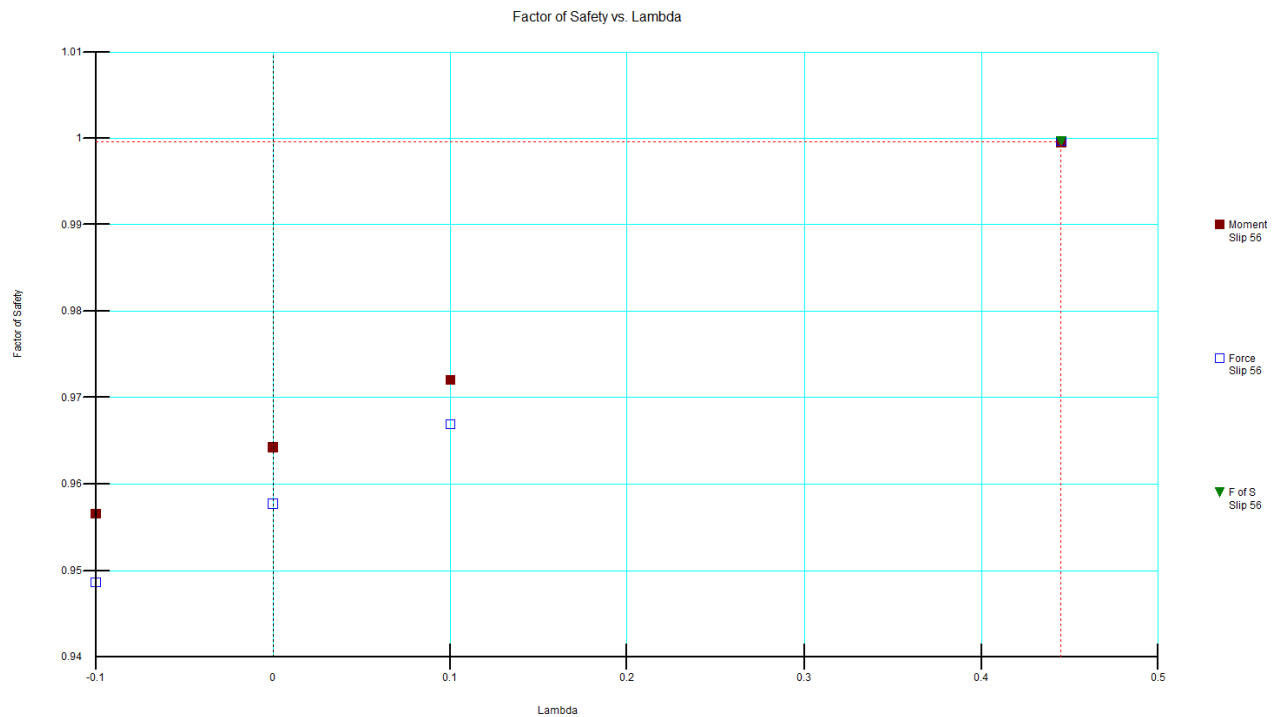
Figure 122 Factor of Safety vs Lambda: Loukidis – Seismic Coefficient#2

Table 108 Results of the non Circular after optimization

Method	Factor of Safety	
	Loukidis et al (2003)	SLOPE/W
Spencer	1.00	1.00

2.40   Rapid Drawdown - Walter Bouldin Dam

Project File: Rapid drawdown with multi-stage.gsz

Document: Rapid drawdown with multi-stage.pdf

Walter Bouldin Dam is a rolled earth fill embankment. The dam is about 60 feet high, sitting on 80 feet of clayey sand and gravel. Overlying the gravel are a layer of cretaceous clay, a zone of micaceous silt, and a clayey silty sand layer that covers the slope. During a rapid drawdown of 32 feet in 5.5 hours the Walter Bouldin Dam failed on February 10, 1975. The stability was analyzed using the 3-stage drawdown procedure proposed by Duncan et al. (1990).

2.40.1   Geometry and Material Properties

Color	Name	Slope Stability Material Model	Unit Weight (pcf)	Effective Cohesion (psf)	Effective Friction Angle (°)	Cohesion R (psf)	Phi R (°)	Piezometric Surface	Piezometric Surface After Drawdown
	Clayey Sandy Gravel	Bedrock (Impenetrable)						1	2
	Clayey Silty Sand	Mohr-Coulomb	128	240	32.7	650	13	1	2
	Cretoceous Clay	Mohr-Coulomb	124	180	19	230	13	1	2
	Micoceous Silt	Mohr-Coulomb	123	220	22.5	450	11	1	2
	Riprap	Mohr-Coulomb	140	0	40	0	0	1	2
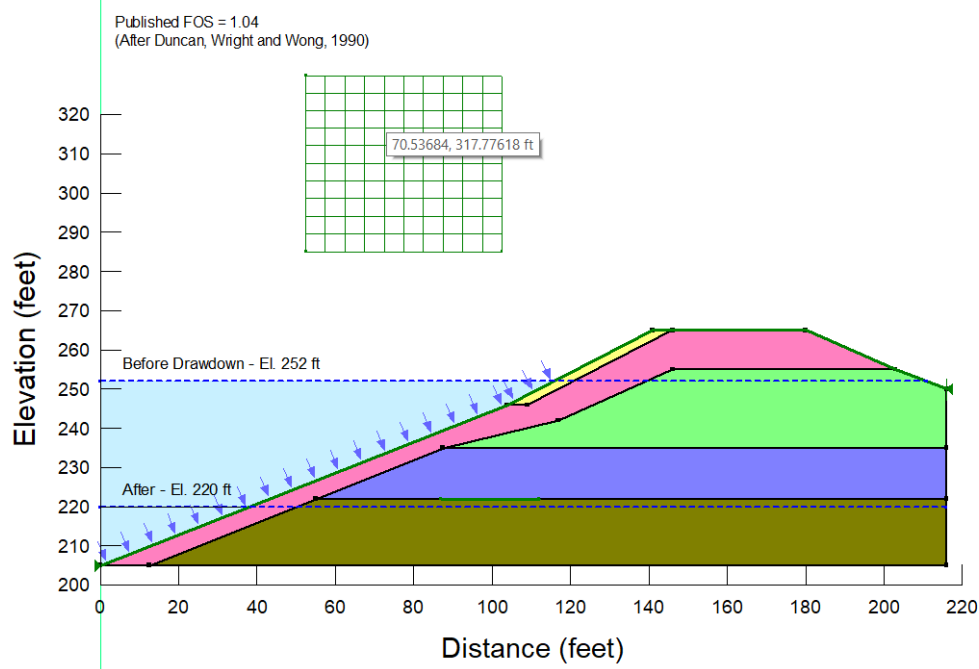
Figure 123 Geometry of the Walter Bouldin Dam

83

2.40.2   Results and Discussions

Duncan et al. (1990) reported a critical factor of safety of 1.04. The factor of safety and location / shape of the critical slip surface closely match the published results.
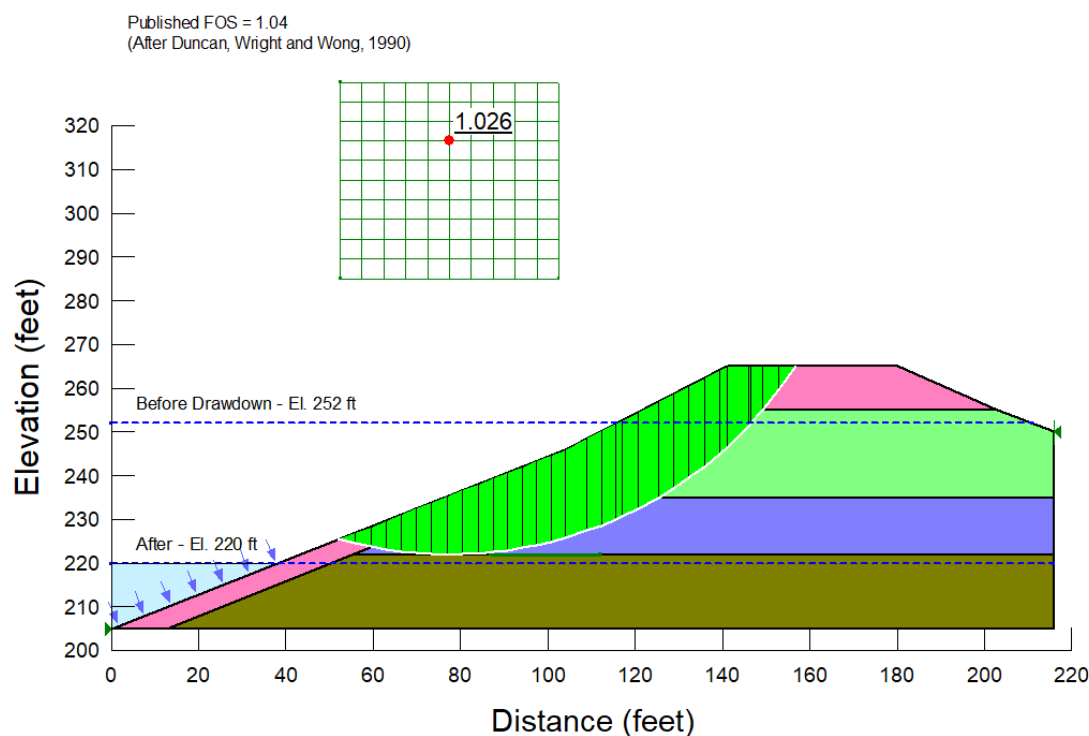
Figure 124 Slip surface location for the Walter Bouldin dam

Table 109 Comparison of FOS with Slope/W for Walter Bouldin Dam

Method	Factor of Safety				Difference (%)
	Slope Stability		Slope/W		
	Moment	Force	Moment	Force	
Bishop	1.002		1.016		-1.397
Spencer	0.999	0.998	1.02		-2.352

Table 110 Comparison of FOS between Slope Stability and Duncan et al. (1990)

	Corps #2	Lowe-Karafiath
Duncan et al. (1990)	0.93	1.09
Slope Stability	1.016	1.034
Difference	9.2%	-5.1%

2.41   Rapid Drawdown - USACE Benchmark

Project File: Staged rapid drawdown - CE Example.gsz

Document: Rapid drawdown with multi-stage.pdf

This benchmark example is created by the United Sates Army Corps of Engineers (USACE) in the Appendix G of the Engineering Manual – EM 1110-2-1902. The rapid drawdown water level is from 103 feet to 24 feet (USACE, 2003).

2.41.1 Geometry and Material Properties

Color	Name	Unit Weight (pcf)	Cohesion' (psf)	Phi' (°)	Phi-B (°)	Cohesion R (psf)	Phi R (°)	Piezometric Line	Piezometric Line After Drawdown
🟨	New Material	135	0	30	0	1,200	16	1	2
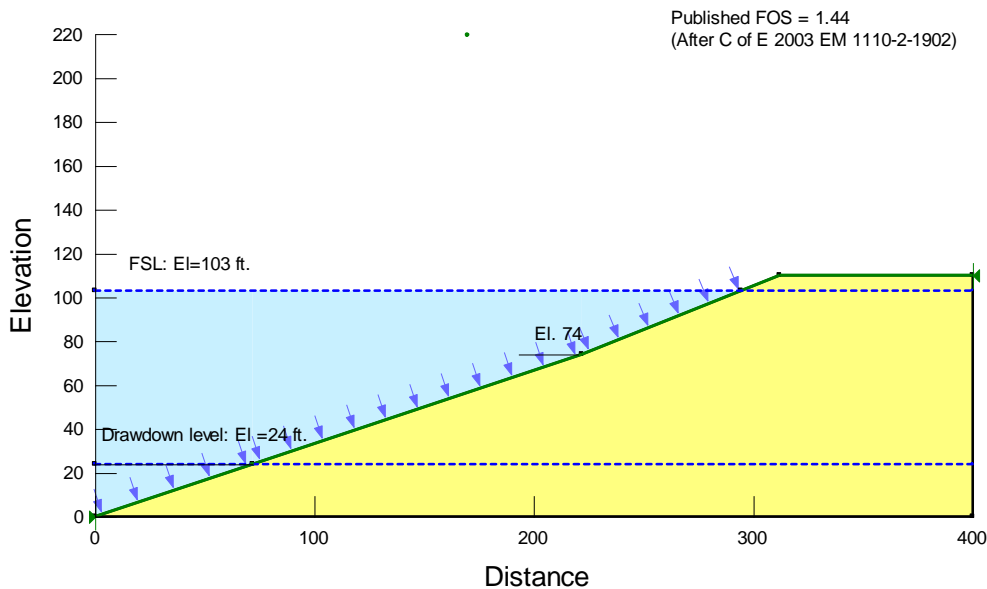
Figure 125 Rapid Drawdown - USACE Benchmark - Geometry

2.41.2 Results and Discussions

USACE (2003) reported a critical factor of safety of 1.44. The factor of safety and location / shape of the critical slip surface closely match the published results.
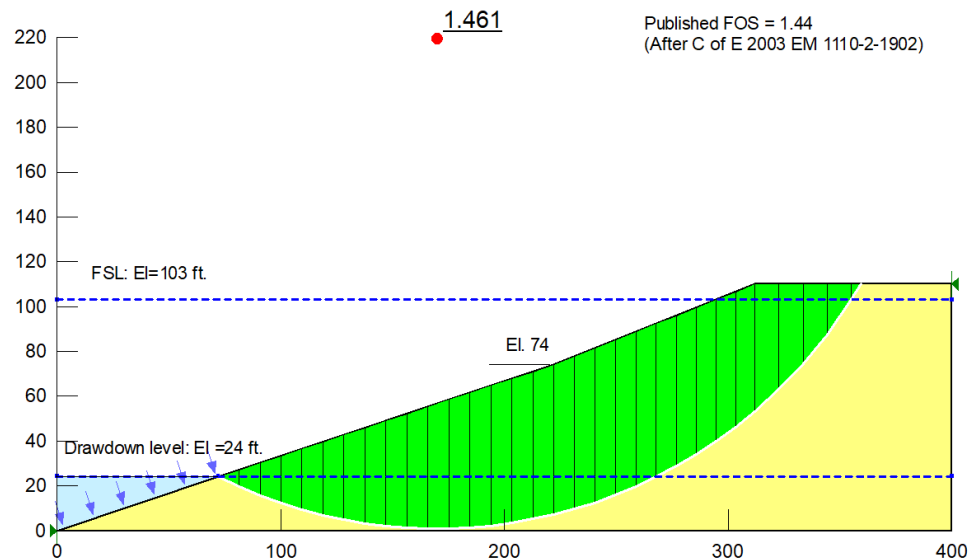
Figure 126 Rapid Drawdown - USACE Benchmark – Critical slip surface

2.42 Rapid Drawdown - Pumped Storage Project Dam

Project File: Staged rapid drawdown - Pumped Storage Project Dam.gsz

Document: Rapid drawdown with multi-stage.pdf

The Pumped Storage Project Dam has a densely compacted, silty clay core. The lower portion of the upstream slope is a zone of random materials with the same strength properties as the core. The upper portion of the upstream slope and the entire downstream slope is a free draining rock fill. For the rapid drawdown analysis, the water level is lowered from 545 feet to 380 feet. The Duncan 3-Stage Rapid Drawdown method is used to calculate the factor of safety and determine the location of the critical slip surface. The implementation of the method is based on the theory presented by Duncan, Wright, and Wong (1990).

2.42.1 Geometry and Material Properties

Color	Name	Slope Stability Material Model	Unit Weight (pcf)	Effective Cohesion (psf)	Effective Friction Angle (°)	Cohesion R (psf)	Phi R (°)	Piezometric Surface	Piezometric Surface After Drawdown
	Compacted Rockfill	Mohr-Coulomb	142	0	37	0	0	1	2
	Silty Clay Core	Mohr-Coulomb	140	0	36	2,000	18	1	2
	Silty Clay Random Zone	Mohr-Coulomb	140	0	36	2,000	18	1	2
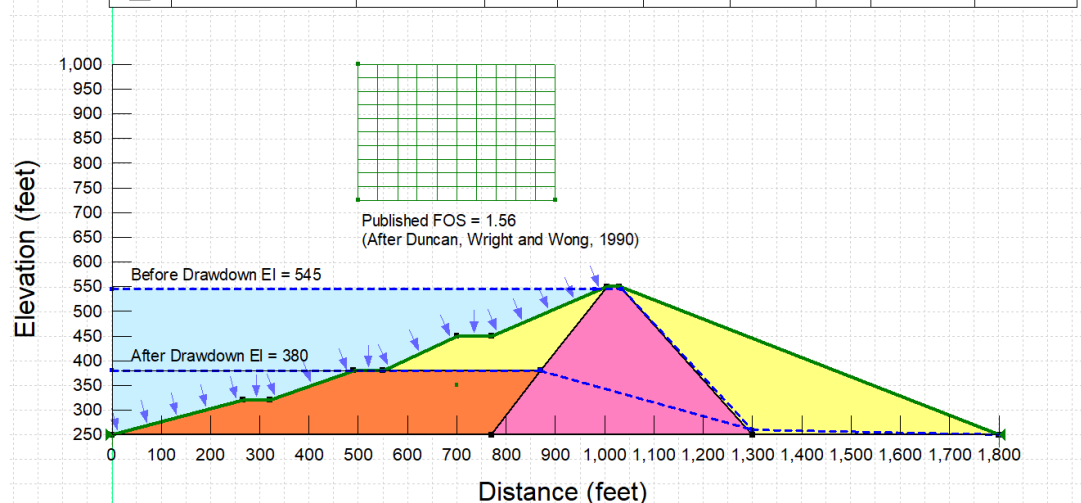
Figure 127 Pumped Storage Project Dam - Geometry

2.42.2 Results and Discussions

Duncan et al. (1990) reported a critical factor of safety of 1.56. The factor of safety and location / shape of the critical slip surface closely match the published results.
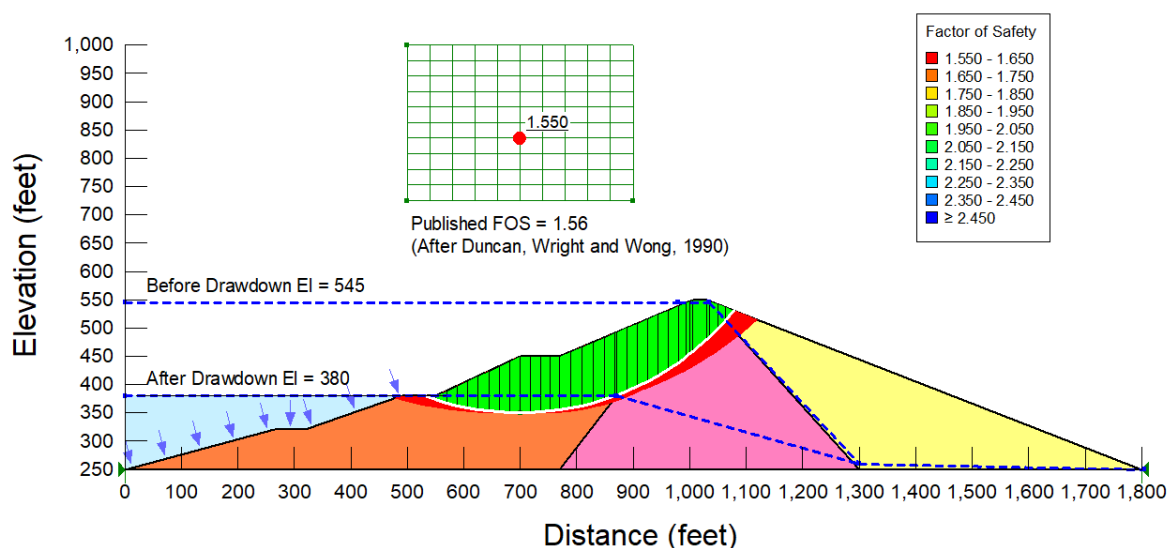
Figure 128 Pumped Storage Project Dam – Critical slip surface

2.43   Rapid Drawdown - Pilarcitos Dam

Project File: Staged rapid drawdown - Pilarcitos Dam.gsz

Document: Rapid drawdown with multi-stage.pdf

The Pilarcitos Dam is a homogeneous rolled earth-fill embankment. The slope failure occurred after the water level was lowered from elevation of 692 to elevation of 657 between Oct. 07 and Nov. 19, 1969.

2.43.1   Geometry and Material Properties

Color	Name	Slope Stability Material Model	Unit Weight (pcf)	Effective Cohesion (psf)	Effective Friction Angle (°)	Cohesion R (psf)	Phi R (°)	Piezometric Surface	Piezometric Surface After Drawdown
	New Material	Mohr-Coulomb	135	0	45	60	23	1	2
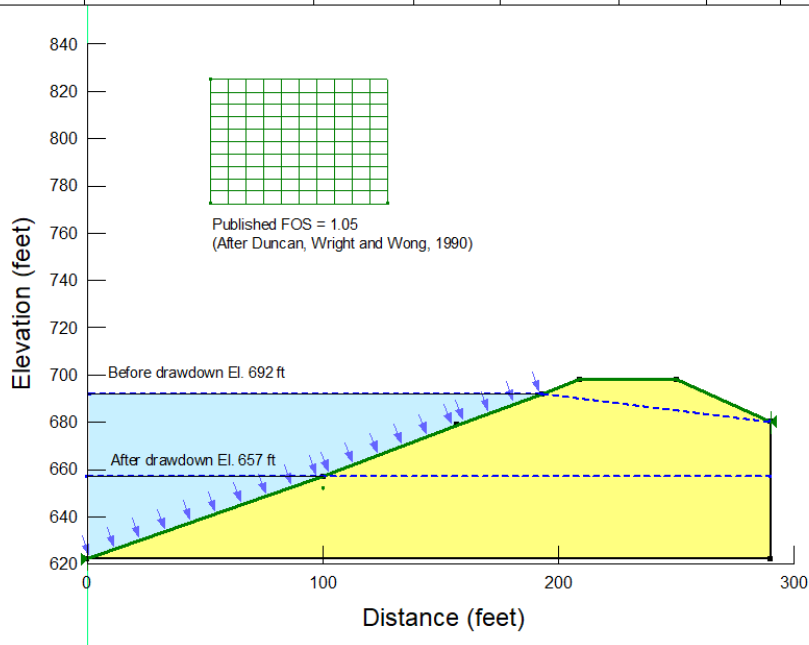
Figure 129 Geometry of the Pilarcitos Dam

2.43.2   Results and Discussions

Duncan et al. (1990) reported a critical factor of safety of 1.05. The factor of safety and location / shape of the critical slip surface closely match the published results.
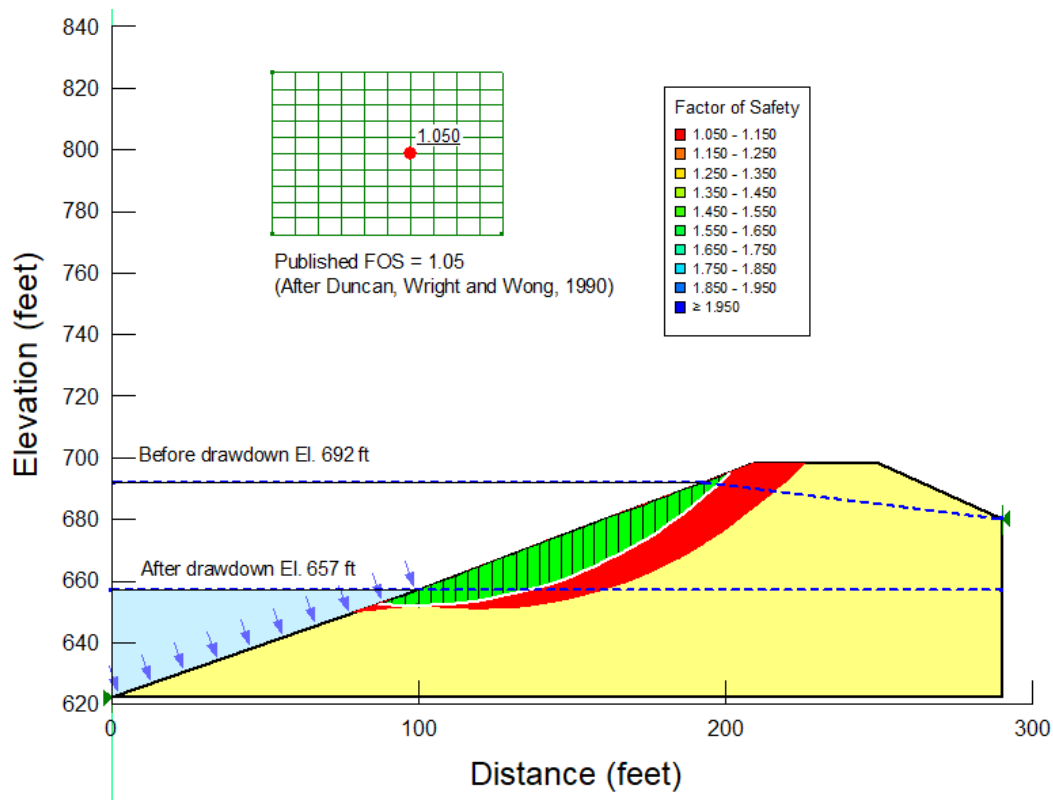
Figure 130 Location of the critical slip surface for the Pilarcitos Dam

2.44 Probability – James Bay Case History

Project File: Probabilistic - James Bay Case History.gsz

In this example, consideration is given to the statistical and spatial variability of the soil properties across the entire length of the soil stratum. The material properties are assumed to have a normal distribution.

2.44.1 Geometry and Material Properties

Figure 131 Geometry of the James Bay Probability model

Table 111 Material Properties of the James Bay Probability model

Material Names	Sat. Unit Wt. (kN/m³)	Cohesion (kPa)	Friction Angle (deg)
Till	20.6	34	29
Lacustrine Clay	20.3	31.2	0
Marine Clay	18.8	34.5	0
Clay Crust	18.8	43	0
Embankment	20	0	30

Table 112 Probability Parameters of the James Bay Probability model

Material Names	Property	Mean	Standard Deviation
Embankment	Phi	30	1
Embankment	Unit Weight	20	1
Marine Clay	c	34.5	8.14
Lacustine Clay	c	31.2	8.65

2.44.2 Results and Discussions

The deterministic solution from SLOPE/W shows excellent agreement to the case history documented by El-Ramly et. al. (2002).

1.460

Color	Name	Slope Stability Material Model	Unit Weight (kN/m³)	Effective Cohesion (kPa)	Effective Friction Angle (°)
	Clay crust	Mohr-Coulomb	18.8	43	0
	Lacustrine clay	Mohr-Coulomb	20.3	31.2	0
	Marine clay	Mohr-Coulomb	18.8	34.5	0
	Sand embankment	Mohr-Coulomb	20	0	30
	Till	Bedrock (Impenetrable)			
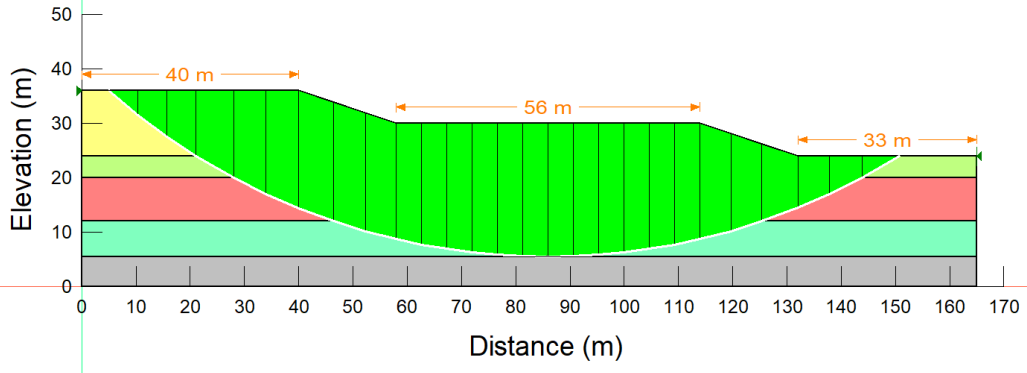
Figure 132 Solution of the James Bay Probability model (sampling every slice) using Bishop method

Table 113 Mean FOS compared with deterministic for James Bay Case History

Sampling Distance	Factor of Safety	
	Deterministic	Mean
Every slice	1.461	1.4605
30m	1.461	1.4601
40m	1.461	1.4600
50m	1.461	1.4613
80m	1.461	1.4606
100m	1.461	1.4578
No Spatial consideration	1.461	1.4611

Table 114 Spatial variability results for the James Bay Probability model

Sampling Distance	Standard Deviation	Probability of failure (%)	Reliability Index
Every slice	0.06537	0.000	7.109
30m	0.12795	0.003	3.596
40m	0.14518	0.050	3.168
50m	0.15446	0.100	2.986
80m	0.19617	0.937	2.348
100m	0.19842	0.990	2.308
No spatial consideration	0.21295	1.340	2.165

2.45 Eurocode 7 – Cutting in Clay

Project File: Eurocode Cutting in Clay.gsz

90

This model was based on the example on page 202 of the book "Designers' Guide to Eurocode 7: Geotechnical Design". The water table line was approximate only since the book did not give the coordinates. A permanent surcharge load of 35 kPa was applied to the crest of the slope. Eurocode 7 Design Approach 3 was selected for the analysis.

2.45.1 Geometry and Material Properties
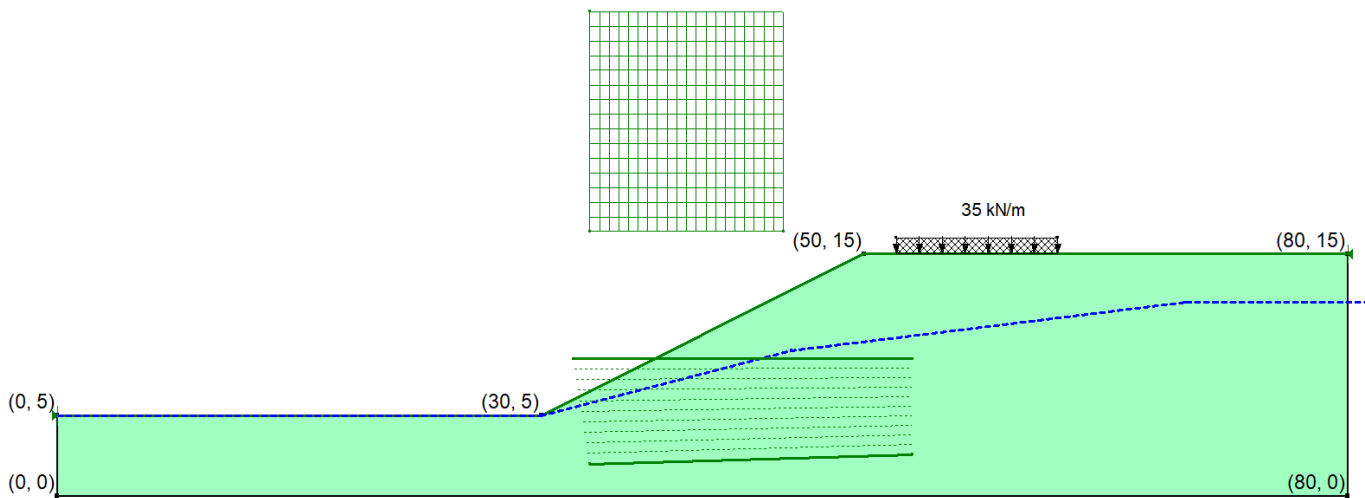
Figure 133 Eurocode 7 example Cutting in Clay: Geometry

Table 115 Eurocode 7 example Cutting in Clay: Material Properties

Material (M-C)	c (kPa)	φ (degrees)	γ (kN/m³)
Clay	10	28	20

2.45.2 Results and Discussions

The results of the analysis are shown in the following table and figures. The Overdesign Factor result published in the book was 1.193 using Bishop's method.

Method	Overdesign Factor	
	Moment	Force
Bishop	1.173	
Janbu		1.033
Spencer	1.174	1.174
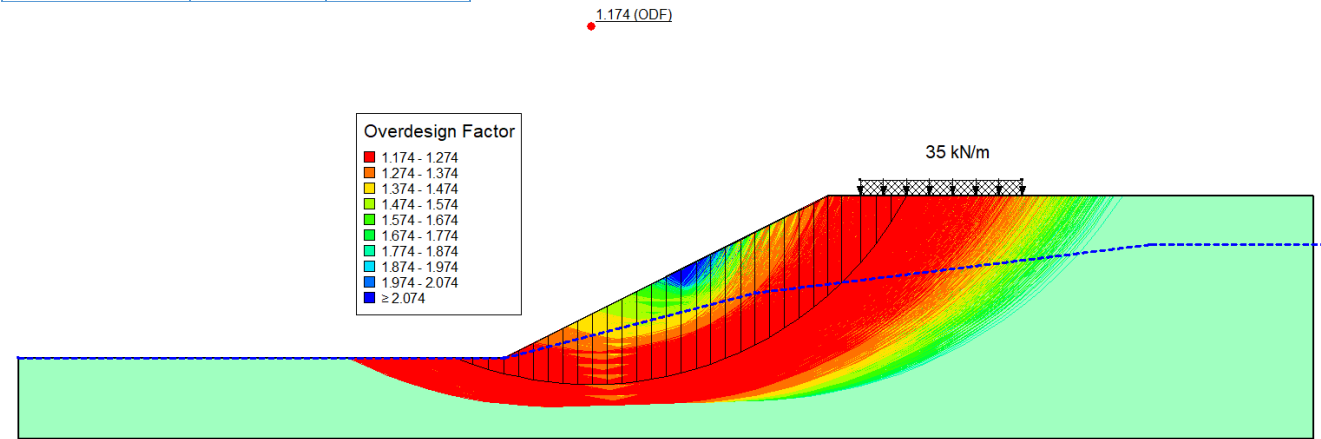
Figure 134 Eurocode 7 example Cutting in Clay: Critical slip surface
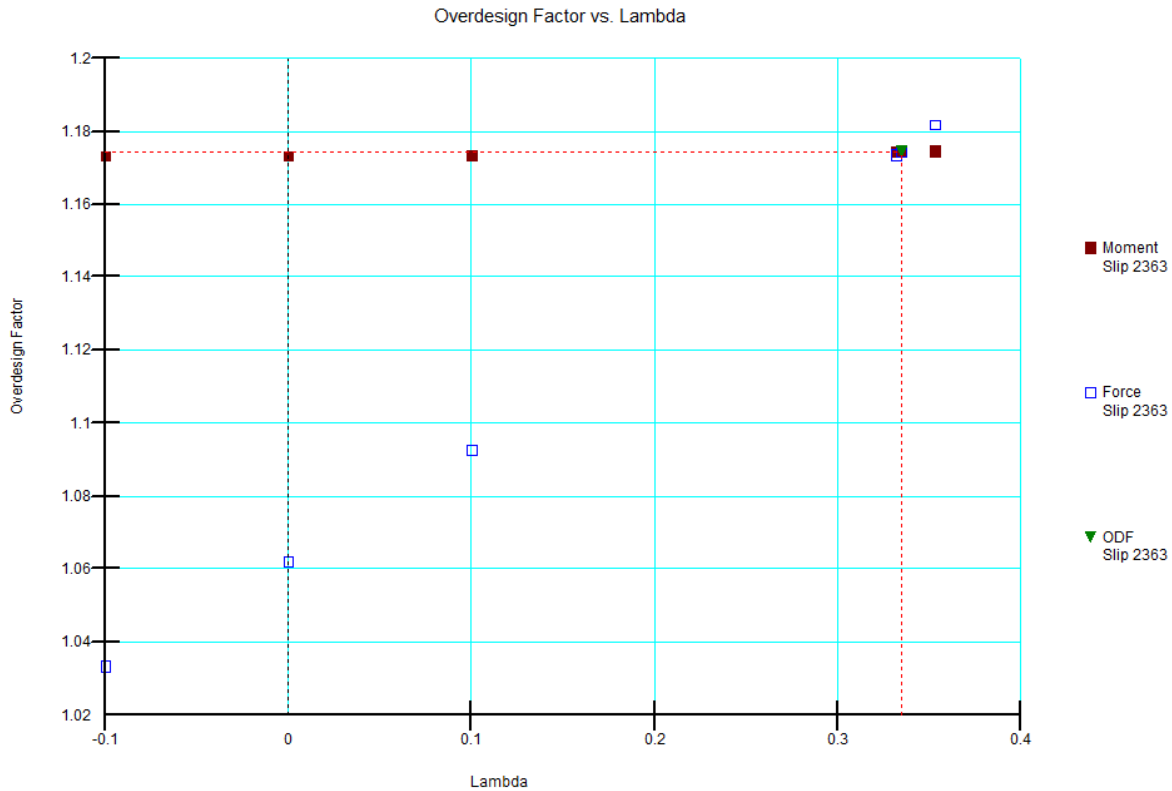
Figure 135 Eurocode 7 example Cutting in Clay: Factor of safety calculations

2.46 Eurocode 7 – Earth Dam

Project File: Eurocode Earth Dam.gsz

This model was based on example 5.12 of the book "Smith's Elements of Soil Mechanics" 8th edition. It was a coupled SEEP/W and SLOPE/W analysis. The slope stability analysis was conducted using Eurocode 7 Design Approach, Combination 2.

2.46.1 Geometry and Material Properties
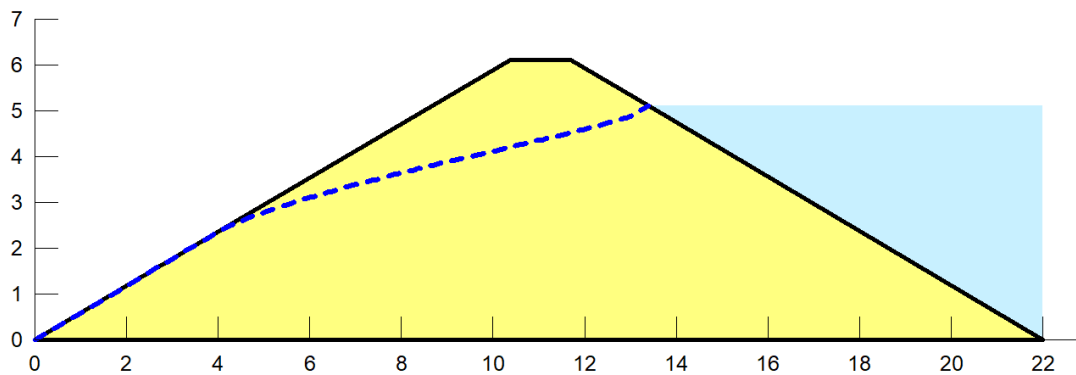
Figure 136 Eurocode 7 Earth Dam: Geometry

Table 116 Eurocode 7 Earth Dam: Material Properties

Material (M-C)	c (kPa)	ϕ (degrees)	γ (kN/m³)
Clay	12	20	19.2

92

2.46.2 Results and Discussions

The results of the analysis are shown in the following table and figures. The Overdesign Factor result published in the book (page 198) was 1.07 using Bishop's method.

Table 117 Eurocode 7 Earth Dam: Material Results

Method	Overdesign Factor	
	Moment	Force
Bishop	1.092	
Janbu		1.017
Morgenstern-Price	1.091	1.091
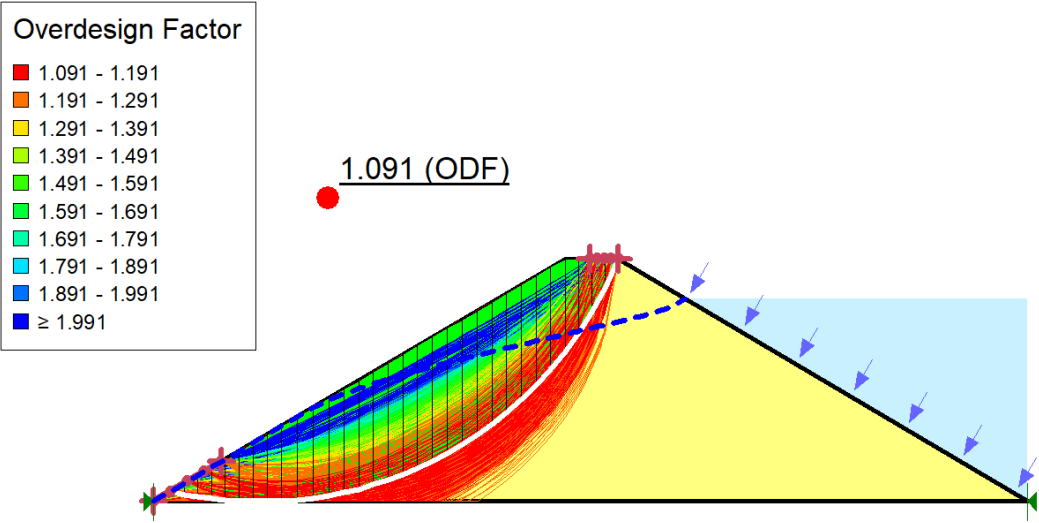
Figure 137 Eurocode 7 Earth Dam: Critical slip surface
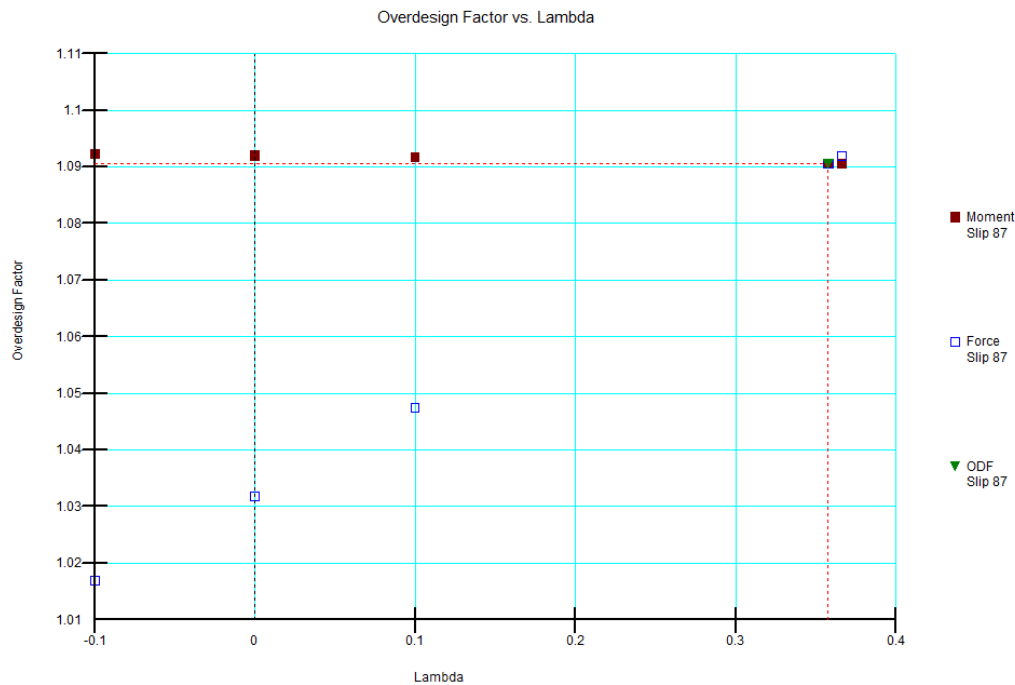
Figure 138 Eurocode 7 Earth Dam: Factor of safety calculations

2.47 Compound Strength vs Anisotropic Function

Project File: Compound Strength vs Anisotropic Function.gsz

This example verifies the Compound Strength and Anisotropic Function material models by comparing the results from a simulation involving a complex faulted geometry. The Cuckoo search technique was employed to locate the critical slip surface. All materials within the fault block are jointed rock masses. The shear strength of the discontinuities is considerably lower than that of the intact rock. The most straightforward way of modelling a jointed rock mass is by means of the Compound Strength model. The Compound Strength model comprises two strength models: one for the intact rock and one for the discontinuity. In addition, the Compound Strength model requires the dip and dip direction of the discontinuity and two angle ranges (A and B) to allow for interpolation of the strengths between that of the intact material and that of the discontinuity.

2.47.1 Geometry and Material Properties

Figure 139 shows the domain and material legend. Table 118 and Table 119 summarize the shear strength properties of the intact rock mass and the discontinuities. The name of the discontinuity comprises the name of the intact rock and the dip of the discontinuity. For example, DG1_40 is a discontinuity dipping at 40 degrees within the intact rock mass DG1. The intact strength is therefore c' = 163 kPa and $\emptyset' = 39$ while the discontinuity has c' = 10 kPa and $\emptyset' = 35$. All other discontinuities within DG1 have the same strength properties and different dip angles.

94

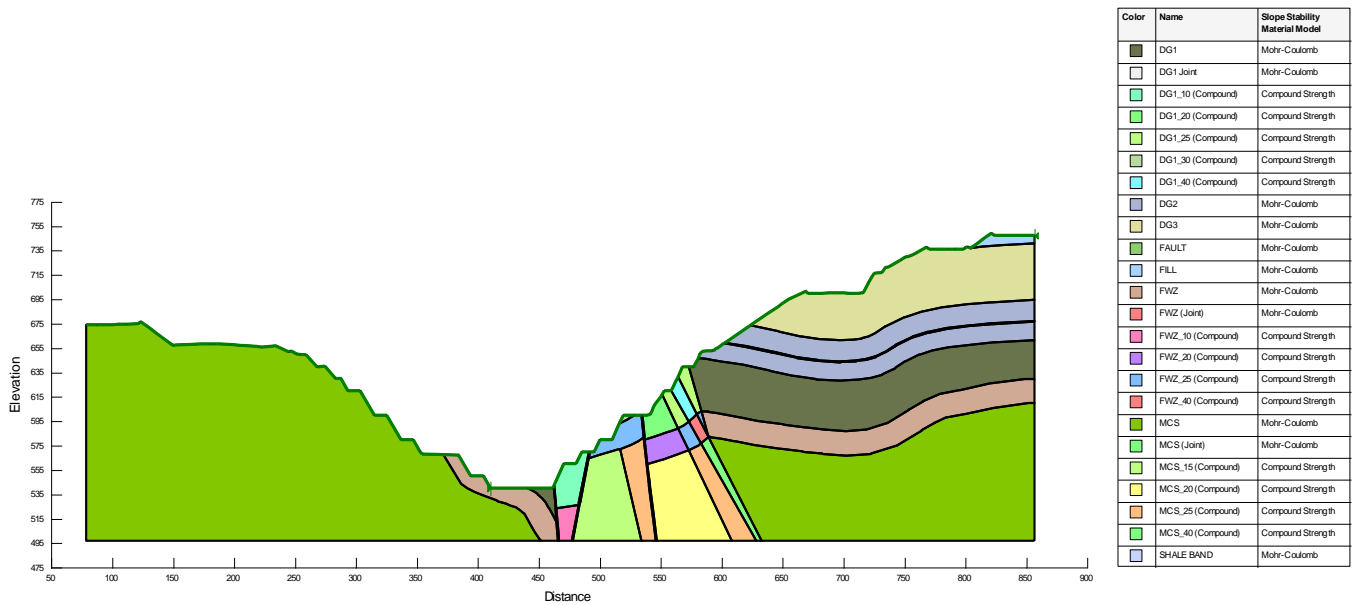| Color	Name	Slope Stability Material Model
	DG1	Mohr-Coulomb
	DG1 Joint	Mohr-Coulomb
	DG1_10 (Compound)	Compound Strength
	DG1_20 (Compound)	Compound Strength
	DG1_25 (Compound)	Compound Strength
	DG1_30 (Compound)	Compound Strength
	DG1_40 (Compound)	Compound Strength
	DG2	Mohr-Coulomb
	DG3	Mohr-Coulomb
	FAULT	Mohr-Coulomb
	FILL	Mohr-Coulomb
	FWZ	Mohr-Coulomb
	FWZ (Joint)	Mohr-Coulomb
	FWZ_10 (Compound)	Compound Strength
	FWZ_20 (Compound)	Compound Strength
	FWZ_25 (Compound)	Compound Strength
	FWZ_40 (Compound)	Compound Strength
	MCS	Mohr-Coulomb
	MCS (Joint)	Mohr-Coulomb
	MCS_15 (Compound)	Compound Strength
	MCS_20 (Compound)	Compound Strength
	MCS_25 (Compound)	Compound Strength
	MCS_40 (Compound)	Compound Strength
	SHALE BAND	Mohr-Coulomb

Figure 139 Geometry of the Section

Table 118 Intact rock strengths via the Mohr-Coulomb Model

	c (kN/m²)	φ' (degrees)	γ (kN/m³)
MCS	139	32	22
FWZ	184	43	30
DG1	163	39	35
DG2	124	32	35
DG3	150	37	35
FILL	10	37	20
FAULT	5	25	20
SHALE BAND	10	22	20

Table 119 Anisotropic Material Properties of the Section_B_ALM1 model

	c1 (kN/m²)	φ1 (degrees)	c2 (kN/m²)	φ2 (degrees)	A (degrees)	B (degrees)	θ (degrees)	γ (kN/m³)
DG1_40	10	35	163	39	5	30	40	35
DG1_30	10	35	163	39	5	30	30	35
DG1_25	10	35	163	39	5	30	25	35
DG1_20	10	35	163	39	5	30	20	35
DG1_10	10	35	163	39	5	30	10	35
FWZ_40	10	32	184	43	5	30	40	30
FWZ_25	10	32	184	43	5	30	25	30
FWZ_20	10	32	184	43	5	30	20	30
FWZ_10	10	32	184	43	5	30	10	30
MCS_40	10	27	139	32	5	30	40	22
MCS_25	10	27	139	32	5	30	25	22
MCS_20	10	27	139	32	5	30	20	22
MCS_15	10	27	139	32	5	30	15	22

2.47.2   Results and Discussions

Despite the complexity of the geology and material strength definitions, the simulations using the Anisotropic Function and Compound Strength models produced the same solutions. The Cuckoo search technique located a

slightly different slip surface for the two cases. The small discrepancy in FoS is the result of how the parameters / strengths are linearly interpolated between the intact rock and discontinuity parameters / strengths. The Compound Strength model linearly interpolates the frictional strength ($\sigma'_n \tan \emptyset'$) while the Anisotropic Function model linearly interpolates the effective friction angle ($\emptyset'$). The linear interpolation of the cohesive strength is the same between both models.
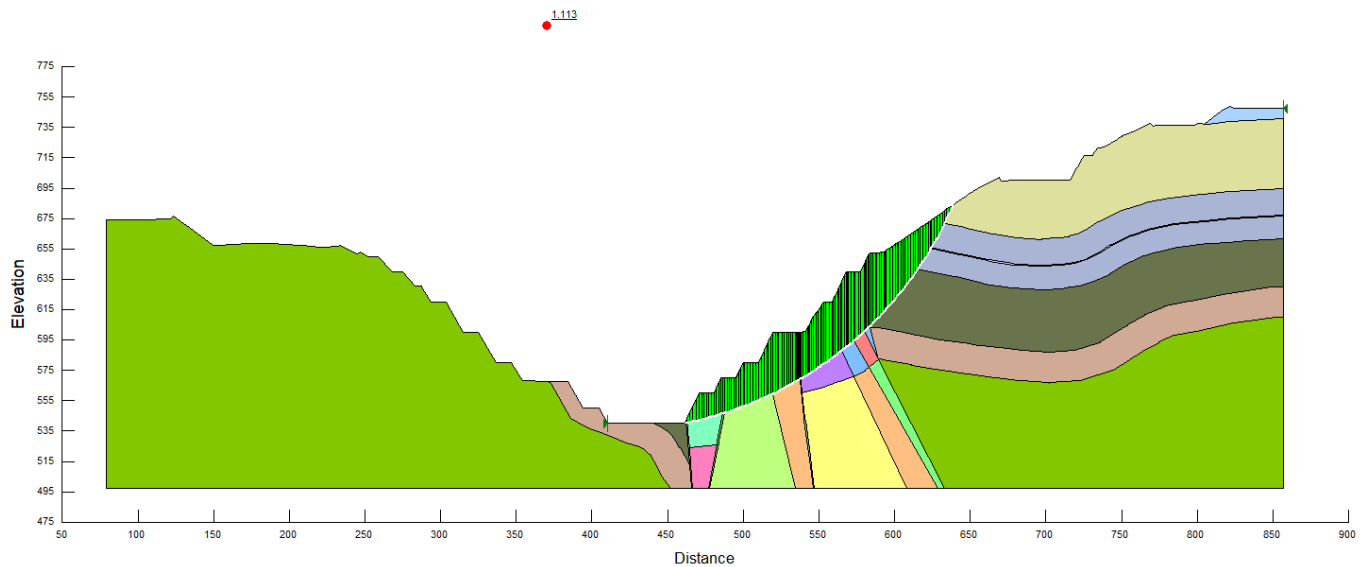

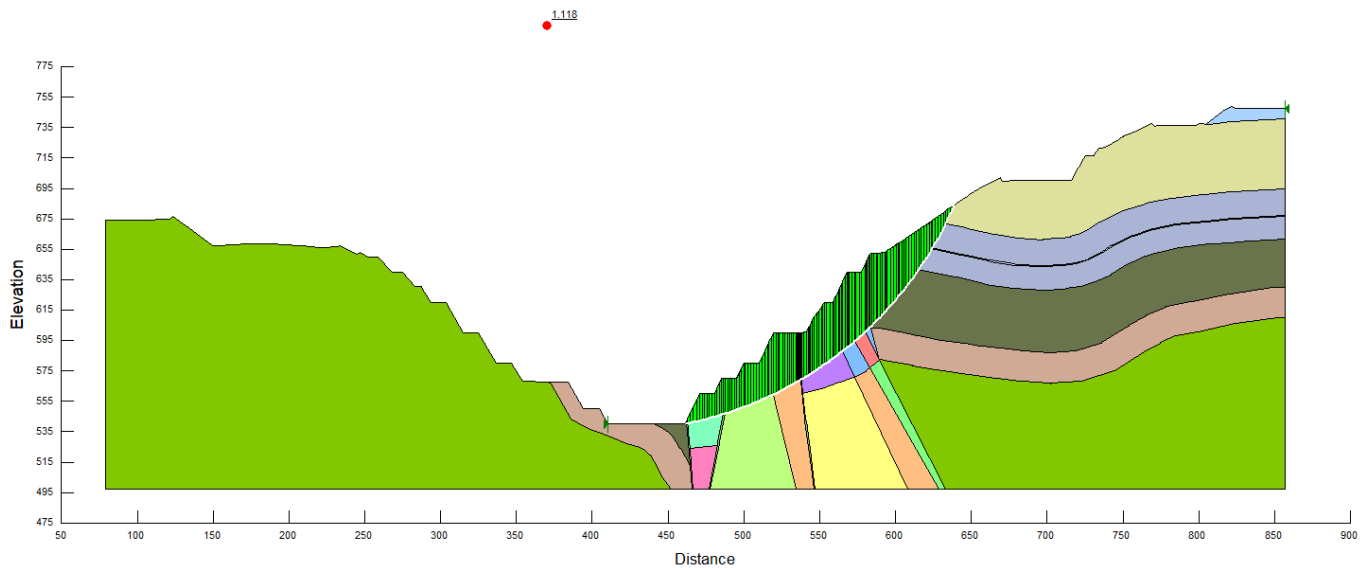**Figure 140 Anisotropic Function model used for all jointed rock within the fault block.**

Figure 141 Compound Strength model used for all jointed rock within the fault block.

96

3 References

Arai, K. and Tagyo, K. (1985), "Determination of Noncircular Slip Surface giving the minimum factor of safety in slope stability analysis", Soils and Foundations. Vol. 25, No.1 pp. 43-51.

Baker, R. (1980), "Determination of the critical slip surface in slope stability computations", International Journal for Numerical and Analytical Methods in Geomechanics, Vol.4, pp. 333-359.

Baker, R. and Leshchinsky, D. (2001), "Spatial Distribution of Safety Factors", Journal of Geotechnical and Geoenvironmental Engineering, February 2001, pp. 135-144.

Baker, R. (2003), "Inter-relations between experimental and computational aspects of slope stability analysis", International Journal for Numerical and Analytical Methods in Geomechanics, No. 27, pp. 379-401.

Baker, R. (1993), "Slope stability analysis for undrained loading conditions", International Journal for Numerical and Analytical Methods in Geomechanics, Vol. 17, pp. 15-43.

Borges, J. L. and Cardoso, A.S. (2002), "Overall stability of geosynthetic-reinforced embankments on soft soils", Geotextiles and Geomembranes, Vol. 20, pp. 395-421.

Brinkgreve, R.B. (2002), Plaxis Version 8 Dynamic Manual, Lisse, Balkema.

Chen, Z. and Shao, C. (1988). "Evaluation of minimum factor of safety in slope stability analysis", Canadian Geotechnical Journal, Vol. 25, pp. 735-748.

Chowdhury, R.N. and Xu, D.W. (1995), "Geotechnical system reliability of slopes", Reliability Engineering and System Safety. Vol. 47, pp. 141-151.

Craig, R. F., (1997), Soil Mechanics, 6th Edition. Routledge, UK June, 1997

Duncan, M.J., (2000), "Factors of Safety and Reliability in Geotechnical Engineering", Journal of Geotechnical of Geoenvironmental Engineering. April pp. 307-316.

Duncan, J.M., and Wright, S.G., 2005, "Soil Strength and Slope Stability", John Wiley & Sons, Inc.

Duncan, J.M., Wright, S.G., and Wong, K.S., 1990, "Slope stability during rapid drawdown", Proceedings of the H. Bolton Seed Memorial Symposium, May, Vol. 2, pp. 253-272.

El-Ramly, H., Morgenstern, N.R. and Cruden, D.M. (2003), "Probabilistic stability analysis of a tailings dyke on presheared clay-shale", Canadian Geotechnical Journal, Vol. 40, pp. 192-208.

FlexPDE 6 (2007). *Reference Manual*, PDE Solutions Inc., Spokane Valley, WA 99206.

FlexPDE 7 (2017). *Reference Manual*, PDE Solutions Inc., Spokane Valley, WA 99206.

Fowler, C.M.R. (1990), An Introduction to Global Geophysics (2nd ed.). Cambridge University Press.

Fredlund, D.G. and Krahn, J. (1977), "Comparison of slope stability methods of analysis", Canadian Geotechnical Journal Vol. 14, No. 3, pp. 429-439.

Ghobrial, F., Karray, M., Delisle, M-C. and Ledoux, C. (2015), Development of spectral pseudo-static method for dynamic clayey slope stability analysis. 68th Canadian Geotechnical Conference, Quebec City, Quebec, Canada.

Giam, P.S.K. and I.B. Donald (1989), "Example problems for testing soil slope stability programs", Civil Engineering Research Report No. 8/1989, Monash University, ISBN 0867469218, ISSN 01556282.

Giam, P.S.K. (1989). "Improved methods and computational approaches to geotechnical stability analysis", Ph.D., Thesis, Department. of Civil Engineering, Monash University, Melbourne, Australia.

Greco, V.R. (1996), "Efficient Monte Carlo technique for locating critical slip surface", Journal of Geotechnical Engineering. Vol. 122, No. 7, July, pp. 517-525.

Hassan, A.M. and Wolff, T.E. (1999), "Search algorithm for minimum reliability index of earth slopes", Journal of Geotechnical and Geoenvironmental Engineering, Vol. 125, No. 4, April 1999, pp. 301-308.

Hungr O., Salgado F.M. and Byrne P.M. (1989), "Evaluation of a three-dimensional method of slope stability analysis", Canadian Geotechnical Journal, Vol. 26, pp. 697-686.

Ireland, H.O. (1954), "Stability analysis of the Congress Street open cut in Chicago", Geotechnique, Vol. 4, pp. 163-168.

Jiang, J-C., Baker, R., and Yamagami, T. (2003), "The effect of strength envelope non linearity on slope stability computations", Canadian Geotechnical Journal, No. 40, pp. 308-325.

Kim, J., Salgado, R., Lee, J. (2002), "Stability analysis of complex soil slopes using limit analysis", Journal and Geotechnical and Geoenvironmental Engineering. Vol. 128, No. 7, July, pp. 546-557.

Kinsler, L.E., Frey A.R., Coppens, A.B., & Sanders J.V. (1999). Fundamentals of Acoustics (4th ed.), Wiley.

Lambe, T., and Whitman, R. (1969). "Soil Mechanics", John Wiley & Sons, New York, N.Y.

Leshchinski D., Baker, R., and Silver, M.L. (1985). "Three dimensional analysis of slope stability", International Journal for Numerical and Analytical Methods in Geomechanics, vol. 9, pp. 199-223.

Li, S.K. and Lumb, P. (1987). "Probabilistic design of slopes", Canadian Geotechnical Journal, Vol. 24, No. 4, pp. 520-535.

Loukidis, D., Bandini, P., and Salgado, R. (2003), "Stability of seismically loaded slopes using limit analysis", Geotechnique, No. 5, pp. 463-479.

Low, B. (1989), "Stability analysis of embankment on soft ground." Journal of Geotechnical Engineering, Vol. 115, No. 2, pp. 221-227.

Malkawi, A.I.H, Hassan, W.F., and Sarma, S.K. (2001), "Global search method for locating general slip surface using Monte Carlo techniques." Journal of Geotechnical and Geoenvironmental Engineering. Vol. 127, No. 8 August, 99. 688-698.

Pham, Ha, (2002), "Slope Stability Analysis using Dynamic Programming Method Combined with a Finite Element Stress Analysis", University of Saskatchewan, Saskatoon, Canada

Pilot, G., Trake, B. and La Rochelle, P. (1982). "Effective stress analysis of the stability of embankments on soft soils", Canadian Geotechnical Journal, Vol. 19, pp. 433-450.

Pockoski, M., and Duncan, J.M., (2000). "Comparison of Computer Programs for Analysis of Reinforced Slopes", Virginia Polytechnic Institute and State University.

Prandtl, L. (1921), "Uber die Eindringungsfestigkeit (Harte) plastischer Baustoffe und die Festigkeit von Schneiben (On the penetrating strength (hardness) of plastic construction materials and strength of curring edges)", Zeitschrift fur Agnewandte Mathematik und Mechanik, Vol. 1, pp. 15-20.

Priest, S. (1993), "Discontinuity analysis for rock engineering", Chapman & Hall, London, pp. 219-226.

Sarma, S.K. (1979). "Stability Analysis of Embankments and Slopes". J. Geotech. Eng. Div. ASCE 105, No. 12, pp. 1511-1524.

Seed, R.B., Mitchell, J.K. and Seed, H.B.. (1990). "Kettlemen Hills Waste Landfill Slope Failure", ASCE Journal of Geotechnical Engineering, 116:669-690.

Sevaldson, R.A., (1956). "The slide in Lodalen, October 6th, 1954". Geotechnique, No. 6, pp. 167-182.

Sheahan, T., and Ho. L., (2003), "Simplified trail wedge method for soil nailed wall analysis", Journal of Geotechnical of Geoenvironmental Engineering, Vol. 17, pp. 117-124.

Silvertri V. (2006), "A three-dimensional slope stability problem in clay", Canadian Geotechnical Journal, Vol. 43, pp. 224-228.

Spencer, E. (1969), "A method of analysis of the stability of embankments assuming parallel inter-slice forces", Geotechnique, Vol. 17, pp. 11-26.

Tandjiria, V., Low. B.K., and Teh, C.I. (2002), "Effect of reinforcement force distribution on stability of embankment", Geotextiles and Geomembranes, No. 20 pp. 423- 443.

Wolff, T.F. and Harr, M.E. (1987), "Slope design for earth dams", Reliability and Risk Analysis in civil Engineering 2, Proceedings of the Fifth International Conference on Applications of Statistics and Probability in Soil and Structural Engineering, Vancouver, BC, Canada, May, 1987, pp. 725-732.

XSTABL, (1999), Slope Stability Reference Manual, Version 5.2, pp 11-26.

Yamagami, T., Jiang, J.C., and Ueno, K. (2000), "A limit equilibrium stability analysis of slope with stabilizing piles", Slope Stability 2000, pp. 343-354.

Yamagami, T. and Ueta, Y. (1988), "Search for noncircular slip surfaces by the Morgenstern-Price method", Proc. 6th Int. Conf. Numerical Methods in Geomechanics, pp. 1335-1340

Zhu, D., Lee, C.F., and Jiang, H.D, (2003), "Generalized framework of limit equilibrium methods for slope stability analysis." Geotechnique, No. 4, pp. 337-395.

Zhu, D., and Lee, C. (2002), "Explicit limit equilibrium solution for slope stability", International Journal for Numerical and Analytical Methods in Geomechanics, No. 26, pp. 1573-1590.